THE JOURNAL
OF
CHEMICAL PHYSICS

VOLUME 8 JUNE, 1940 NUMBER 6

Calculation of Dipole Moments from Rates of Nitration of Substituted Benzenes and Its Significance for Organic Chemistry

TAIKEI RI* AND HENRY EYRING
Princeton University, Princeton, New Jersey
(Received March 6, 1940)

(1) From a set of assumptions which seem reasonable *a priori*, the authors calculate the charge distributions in the molecules of mono-substituted benzenes, and the dipole moments of the latter from reaction rate data alone. These coincide very well with the observed moments. (2) From the dipole moments of aromatic and aliphatic compounds, the ortho-, meta- and para-percentages during nitration were calculated. These also accord satisfactorily with the experimental values. (3) It is concluded that these two facts give a quantitative basis to the usual explanation about the orienting power of substituents of benzene. (4) The nitration of benzene is an ionic reaction: The nitrating agent $X \cdot NO_2$ dissociates into X^- and NO_2^+ in the activated complex, and the latter ion interacts with the reacting carbon. The activation free energy is reduced by the amount of the electrostatic interaction, i.e., $4.80 \cdot 10^{-10}\epsilon_y/(rD)$. Here ϵ_y is the charge on the reacting carbon, r, the distance between NO_2^+ and the reacting carbon in the activated complex, D, the dielectric constant of the medium between NO_2^+ and the reacting carbon. (5) The authors find that $r=1.6$A and $D=1$ approximately, independent of the nature of the reacting media. The consequences of this theory are outlined. (6) Further this interpretation of reaction rates provides, for the first time, a method of calculating the atomic charges in the molecules as distinguished from the usual dielectric measurements which lead only to dipole moments.

1. INTRODUCTION

IT is a well-known fact that some substituents of benzene e.g., CH_3, OH, NH_2, halogens, etc. act as ortho- and para-orienting while NO_2, COOH, SO_3H, etc. cause reaction in the meta-position when mono-substituted benzenes are subjected to substitution reactions, e.g., nitration, halogenation, sulphonation, etc. This is explained in modern organic chemistry by the following two assumptions:

(a) An ortho- and para-orienting substituent makes the electron density on the corresponding carbon atoms greater than that on the meta-atom by inductive and resonance effect, while a meta-orienting one acts in the opposite way.

(b) Substituting agents are electrophilic,[1] i.e., electron-seeking, because of their positive electric nature. Thus it reacts most easily with that carbon atom which is surrounded by the greatest number of electrons.

Assuming this explanation to be correct then the ortho-, meta- and para-percentages, which are proportional to the reaction rates at the corresponding carbon atoms, should provide a means of determining the charge distribution and consequently also permit the calculation of the dipole moments of such molecules from rate data alone. If dipole moments calculated in this way from rates coincide with the observed values, then the above qualitative explanation for the orienting power of substituents will be

* Assistant Professor, Kyoto Imperial University, Japan.

[1] Ingold, J. Chem. Soc. 1120 (1933).

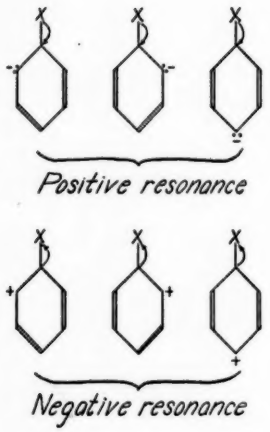

FIG. 1.

shown to have a considerably more substantial basis. Also assumption (b) which organic chemists make from qualitative considerations only will be much more precisely formulated.

In the present work we have calculated the moments of mono-substituted benzenes from the ortho-, meta- and para-percentages of the substituents after nitration since they have been studied more completely than other substitution reactions. Afterwards the converse calculation is made, i.e., the percentages of the nitrated products are calculated from the dipole moments alone. As far as we know, this is the first attempt at such a calculation, although there is a qualitative statement regarding the relation between ortho, meta- and para-substitution and dipole moments, which has been known as "Sutton's rule."[2]

2. Model Assumed for the Activated Complex

In nitration of mono-substituted benzene, the following assumptions are made:

(1) The nitrating agent is ionized into a negative ion and an NO_2^+ which in the activated complex lies adjacent to the carbon atom with which it is to react.

(2) A substituent of benzene changes the electric charge on the six-carbon atoms, as is usually assumed, by both an inductive and a resonance effect.

(3) The inductive effect induces equal charges, ϵ_i, on the six-carbon atoms of benzene and a charge $-6\epsilon_i$ on the inductive group. This charge may be either positive or negative. In first approximation, we assume further that the charge, ϵ_r, which also may be positive or negative, accumulates on each of the two ortho- and one para-atoms by resonance with the three bond structures in Fig. 1, there being no corresponding effect at the meta-position. (In Fig. 1 the curved arrows between X and the substituted carbon atoms indicate the directions of electron movements.)

(4) The charge $3\epsilon_r$ on the ortho- and para-carbons is balanced by a charge of $-\frac{3}{2}\epsilon_r$ on the substituent group and $-\frac{3}{2}\epsilon_r$ on the carbon atom to which the latter is bonded.

Therefore, the charge distribution in a molecule can be represented by Fig. 2 and the following formulas, combining assumptions (3) and (4),

$$\begin{aligned} &\text{(a)} \quad \epsilon_m = \epsilon_i, \\ &\text{(b)} \quad \epsilon_p = \epsilon_0 = \epsilon_m + \epsilon_r, \\ &\text{(c)} \quad \epsilon_1 = \epsilon_m - \tfrac{3}{2}(\epsilon_p - \epsilon_m), \\ &\text{(d)} \quad \epsilon_x = -6\epsilon_x - \tfrac{3}{2}(\epsilon_p - \epsilon_m), \end{aligned} \tag{1}$$

where ϵ_1 represents the charge on the carbon attached to the substituent group X, and ϵ_x the charge on X. The location of the other ϵ's is indicated by the subscripts.

(5) We assume further that the electrostatic interaction between the reacting carbon atom and NO_2^+ changes the activation free energy $\Delta F^\ddagger$ for the nitration of benzene by the amount, $\epsilon_y\epsilon_n/(rD)$. The velocity constant at a carbon atom for mono-substituted benzene is then given

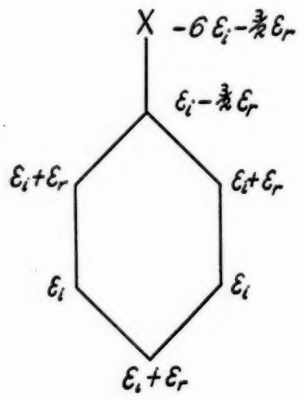

FIG. 2.

[2] Sutton, Proc. Roy. Soc. **133A**, 668 (1931), Groves and Sugden, J. Chem. Soc. 973 (1935).

by the equation

$$k_y = \kappa \frac{kT}{h} e^{-[\Delta F^{\ddagger} + \epsilon_y \epsilon_n/(rD)]/kT}, \qquad (2)$$

where ϵ_y and ϵ_n are the charges on the reacting carbon atom and NO_2^+, respectively, the latter being taken as $4.80 \cdot 10^{-10}$ e.s.u. r is the distance between the carbon and NO_2^+ which is always taken as 1.6A in this calculation. D is the dielectric constant of the medium between NO_2^+ and the carbon atom which we take equal to unity. The other notation has the usual meaning.[3]

3. Calculation of Charge Distributions in Molecules and of Dipole Moments

If k_H is the rate constant at a carbon atom of benzene, the following equation follows immediately from Eq. (2),

$$\frac{k_y}{k_H} = e^{-[\epsilon_y \epsilon_n/(rD)]/kT}. \qquad (3)$$

Here, k_y/k_H can be obtained from the fractions χ_0, χ_m and χ_p of ortho-, meta- and para-substituents after nitration together with the relative nitrated amounts k_H' and k_x' of benzene and substituted benzene respectively in a competitive reaction, since we can write down immediately the following relations:

$$\begin{aligned} &(a) \quad k_0/k_H = 3\chi_0(k_x'/k_H'), \\ &(b) \quad k_m/k_H = 3\chi_m(k_x'/k_H'), \qquad (4)^* \\ &(c) \quad k_p/k_H = 6\chi_p(k_x'/k_H'). \end{aligned}$$

Thus, the charge ϵ_m and ϵ_p are calculated from (3) and (4), and consequently the entire charge distribution in the molecule of mono-substituted benzene is obtained using Eq. (1).

The dipole moment of the molecule is given by the equation

$$\mu = \epsilon_x(r_x + r_b) + (\epsilon_1 - \epsilon_m) r_b, \qquad (5)$$

where r_b is the length of a C−C bond in the benzene nucleus and r_x is the distance between the substituent X and the carbon to which it is attached. Thus, if we assume $\epsilon_0 = \epsilon_p$ as first approximation, the Eq. (4a) is not necessary to compute dipole moments. The calculations of dipole moments to be given next, are based on this assumption. However this assumption is not strictly correct, as will be discussed later in the refinement of the theory, which is necessary to take account of the difference in rates in the ortho- and para-substitution, i.e., of the difference between the charges in ortho- and para-position. We shall hereafter use the symbol (ϵ_0) for the charge obtained from the rate of the ortho-position, to denote that it is different from the charge obtained from the simple assumption $\epsilon_p = \epsilon_0$. When we use (ϵ_0) also for the calculation of dipole moments it changes our results only by about 5 percent, as will be shown later. This does not affect significantly the agreement with experiment.

The values r_b and r_x used in the calculation are tabulated in Table I.[4] The r_x values in this table represent the bond lengths between substituted carbon atoms and the atoms in the substituents which combined directly with the former.

At first, results will be given, which are obtained by making use of the studies of Ingold and collaborators on competitive nitration. Generally the percentages of the various substitution products are independent of the reacting media. This is a justification for taking D constant independent of the solvent. This result also indicates that the electrostatic effect of other carbons than the one being attacked do not contribute appreciably to the activation energy,

Table I. $r_b = 1.39$A.

	CH_3	CH_2Cl	$CHCl_2$	CCl_3	F	Cl
r_x(A)	1.50	1.50	1.50	1.50	1.40	1.69

Br	I	COOH	$COOCH_3$	$COOC_2H_5$	NO_2
1.88	2.05	1.54	1.54	1.54	1.46

[3] Eyring, J. Chem. Phys. **3**, 107 (1935), Wynne-Jones and Eyring, J. Chem. Phys. **3**, 492 (1935).

* There are six positions for nitration of benzene while there are two for ortho- and meta- and one for paranitration in the case of substituted benzene. Consequently, $k_0/k_H = (\chi_0 k_x'/2)/(k_H'/6)$, $k_m/k_H = (\chi_m k_x'/2)/(k_H'/6)$ and $k_p/k_H = (\chi_p k_x')/(k_H'/6)$.

[4] These values were taken from Brockway and Beach (Rev. Mod. Phys. **8**, 231 (1936), Am. Ass. Adv. Sci. No. 7, p. 88 (1939)).

TABLE II.[8] *Nitration of toluene.* $\mu_{calc}=0.48$; $\mu_{obs}=0.44$.

	273°K $k_x'/k_H'=27$			303°K $k_x'/k_H'=22$			MEAN FREE ENERGIES AND CHARGE DISTRIBUTION	
	%	k_y/k_H	$\frac{\epsilon_y\epsilon_n}{rD}$ (CAL./MOLE)	%	k_y/k_H	$\frac{\epsilon_y\epsilon_n}{rD}$ (CAL./MOLE)	$\frac{\epsilon_y\epsilon_n}{rD}$ (CAL./MOLE)	$\epsilon_y\cdot10^{10}$ (E.S.U.)
o	57.2	46.31	−2071	57.3	37.8	−2178	−2125	(−0.0491)*
m	3.1	2.5	− 497	4.2	2.77	− 611	− 554	−0.0128
p	39.7	64.3	−2247	38.5	50.8	−2354	−2301	−0.0532
1								0.0478
X								0.137

* These numbers within the parentheses in this and the following tables are the charges (ϵ_0) of the ortho-positions calculated from the rates.

TABLE III.[9] *Nitration of ethylbenzoate.* $\mu_{calc}=-1.31$; $\mu_{obs}=-1.91$.

291°K $k_x'/K_H'=0.00367$.

	%	k_y/K_H	$\frac{\epsilon_y\epsilon_n}{rD}$ (CAL./MOLE)	$\epsilon_y\cdot10^{10}$ (E.S.U.)
o	27.5	0.00303	3338	(0.0772)
m	68.9	0.00759	2809	0.0649
p	3.6	0.000793	4109	0.0950
1				0.0198
X				−0.430

as such an interaction would be modified by the dielectric constant of the media. Because of this constancy we followed Bird and Ingold[5] in using mean percentages obtained from experiments in different media and at different temperatures.

The method of averaging of the ortho-, meta- and para-percentages obtained under different conditions was as follows: By the equations

$$\Delta F_{pm}^{\ddagger}=\frac{(\epsilon_p-\epsilon_m)\epsilon_n}{rD}=-kT\ln\frac{2\chi_p}{\chi_m} \qquad (6)$$

and

$$\Delta F_{om}^{\ddagger}=\frac{((\epsilon_0)-\epsilon_m)\epsilon_n}{rD}=-kT\ln\frac{\chi_o}{\chi_m} \qquad (7)$$

obtained from Eqs. (2) and (4), the mean free energies $\Delta F_{pm}^{\ddagger}$ and $\Delta F_{om}^{\ddagger}$ are averaged regardless of the conditions under which the nitration was conducted. If the mean free energies are then put back into Eqs. (6) and (7), one can now calculate "mean percentages" at any desired temperature. This method is the same in principle as that used by Scheffer,[6] by Bradfield and Jones,[7] and by Bird and Ingold.[5] Ingold and collaborators showed also that the rate ratios for substituted benzenes to benzene for nitration, i.e., k_x'/k_H' are independent of the reacting media. Thus mean values of k_x'/k_H' in different media were used in our calculations.

In the following Tables II, III, IV, V, VI and VII, the percentages were obtained by the above procedure making use of Table III of the paper of Bird and Ingold.[5] The rate ratios, k_x'/k_H', were taken from the data of the literature as referred to in the following tables.

To simplify our calculation of dipole moments, we have taken the total charge, ϵ_x, on the substituent X as being located on that atom attached to the carbon atom 1 of the benzene ring.

[5] Bird and Ingold, J. Chem. Soc. 918 (1938).

[6] Scheffer, Proc. K. Akad. Wetensch. Amsterdam, **15**, 118 (1913).

[7] Bradfield and Jones, J. Chem. Soc. 1006, 3073 (1928).

TABLE IV.[5] *Nitration of chlorobenzene.* $\mu_{calc}=-1.54$; $\mu_{obs}=-1.55$.

	273°K $k_x'/k_H'=0.0269$			298°K $k_x'/k_H'=0.0322$			308°K $k_x'/k_H'=0.0364$			MEAN FREE ENERGIES AND CHARGE DISTRIBUTION	
	%	k_y/k_H	$\frac{\epsilon_y\epsilon_n}{rD}$ (CAL./MOLE)	%	k_y/k_H	$\frac{\epsilon_y\epsilon_n}{rD}$ (CAL./MOLE)	%	k_y/k_H	$\frac{\epsilon_y\epsilon_n}{rD}$ (CAL./MOLE)	$\frac{\epsilon_y\epsilon_n}{rD}$ (CAL./MOLE)	$\epsilon_y\cdot10^{10}$ (E.S.U.)
o	28.2	0.0228	2041	31.0	0.0300	2067	32.1	0.0351	2041	2050	(0.0473)
m	(0.2)	0.000164	4705	(0.2)	0.000193	5040	(0.2)	0.000218	5138	4961	0.115
p	71.8	0.116	1163	69.0	0.133	1189	67.9	0.148	1164	1172	0.0271
1											0.247
X											−0.558

TABLE V.[5] *Nitration of bromobenzene.* $\mu_{calc} = -1.68$; $\mu_{obs} = -1.53$.

	273°K $k_x'/k_H' = 0.0246$			298°K $k_x'/k_H' = 0.0305$			308°K $k_x'/k_H' = 0.0321$			MEAN FREE ENERGIES AND CHARGE DISTRIBUTION	
	%	k_y/k_H	$\frac{\epsilon_y\epsilon_n}{rD}$ (CAL./MOLE)	%	k_y/k_H	$\frac{\epsilon_y\epsilon_n}{rD}$ (CAL./MOLE)	%	k_y/k_H	$\frac{\epsilon_y\epsilon_n}{rD}$ (CAL./MOLE)	$\frac{\epsilon_y\epsilon_n}{rD}$ (CAL./MOLE)	$\epsilon_y \cdot 10^{10}$ (E.S.U.)
o	39.0	0.0288	1915	4.14	0.0379	1928	42.4	0.0405	1954	1932	(0.0446)
m	(0.2)	0.000148	4761	(0.2)	0.000183	5072	(0.2)	0.000193	5211	5015	0.116
p	61.0	0.0900	1300	58.6	0.107	1317	57.6	0.110	1345	1321	0.0305
1											0.244
X											−0.568

The results for toluene and ethylbenzoate are given in Tables II[8] and III,[9] respectively, together with k_x'/k_H' used in the calculations. The agreement here is satisfactory.

The dipole moment −1.31 calculated in this case is that due to resonance and induction in the benzene ring. The extra 0.60 Debye unit observed is to be attributed to the rest of the molecule.

Next we shall give the results for halobenzenes. Usually halobenzenes are assumed not to produce meta-substituted products. But this is not strictly true. Thus Holleman (see Bird and Ingold[10]) found 0.3 percent of the meta-product in the nitration of bromobenzene. The authors have taken 0.2 percent for the amount of meta-products which lies within the usual experimental error. This value is used in Tables IV, V, VI and VII for the calculation.

The agreement between the calculations and experiments in these cases also is very good. Here, however, it hinges on the approximate correctness of our estimation of the meta-percentages. We also found, as will be shown in a later paper, the same ϵ_m from a study of acid and base-strengths and from side chain reactivities of meta-halogenated compounds. Therefore, our estimation of the meta-products is quite reasonable.

For the compounds which have not yet been competitively nitrated in the presence of benzene the dipole moments were calculated by the following procedure.

TABLE VI.[5*] *Nitration of iodobenzene.* $\mu_{calc} = -1.27$; $\mu_{obs} = -1.30$.

	291°K $k_x'/k_H' = 0.18$			
	%	k_y/k_H	$\frac{\epsilon_y\epsilon_n}{rD}$ (CAL./MOLE)	$\epsilon_y \cdot 10^{10}$ (E.S.U.)
o	43.1	0.232	841	(0.0194)
m	(0.2)	0.00108	3931	0.0909
p	56.9	0.613	282	0.00651
1				0.218
X				−0.419

* In the competitive nitration of iodo- and fluorobenzene, there are considerable errors in k_x'/k_H'. Especially in the case of iodobenzene, the values of k_x'/k_H' change within the range 0.1–0.3 with no distinction for the temperatures between 0° and 35°, under which the experiments were carried out. Therefore, in the calculation of these cases, we used the mean values of k_x'/k_H' at 18°, which were given by these authors. Since they have not determined the ortho- meta- and para-percentages of the substituents of these compounds, we used the mean percentages at 18° obtained from Holleman's values (Chem. Rev. 1, 187 (1924)).

TABLE VII.[5] *Nitration of fluorobenzene.* $\mu_{calc} = -1.20$; $\mu_{obs} = -1.45$.

	291°K $k_x'/k_H' = 0.15$			
	%	k_y/k_H	$\frac{\epsilon_y\epsilon_n}{rD}$ (CAL./MOLE)	$\epsilon_y \cdot 10^{10}$ (E.S.U.)
o	14.6	0.0653	1570	(0.0363)
m	(0.2)	0.00090	4036	0.0933
p	85.4	0.768	152	0.00351
1				0.181
X				−0.473

First, Eq. (6) is used, where $2\chi_p/\chi_m$ is known experimentally. Therefore, if ϵ_m of a molecule is known by another method, ϵ_p can be calculated. We assume that the inductive part of the dipole moment of mono-substituted benzene is equal to the moment μ_{ali} of the corresponding substituted tertiary aliphatic compound, i.e.,

$$-6\epsilon_m(r_b + r_x) = \mu_{ali}. \qquad (8)$$

Equation (8) permits us to calculate ϵ_m from μ_{ali}, and consequently we can now calculate the

[8] Ingold, Lapworth, Rothstein and Ward, J. Chem. Soc. 1959 (1931); Bird and Ingold, *ibid.* 918 (1938). The dipole moments in Debye units in this and the following tables, are the mean values of the data in Trans. Faraday Soc. **30**, Appendix (1934). The signs for the direction of the dipole moments are the customary ones.

[9] Ingold and Smith, J. Chem. Soc. 905 (1938).

[10] Reference 5, p. 923.

TABLE VIII.[11] *Nitration of nitrobenzene.* $\mu_{ali}=-3.29$ *(nitro-n-butane).* $\mu_{calc}=-3.63$; $\mu_{obs}=-3.81$.

	243°K		303°K		MEAN FREE ENERGIES AND CHARGE DISTRIBUTION	
	%	$\frac{(\epsilon_y-\epsilon_m)\epsilon_n}{rD}$ (CAL./MOLE)	%	$\frac{(\epsilon_y-\epsilon_m)\epsilon_n}{rD}$ (CAL./MOLE)	$\frac{(\epsilon_y-\epsilon_m)\epsilon_n}{rD}$ (CAL./MOLE)	$\epsilon_y\cdot10^{10}$ (E.S.U.)
o	6.4	1287	8.2	1443	1365	(0.223)
m	93.2		91.1			0.191
p	0.25	2514	0.7	2438	2476	0.248
1						0.105
X						−1.23

whole charge distribution in a molecule. The following results were obtained by this procedure. (When there is no datum for the tertiary compound, the value for a compound which has a structure as similar as possible to the latter is used.) In Tables VIII–XIII,[11–14] the charges in the ortho-positions were calculated by Eq. (7).

In these cases also, the calculated dipole moments accord very well with the observed values.

We applied this method to the calculation of the dipole moments of ethylbenzoate using $\mu_{ali}=-1.78$ for ethylbutyrate and the ortho-, meta- and para-percentages in Table III. The charges (ϵ_0), ϵ_m, ϵ_p, ϵ_1 and ϵ_x are (0.114), 0.101, 0.131, 0.0562 and −0.653, respectively, and $\mu_{cal}=-1.98$. Considering this excellent agreement between the calculated and observed moment ($\mu_{obs}=-1.91$), the explanation concerning the discrepancy between the latter and the calculated moment from the rate data alone is apparently valid.

[11] Holleman and Buryn, Rec. trav. chim. **19**, 79 (1900).
[12] Holleman, Rec. trav. chim. **18**, 265 (1899).
[13] Holleman, *Direkte einfuhrung von Substituenten in der Benzolkernen* (1910), p. 125.
[14] Holleman, Vermeulen and de Mooy, Rec. trav. chim. **33**, 1 (1914).

4. REFINEMENT OF THE THEORY

In the above calculations, we assumed $\epsilon_0=\epsilon_p$. But actually because the charge in the ortho-position is in closer proximity to the charge ϵ_1 on the substituted carbon, the corresponding structure will occur to a somewhat different extent than does the para-structure. The quantum-mechanical consideration of this will be given later, when the theory of the charge distribution in the molecule of substituted benzene, will be discussed.[15] Here we shall use the empirical formula

$$(\epsilon_0)=\epsilon_p+\frac{\epsilon_1-\epsilon_p}{15} \tag{9}$$

or

$$(\epsilon_o)=\epsilon_p+\frac{\epsilon_1-\epsilon_m}{8}, \tag{9'}$$

to correct the charges on the orthocarbon atoms of the molecule, when it is necessary to obtain the actual charges (ϵ_0) on the orthocarbons from the charges ϵ_p. (Both Eqs. (9) and (9′) work almost equally well. We will consider which is

[15] Wheland and Pauling, J. Am. Chem. Soc. **57**, 2086 (1935); E. Hückel, Zeits. f. Physik **72**, 310 (1931); E. Hückel and W. Hückel, Nature **129**, 937 (1932); E. Hückel, Zeits f. physik. Chemie **B35**, 163 (1937).

TABLE X.[13] *Nitration of methylbenzoate.* $\mu_{ali}=-1.65$ *(methylvalerate).* $\mu_{calc}=-1.83$; $\mu_{obs}=-1.86$.

	243°K		303°K		MEAN FREE ENERGIES AND CHARGE DISTRIBUTION	
	%	$\frac{(\epsilon_y-\epsilon_m)\epsilon_n}{rD}$ (CAL./MOLE)	%	$\frac{(\epsilon_y-\epsilon_m)\epsilon_n}{rD}$ (CAL./MOLE)	$\frac{(\epsilon_y-\epsilon_m)\epsilon_n}{rD}$ (CAL./MOLE)	$\epsilon_y\cdot10^{10}$ (E.S.U.)
o	23.6	552	25.7	599	576	(0.1062)
m	74.4		69.8			0.0929
p	2.0	1405	4.5	1227	1316	0.123
1						0.0473
X						0.603

TABLE IX.[12] *Nitration of benzoic acid.* $\mu_{ali}=-0.73$ *(butyric acid).* $\mu_{calc}=-1.02$; $\mu_{obs}=-1.0$.

	243°K		273°K		303°K		MEAN FREE ENERGIES AND CHARGE DISTRIBUTION	
	%	$\frac{(\epsilon_y-\epsilon_m)\epsilon_n}{rD}$ (CAL./MOLE)	%	$\frac{(\epsilon_y-\epsilon_m)\epsilon_n}{rD}$ (CAL./MOLE)	%	$\frac{(\epsilon_y-\epsilon_m)\epsilon_n}{rD}$ (CAL./MOLE)	$\frac{(\epsilon_y-\epsilon_m)\epsilon_n}{rD}$ (CAL./MOLE)	$\epsilon_y\cdot10^{10}$ (E.S.U.)
o	14.4	855	18.8	784	22.3	738	792	(0.0594)
m	85.0		80.2		76.5			0.0411
p	0.6	2049	1.3	1852	1.2	2074	1992	0.0871
1								−0.0342
X								−0.316

TABLE XI.[14] *Nitration of benzylchloride.* $\mu_{ali} = -1.98$ (*1-chloro-2-methylpropane*). $\mu_{calc} = -1.69$; $\mu_{obs} = -1.82$.

298°K			
	%	$\frac{(\epsilon_y - \epsilon_m)\epsilon_n}{rD}$ (CAL./MOLE)	$\epsilon_y \cdot 10^{10}$ (E.S.U.)
o	40.9	1342	(0.083)
m	4.2		0.114
p	54.9	−1924	0.070
1			0.180
X			−0.617

TABLE XII.[14] *Nitration of benzalchloride.* $\mu_{ali} = -2.06$ (*1,1-dichloropropane*). $\mu_{calc} = -1.95$; $\mu_{obs} = -2.04$.

298°K			
	%	$\frac{(\epsilon_y - \epsilon_m)\epsilon_n}{rD}$ (CAL./MOLE)	$\epsilon_y \cdot 10^{10}$ (E.S.U.)
o	23.3	220	(0.122)
m	33.8		0.117
p	42.9	−549	0.104
1			0.136
X			−0.683

TABLE XIII.[14] *Nitration of phenylchloroform.* $\mu_{ali} = -1.54$ (*methychloroform*). $\mu_{calc} = -1.48$; $\mu_{obs} = -2.11$. (*This value is lower than the observed value, probably because of the lack of a satisfactory value for* μ_{ali}.)

298°K			
	%	$\frac{(\epsilon_y - \epsilon_m)\epsilon_n}{rD}$ (CAL./MOLE)	$\epsilon_y \cdot 10^{10}$ (E.S.U.)
o	6.8	1328	(0.118)
m	64.5		0.0876
p	28.7	−68.7	0.0892
1			0.0900
X			−0.524

best from a theoretical point of view at a later date.)

We assume the difference in charge between ϵ_p and (ϵ_0) accumulates on the substituted carbon 1 and substituting group X equally, according to our assumption (4) made in the model for the activated complex. Then the corrected charges on these two atoms will be given by the following equations:

$$\left.\begin{aligned}(\epsilon_1) &= \epsilon_1 + \epsilon_p - (\epsilon_0),\\ (\epsilon_x) &= \epsilon_x + \epsilon_p - (\epsilon_0).\end{aligned}\right\} \qquad (10)$$

Here, parentheses around the symbol for charge indicate the charge has been corrected in the way which follows from Eqs. (9) or (9′) and (10). The corrected moments together with (ϵ_0),* (ϵ_1) and (ϵ_x) are given in Table XIV.

From Table XIV, it will be concluded that this correction often makes the calculated dipole moments slightly worse. The difference is usually of the order of 5 percent, and consequently it does not affect significantly our previous conclusions. A slight change in the value 1.6A for the distance between NO_2^+ and the carbon being substituted would reduce the discrepancy between the calculated and observed dipole moments.

Because the use of the refined theory to calculate the "refined" dipole moments does not improve them but, if anything, makes them slightly worse, it is interesting to note that one can assume the "approximate" calculation of dipole moments is correct. In this case one interprets the difference between the ortho- and para-percentages not as due to different charges at these positions but as due to the difference in charge in the two neighboring positions. Thus a para-position is flanked by two meta-positions while an ortho-position is flanked by a meta-position on one side and ϵ_1 on the other. If the distance, r', from the charge ϵ_1 to the substituting group and D', the effective dielectric constant, satisfies the equation $r'D' = 8 \times 1.6$, then the free energy of activation in the ortho-position will differ from that in the para-position by the amount, $(\epsilon_1 - \epsilon_m)\epsilon_n/(8 \times 1.6)$, or we can say that the apparent charge in the ortho-position is given by Eq. (9′). Actually this interpretation leaves us with our original "approximate" dipole moments. One can, however, only justify neglecting the effect of the larger charge on the original substituent in the benzene on the basis of a larger effective dielectric constant and a somewhat greater distance. This assumption that the flanking charges contribute in an important way to the free energy of activation would necessitate other obvious changes in the calculation of the dipole moments. The results are in less satisfactory agreement with experiment, so that we prefer the assumption that there is a different charge in the ortho- and para-position.

* The charges (ϵ_0) in Table XIV are the values obtained from rates, and not the values obtained by Eq. (9) or (9′).

TABLE XIV.

	$C_6H_5CH_3$	$C_6H_5COOC_2H_5$	C_6H_5Cl	C_6H_5Br	C_6H_5I	C_6H_5F
$(\epsilon_0)\cdot 10^{10}$	−0.0491	0.0772	0.0474	0.0446	0.0194	0.0363
$(\epsilon_1)\cdot 10^{10}$	0.0437	0.0376	0.227	0.230	0.205	0.148
$(\epsilon_x)\cdot 10^{10}$	0.133	−0.412	−0.578	−0.582	−0.432	−0.506
μ_{refined}	0.46	−1.25	−1.62	−1.74	−1.33	−1.34
μ_{obs}	0.44	−1.91	−1.56	−1.53	−1.30	−1.45
μ_{approx}	0.48	−1.31	−1.54	−1.68	−1.27	−1.20
	$C_6H_5NO_2$	C_6H_5COOH	$C_6H_5COOCH_3$	$C_6H_5CH_2Cl$	$C_6H_5CHCl_2$	$C_6H_5CCl_3$
$(\epsilon_0)\cdot 10^{10}$	0.223	0.0594	0.106	0.083	0.122	0.118
$(\epsilon_1)\cdot 10^{10}$	0.130	−0.0065	0.0643	0.163	0.118	0.0610
$(\epsilon_x)\cdot 10^{10}$	−1.20	−0.288	−0.586	−0.630	−0.701	−0.553
μ_{refined}	−3.50	−0.910	−1.76	−1.76	−2.03	−1.64
μ_{obs}	−3.81	−1.00	−1.86	−1.82	−2.04	−2.11
μ_{approx}	−3.63	−1.02	−1.83	−1.69	−1.95	−1.48

5. Calculation of Ortho-, Meta- and Para-Percentages of Nitrated Products from Dipole Moments Alone

From the above results, it is clear that there is the possibility of calculation of ortho-, meta- and para-percentages of nitrated products from the dipole moments of aromatic and aliphatic compounds. To do this, the authors assumed that $\mu_{\text{aro}}-\mu_{\text{ali}}$ is equal to the resonance part of μ_{aro}, i.e.,

$$\mu_{\text{aro}}-\mu_{\text{ali}}=-\tfrac{3}{2}(\epsilon_p-\epsilon_m)(r_x+2r_b). \qquad (11)$$

Eq. (11) is easily obtained from the charge distribution in Fig. 2. Combining (11) and (8), we can calculate ϵ_m and ϵ_p, consequently, the whole charge distribution in a molecule follows from a knowledge of μ_{ali} and μ_{aro}. However, it must be kept in mind that in this case the charge (ϵ_0) on the ortho-atom must be used, which is obtained from (9) or (9′). Introducing the charges (ϵ_0), ϵ_m and ϵ_p in Eqs. (6) and (7), the fractions χ_0, χ_m and χ_p are calculated. In the following, the results are given together with μ_{ali} and $\mu_{\text{aro}}-\mu_{\text{ali}}$ used in the calculation.*

From the above results, it can be understood that the agreement between the calculated and observed percentages is quite good considering that there is a considerable percentage of error in $\mu_{\text{aro}}-\mu_{\text{ali}}$, due to its small value. Especially, in the case of nitrobenzene, the ortho-percentage is smaller than the para-percentage in the calculation, while the opposite is true experimentally. This is, of course, due to the error in $\mu_{\text{aro}}-\mu_{\text{ali}}$ in this case. We did not try this calculation in the other cases, partly because of the lack of the values of μ_{ali} as in the cases of fluorobenzene and toluene, and partly because of the small values of $\mu_{\text{aro}}-\mu_{\text{ali}}$, which are between 0.1–0.2, and consequently contain large percentage errors.

It is noteworthy here that the ϵ_m's of the chloro-, bromo- and iodobenzene in Tables XV, XVI and XVII accord very well with those given in Tables IV, V and VI, respectively, which were calculated making the assumption that the percentages of meta-nitrated products of these compounds is in all cases 0.2 percent. This agreement indicates this assumption is not unreasonable.

6. Discussion

We have shown above that the correct dipole moments of substituted benzenes can be calculated from the ortho-, meta- and para-percentages of the substituents after nitration, and that conversely the latter can be calculated from the dipole moments alone. This agreement shows the substantial correctness of our assumptions. However, we will now discuss them in more detail.

Benford and Ingold[16] studied kinetically the nitration of benzene and substituted benzenes in CH_3NO_2 solution, and found that this reaction is zero order. They explained this fact by the assumption that the rate determining step is (b)

* The charges (ϵ_0) in the following tables were obtained using Eq. (9).

[16] Benford and Ingold, J. Chem. Soc. 929 (1938).

TABLE XV. *Nitration of chlorobenzene.* $\mu_{ali}=-2.15$ *(tertiary chlorobutane).* $\mu_{aro}-\mu_{ali}=0.59$.

	$\epsilon_y\cdot10^{10}$	$\frac{(\epsilon_y-\epsilon_m)\epsilon_n}{rD}$ (CAL./MOLE)	273°K		298°K	
			$(\%)_{CALC}$	$(\%)_{OBS}$	$(\%)_{CALC}$	$(\%)_{OBS}$
o	(0.0429)	−3160	37.4	28.2	39.8	31.0
m	0.116		0.1		0.2	
p	0.0282	−3810	62.5	71.8	60.0	69.0
1	0.248					
X	−0.564					

TABLE XVI. *Nitration of bromobenzene.* $\mu_{ali}=-2.15$ *(tertiary bromobutane).* $\mu_{aro}-\mu_{ali}=0.62$.

	$\epsilon_y\cdot10^{10}$	$\frac{(\epsilon_y-\epsilon_m)\epsilon_n}{rD}$ (CAL./MOLE)	273°K		298°K	
			$(\%)_{CALC}$	$(\%)_{OBS}$	$(\%)_{CALC}$	$(\%)_{OBS}$
o	(0.0389)	−3203	37.4	39.0	39.8	41.4
m	0.113		0.1		0.2	
p	0.0240	−3853	62.5	61.0	60.0	58.6
1	0.247					
X	−0.544					

TABLE XVII. *Nitration of iodobenzene.* $\mu_{ali}=-1.95$.* $\mu_{aro}-\mu_{ali}=0.65$.

	$\epsilon_y\cdot10^{10}$	$\frac{(\epsilon_y-\epsilon_m)\epsilon_n}{rD}$ (CAL./MOLE)	273°K		298°K	
			$(\%)_{CALC}$	$(\%)_{OBS}$	$(\%)_{CALC}$	$(\%)_{OBS}$
o	(0.0199)	−3229	37.7	41.7	40.0	43.7
m	0.0945		0.1		0.2	
p	0.0050	−3874	62.2	58.3	59.8	56.3
1	0.229					
X	−0.433					

* The dipole moment of tertiary iodobutane is −2.13, and the dipole moment of phenyliodide is −1.30, so $\mu_{aro}-\mu_{ali}=0.83$. If we calculate the charges ϵ_m and ϵ_p of C_6H_5I, using this μ_{ali}, and $\mu_{aro}-\mu_{ali}$, then ϵ_p becomes negative. This is in disagreement with the experimental fact, because we know that the nitration of iodobenzene is slower than that of benzene. Because of the uncertainty of the dipole moment of tertiary butyl iodide, we used −1.95 for μ_{ali}, which is the mean value of the dipoles moments of the latter and that of 1-iodobutane ($\mu=-1.76$).

TABLE XVIII. *Nitration of nitrobenzene.* $\mu_{ali}=-3.29$ *(nitro-n-butane).* $\mu_{aro}-\mu_{ali}=-0.52$.

	$\epsilon_y\cdot10^{10}$	$\frac{(\epsilon_y-\epsilon_m)\epsilon_n}{rD}$ (CAL./MOLE)	273°K		298°K	
			$(\%)_{CALC}$	$(\%)_{OBS}$	$(\%)_{CALC}$	$(\%)_{OBS}$
o	(0.260)	2944	0.4	6.4	0.7	7.9
m	0.192		96.0	93.4	94.7	91.6
p	0.274	3550	3.6	0.2	4.6	0.5
1	0.069					
X	−1.28					

in the following series of reactions:

$$CH_3NO_2\rightarrow CH_2:NO\cdot OH, \quad (a)$$

$$CH_2:NO\cdot OH+HO\cdot NO_2\rightarrow CH_2:NO\cdot O\cdot NO_2+H_2O, \quad (b)$$

$$CH_2:NO\cdot O\cdot NO_2+C_6H_6\rightarrow C_6H_5\cdot NO_2+CH_2:NO\cdot OH. \quad (c)$$

They concluded also qualitatively, having studied solvent effects upon the nitration, that the efficiency of the nitrating agents $X\cdot NO_2$ ($X=CH_2:NO\cdot O-$ in the above case) depends upon the electron affinities of the X groups for the electrons of the bonds $X-NO_2$, as indicated, for instance, by acid strength of X·H. Thus

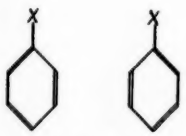

FIG. 3.

Kékulé structures

$SO_4H \cdot NO_2$ is more reactive than $CH_3CO \cdot O \cdot NO_2$, and the latter is more reactive than $HO \cdot NO_2$.

Basing our results on these experimental facts, we assumed that $X \cdot NO_2$ dissociates into X^- and NO_2^+ in the activated complex (assumption (1)), and that the latter acts on the charge ϵ_y of the reacting carbon atoms, reducing the activation free energy by the amount of the electrostatic interaction, $\epsilon_y \epsilon_n/(rD)$ (assumption (5)). These assumptions, therefore, seem reasonable *a priori*. However, some remarks must be made on the values of r and D, which were taken as 1.6A and unity, respectively, in our calculations.

Calculations of potential surfaces for activated complexes indicate that those atomic distances which are changing are often around 10 percent larger than the normal distances. Therefore we have chosen 1.6A for the distance $C-NO_2^+$ in the activated complex, since the normal distance $C-NO_2$ is 1.46A. Our justification for taking D constant and independent of solvents has already been given, i.e., the constancy of ortho-, meta- and para-percentages regardless of the reacting media. In general, the macroscopic dielectric constants measured by the usual experimental method have no meaning for phenomena occurring at atomic distances, since most of the interatomic lines of force do not pass through the solvent. Actually, Debye[17] takes D equal to 2 or 3 independent of solvent when he discusses phenomena at molecular distances. In our case, moreover, there is no solvent molecule between the reacting carbon and NO_2^+ in the activated complex. Therefore, it is reasonable to take D equal to unity. The agreement between the moments calculated and observed shows these values are highly satisfactory. Interactions between non-neighboring atoms will be smaller both because of the distance and because of the dielectric constant and in this approximation are neglected.

[17] Debye, *Dipolmoment und chemische Struktur* (Leipzig, 1929); *Polar Molecules* (1929).

Thus we can conclude from the agreement between the experiments and our results that nitration is an ionic process, since these calculations rest on assumption (1) and (5). We have also found that organic reactions such as esterification, saponification (hydrolysis), benzoylation, and quaternary salt formation can be treated in the same way from the study of side chain reactivities. This material will be presented for publication soon. Thus all these reactions are ionic as organic chemists usually assume. That there is a close correlation between the reactions considered here and many other processes is shown for example by the interesting results of Hammett.[18] Interesting but quite different treatments of these questions are also to be found in the recent reports of Jenkins[19] and of Westheimer and Shookhoff.[20]

We assume the same inductive effect on the six carbon atoms of the benzene nucleus (assumption (3)). This is based on findings that can be discussed in sufficient detail only in a subsequent paper. However, a double bond in a side chain of benzene ring acts as a conductor as shown by the induction of charge from the ring on atoms in the side chains. By resonance with the two Kékulé bond structures in Fig. 3, all the C−C bonds partake of the nature of double bonds as is evidenced by the fact that the length of a C−C bond in benzene is longer than that of an aliphatic C=C bond, but shorter than that of an aliphatic C−C bond. For this reason we assume the benzene ring acts as a conductor in the induction, i.e., the charges ϵ_i produced by induction on each of the six carbon atoms are equal to each other. We assumed further as a first approximation that the same charges ϵ_r accumulate on each of the two ortho- and one para-atoms by resonance. The approximate correctness of this assumption has already been discussed, as well as a refinement of this simple assumption. Although this refinement does not effect significantly the calculation of dipole moments from rates, it is important in the converse calculation, i.e., in the calculation of

[18] Hammett, J. Am. Chem. Soc. **59**, 96 (1937); Trans. Faraday Soc. **34**, 156 (1938).

[19] Jenkins, J. Chem. Soc. 1780 (1939).

[20] Westheimer and Shookhoff, J. Am. Chem. Soc. **62**, 269 (1940).

TABLE XIX.

Charge \ Substituents	F	Cl	Br	I
$\epsilon_m \cdot 10^{10}$	0.0933 (*n*)*	0.115 (*n*)	0.116 (*n*)	0.0909 (*n*)
$(\epsilon_p - \epsilon_m) \cdot 10^{10}$	−0.090 (*n*)	−0.088 (*n*)	−0.085 (*n*)	−0.084 (*n*)
Charge \ Substituents	COOH	$COOCH_3$	$COOC_2H_5$	NO_2
$\epsilon_m \cdot 10^{10}$	0.0411 (*m*)*	0.0929 (*m*)	0.0649 (*n*)	0.191 (*m*)
$(\epsilon_p - \epsilon_m) \cdot 10^{10}$	0.0460 (*n*)	0.0300 (*n*)	0.0301 (*n*)	0.057 (*n*)
Charge \ Substituents	CH_3	CH_2Cl	$CHCl_2$	CCl_3
$\epsilon_m \cdot 10^{10}$	−0.0128 (*n*)	0.114 (*m*)	0.117 (*m*)	0.0876 (*m*)
$(\epsilon_p - \epsilon_m) \cdot 10^{10}$	−0.0404 (*n*)	−0.044 (*n*)	−0.013 (*n*)	0.0016 (*n*)

* Here (*n*) and (*m*) represent the values obtained from the nitration and the dipole moments, respectively.

ortho-, meta- and para-percentages from dipole moments alone.

It is not likely that our simple rules for charge distribution in terms of ϵ_m and ϵ_p will remain unchanged as we accumulate more experimental evidence and improve the theory. However, in their present unfinished form these rules are surprisingly successful.

We collect the values of ϵ_m and $\epsilon_p - \epsilon_m$ in Table XIX. Here, as stated above, ϵ_m represents the charge induced on each of the carbon atoms of the benzene nucleus, and $\epsilon_p - \epsilon_m$ represents the charge accumulated on one of the ortho- or para-carbons by the resonance effect.

ϵ_m and $\epsilon_p - \epsilon_m$ in Table XIX, therefore, give the inductive and resonance effects in the substituted benzenes both as regards direction and magnitude. Thus toluene is the only compound in Table XIX which accumulates negative charge in the benzene ring both by the inductive and resonance effects, and it has the greatest reactivity for nitration.

(Here the negative signs in this table show the charges are negative; they must not be confused with the usual positive and negative notations indicating the directions of the inductive and resonance effects, since positive induction, for example, means that negative charge is induced in the benzene nucleus as in toluene, and vice versa. Thus in halobenzenes, the inductions are negative, and resonance positive, while in COOH, $COOCH_3$, $COOC_2H_5$ and NO_2 groups they are both negative.)

It is very interesting to notice that $\epsilon_p - \epsilon_m < 0$ in the case of ortho- and para-orienting groups, and $\epsilon_p - \epsilon_m > 0$ in the case of meta-orienting groups. These relations show clearly that the former groups make the electron densities on ortho- and para-atoms greater than those on meta-atoms, while the latter act in the opposite way. Thus, we can see that the usual explanation on the orienting power of substituents is reasonable, being established by the quantitative evidence given above. Our theory, however, goes beyond such qualitative pictures to a definite model which permits us to calculate quantitative results.

Far Ultraviolet Absorption Spectra of Some Aliphatic Ketones

A. B. F. DUNCAN
Department of Chemistry, University of Rochester, Rochester, New York
(Received March 13, 1940)

Absorption spectra of methyl *n*-propyl, methyl isopropyl and diethyl ketones between 2000 and 1500A were found. The electronic transitions and their vibrational structure are discussed in comparison with acetone and methyl ethyl ketone. It is concluded that most transitions are probably of a Rydberg type, leading to ionization potentials in the neighborhood of 10 ev.

THE absorption spectra of acetone and methyl ethyl ketone in the Schumann region have been studied in some detail,[1] but spectra of the higher ketones have not been reported. It should be expected that the general features of the spectra in this region would be the same for all ketones, but it seemed of interest to study some of the details of the spectra of diethyl, methyl isopropyl and methyl *n*-propyl ketones. The vibration frequencies[2] in the normal electronic state, as well as other physical constants remain remarkably constant as we go from acetone to these ketones.

Apparatus and Experimental Procedure

The first plates were taken in a one-meter spectrograph at Brown University.[1a] The source was the usual Lyman continuum, and the ketone vapors in the spectrograph were separated from the light source only by the narrow slit. In this way the wave-length region from 2200 to 800 was covered. The pressure of the vapors was very uncertain and varied during an exposure, due probably to absorption by the wax gaskets of the spectrograph. This resulted in loss of definition in the vibrational structure.

The final plates were made with a normal incidence vacuum spectrograph built here recently by the writer. It contains a 2-meter radius 120,000-line grating, ruled on glass by R. W. Wood. The dispersion in the first-order ultraviolet is about 4.145A/mm. The light source was an uncondensed discharge in hydrogen operated usually with 1 amp. at 4000 volts. Exposure times were 20–30 minutes with Eastman III–O ultraviolet sensitive plates. In most cases a fused quartz absorption cell 20 cm long was used between source and slit. The plane polished windows which were fused on transmitted to 1560A. In other cases (especially with diethyl ketone) the 4-meter column of the spectrograph tube was used. To avoid possible decomposition products during exposure the vapor could be passed through the cell in a current of pure nitrogen at different fixed rates. Pressures were fixed by immersion of the liquid ketone in a CO_2-ether hand-regulated thermostat or in ice-salt mixtures in which the nitrogen was also precooled. The actual vapor pressures were measured, and the useful ranges were 0.3–2.5 mm for the cell and 0.0025–0.5 for the longer columns. These ranges were covered systematically with a large number of exposures.

The ketones, obtained from Eastman Kodak, all gave tests for acids, oxidizing agents (with $Fe^{++}+CNS^-$), and biacetyl. A negative chemical test showed that the latter could not have a partial pressure greater than 2×10^{-5} mm, but the four strongest bands[3] were found on the first plates. The ketones were washed with dilute $NaHSO_3$ and Na_2CO_3 solutions, then with many small portions of water. After drying they were fractionated in a current of nitrogen. All samples used boiled within 0.2° of the reported boiling point and showed none of the above impurity. While biacetyl is probably exceptional in its large absorption coefficient in this region, this shows that experimental data on the spectra of organic compounds must be examined rather critically.

Lines of NI at 1745.246 and 1742.734A

[1] (a) Noyes, Duncan and Manning, J. Chem. Phys. **2**, 717 (1934). (b) A. B. F. Duncan, J. Chem. Phys. **3**, 131 (1935). (c) Duncan, Ells and Noyes, J. Am. Chem. Soc. **58**, 1454 (1936).
[2] Kohlrausch and Koppl, Zeits. f. physik. Chemie **B24**, 370 (1934).
[3] V. R. Ells, J. Am. Chem. Soc. **60**, 1864 (1938).

appeared on most plates and were used as primary standards. In addition SiI 1989.01 and CI 1930.900 [4] appeared on all plates. From these a few additional lines of silicon were identified.

Results

Although photographs were made down to 800A for the three ketones over considerable range of pressure, nothing but general absorption could be found below 1500A. Not even maxima which might be correlated with high electronic terms were apparent. Between 1500 and 2000A three well-marked transitions were found except for diethyl ketone, for which the second (expected at about 1720A) is unaccountably missing. The longer wave-length transition of this ketone is also unaccompanied by vibrational structure, in contrast to all other ketones studied.

Before discussing the spectra of these ketones, the spectrum of acetone must be mentioned, since the more numerous electronic energy levels are more clearly marked and serve as a basis for comparison with the higher ketones. Reconsideration of the results published in 1934[1b] still does not explain all the details; to do this, probably additional experiments with the higher dispersion available here are necessary and are planned. But some features not stressed in this earlier paper should be mentioned. (1) The most prominent feature of the spectrum as a whole is the Rydberg series reported leading to an ionization potential of 10.20 ev (using more recent values of the fundamental constants). If the Rydberg denominator is written $(n+0.505)$ instead of $(n-0.495)$ retaining $\nu_\infty = 82{,}767$ we get for $n=1$ the value 34,318 cm^{-1}. The maximum in the near ultraviolet absorption is at 35,400 ($\pm$ about 700) cm^{-1}. The intensity for $n=2$ is about 10^3 times the intensity of $n=1$, but there may be an explanation for this not included in recent theory. (2) The second most prominent features in the far ultraviolet, appearing at pressures only slightly greater than this Rydberg series, are the band systems beginning at 51,171 and 69,300. These have similar vibrational structure though that of the former is much more elaborate. Also the vibrational structure in the region 72,000–78,000 is complicated and probably

[4] Boyce and Robinson, J. Opt. Soc. Am. **26**, 133 (1936).

Table I. *Electronic term values* ($\nu_\infty - \nu$ *in* cm^{-1}).

Oxygen (atom)		Acetone	Formaldehyde
36,069	$3s(^5S)$	(46,367)	—
33,043	$3s(^3S)$	31,601	—
14,358	$4s(^5S)$	17,554	23,440
13,612	$4s(^3S)$	13,456	16,230
7721	$5s(^5S)$	8933	10,040
7425	$5s(^3S)$	7396	8410
4818	$6s(^5S)$	5407	5960
4671	$6s(^3S)$	—	5110

associated with more than one electronic transition. The result is that a second series can be proposed (which was found in 1934 but rejected because of intensity anomalies): $\nu = 82{,}772 - R/(1+0.865)^2$, $n=1, 2, 3, \cdots$. Calculated values for $n=1, 2, 3, 4$ are 51,171, 69,353, 75,376 and 78,085. Observed values are 51,171, 69,316, and 75,376. Objections to the series are (a) failure to observe 78,085 while bands at 77,646 and 77,483 are observed and (b) 69,316 is less intense than 75,376 or 51,171. In favor of this second series is the obvious mathematical fit (perhaps an objection) and the fact that Price[5] observed two series in formaldehyde converging to the same ionization potential.

If the two series are real (including $n=1$ of the first series), it is possible to explain by Rydberg transitions all the electronic transitions of acetone except the weak absorption between 60,000 and 69,000 (two electronic transitions with complicated vibrational structure about 10^{-3} as strong as the other absorption below 51,000) and a strong band appearing at low pressures at 72,529. If all the Rydberg transitions are of the type $2p_0 \rightarrow ns$, involving practically atomic orbitals, we may expect a very rough agreement with term values in oxygen. Table I shows these values[6] and the results of Price in the same range of n values. These values are obtained by subtracting the origins of the

Table II. *Electronic transitions of the ketones* (cm^{-1}).

	I	II	III	IV
Acetone	36,400	51,171	60,086	65,213
Methyl ethyl	36,100	50,634	58,110	63,525
Methyl *n*-propyl	35,840	50,699	58,200	63,500
Methyl isopropyl	35,460	50,460	57,566	63,030
Diethyl	35,970	50,700	—	63,300

[5] W. C. Price, J. Chem. Phys. **3**, 256 (1935).
[6] Bacher and Goudsmit, *Atomic Energy States* (1932).

TABLE III. *Vibrational transitions of the ketones.*

METHYL ETHYL		METHYL ISOPROPYL		METHYL *n*-PROPYL	
50,634	ν_0	50,460	ν_0	50,699	ν_0
50,857	$\nu_0+\omega_6$				
51,209	$\nu_0+\omega_4$	50,836	$\nu_0+\omega_4$	51,313	$\nu_0+\omega_4$
51,915	$\nu_0+\omega_1$	51,791	$\nu_0+\omega_1$	51,889	$\nu_0+\omega_1$
53,119	$\nu_0+2\omega_1$	51,279	$\nu_0+\omega_2$		
52,426	$\nu_0+\omega_1+\omega_4$	52,099	$\nu_0+2\omega_2$		
$\omega_1=1281$		$\omega_1=1231$		$\omega_1=1190$	
$\omega_4=$ 575		$\omega_4=$ 388		$\omega_4=$ 614	
$\omega_6=$ 220		$\omega_2=$ 819			

electronic transitions from the spectroscopic ionization potential I for formaldehyde and acetone. The agreement in order of magnitude lends some support to the idea that of these transitions (except possibly 36,400 cm^{-1} in acetone) are really Rydberg transitions of the above mentioned type.

The observed transitions of the other ketones are shown in Table II, where corresponding values for acetone and methyl ethyl ketone are included. Transitions number I, in the near ultraviolet, were measured in the liquid state in most cases, where only maxima occur. These values are quite uncertain while measurements for transitions II, III and IV have at most an uncertainty of about 20 cm^{-1}. The shift toward longer wave-lengths of the absorption maximum which occurs when the hydrogens of acetone are substituted by simple radicals has been discussed for transitions I.[7] The shifts in the other transitions are to be associated with changes in the pure electronic terms as a consequence of change in structure.

In all of the latter transitions, substitution of the first hydrogen by methyl (acetone to methyl ethyl ketone) produces the greatest shift. A further shift is produced only when an α hydrogen is substituted to give an unsymmetrical structure (methyl ethyl to methyl isopropyl). Substitution to produce a symmetrical structure (diethyl) or β substitution indeed seems to show shifts mostly in the opposite direction, but these are relatively small. It is to be noted also that shifts are larger for III and IV than for II.

A qualitative explanation of these shifts can be given[8] if it is admitted that all these transitions except III are $2p_0 \rightarrow ns$, since because of their spherical distribution the s orbitals penetrate the alkyl groups and are affected by changes in them. Shifts in IV would be greater than in II, since II are $3s$ while IV are $4s$ terms. While it is evident that shifts in III are even larger than in IV, any attempt to revise the present analysis in order to include transitions III in $2p_0 \rightarrow ns$ would cause greater intensity difficulties and necessarily exclude a transition which was 10^3 more intense. Possibilities of excitation of other electrons are obviously not excluded when the electronic structures of ketones suggested by Mulliken[9] are considered. While the ionizations potentials corresponding to the removal of $2p_0$ cannot be predicted quantitatively for these ketones, they should be only slightly less than 10.2 ev, and it might be guessed that methyl isopropyl would have the lowest.

Transition II is associated with vibrational transitions in the propyl ketones. No vibrational structure could be found for diethyl ketone, and no structure for the propyl ketones was found in III and IV. The long wave edges, which appear sharper, are given in Table III with probable assignments. The data for methyl ethyl ketone is not new, but is included for comparison. ω_1 is found in all ketones studied and is probably the carbonyl frequency. We hope to decide if this is true in acetone from proposed measurements on acetone-d_6. Little can be said about ω_4, ω_2 and ω_6 except to point out that because of their magnitude they probably represent deformation of the carbon-oxygen framework. It is perhaps stretching a point to assign C_{2v} symmetry to acetone though for normal vibrations involving little hydrogen motion it is a permissible approximation. However it is doubtful if the higher ketones possess even C_s (plane) symmetry but probably only C_1. Hence all vibrations (and overtones) should be permitted in the excited electronic states. There is little hope at present of calculating relative intensities, so we cannot say why so few vibrations actually appear or which are to be expected. But it is a striking fact that very few appear.

[7] K. L. Wolf, Zeits. f. physik. Chemie **B2**, 39 (1929).

[8] Compare the discussion of the alkyl halides by W. C. Price, J. Chem. Phys. **4**, 547 (1936), where references to discussion by R. S. Mulliken will be found.

[9] R. S. Mulliken, J. Chem. Phys. **3**, 564 (1935).

Note on the Infra-Red Absorption Spectra of the Vapors of DCOOH and DCOOD

R. C. HERMAN AND V. WILLIAMS
Palmer Physical Laboratory, Princeton University, Princeton, New Jersey
(Received February 28, 1940)

IN order to complete the set of infra-red spectra of the deuterated formic acids begun by Bonner and Hofstadter[1] (HCOOH) and Hofstadter[2] (HCOOD), the dimer and monomer spectra of the vapors of DCOOH and DCOOD have been obtained in the region 1 to 15μ. We hoped that sufficiently regular shifts in band positions would appear from one spectrum to the next so that approximate calculations would enable us to make assignments of bands whose frequencies lie below 1700 cm^{-1}.

Heavy formic acid (DCOOD) was prepared by the thermal decomposition of anhydrous deuterated oxalic acid [$(COOD)_2$] in vacuum at about 180°C. The deuterated oxalic acid was obtained by exchanging anhydrous oxalic acid (Kahlbaum) with 99.6 percent D_2O and was dehydrated by heating under vacuum. The

[1] L. G. Bonner and R. Hofstadter, J. Chem. Phys. **6**, 531 (1938).
[2] R. Hofstadter, J. Chem. Phys. **6**, 540 (1938).

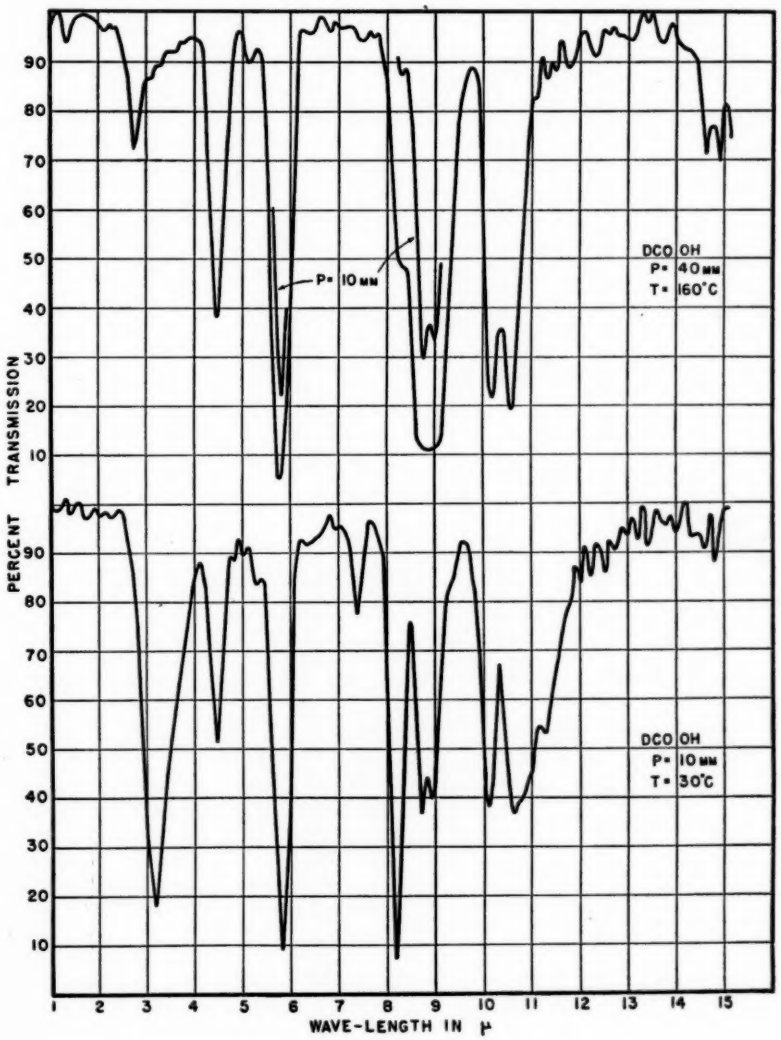

FIG. 1. Absorption spectrum of DCOOH. Cell length 22 cm.

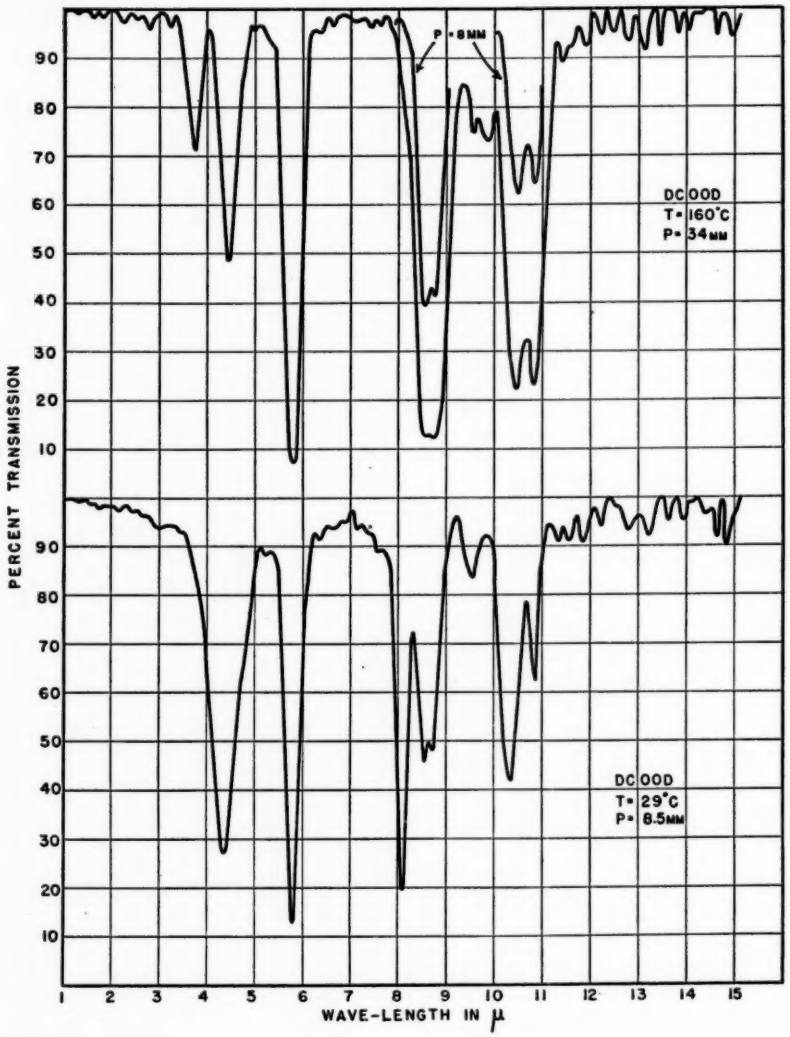

FIG. 2. Absorption spectrum of DCOOD. Cell length 22 cm.

DCOOD was purified by several vacuum distillations after pumping off the CO_2. The DCOOH was prepared by exchanging the DCOOD several times with H_2O. Anhydrous copper sulfate was used to dehydrate the acid between exchanges.

TABLE I.

DCOOD				DCOOH			
DIMER		MONOMER		DIMER		MONOMER	
2325 cm^{-1}	ν(ODO), ν(CD)	2680 cm^{-1}	ν(OD)	3175 cm^{-1}	ν(OHO)	3633 cm^{-1}	ν(OH)
1719	ν(C=O)	2265	ν(CD)	2248	ν(CD)	2250	ν(CD)
1243		1730	ν(C=O)	1730	ν(C=O)	1730	ν(C=O)
1178		1178		1358		1206	
1150		1143		1224		1146	
1052		1052		1150		1114	
974		1015		1121		982	
927		957		990		946	
		926		944*		678	
				887			

* Broad.

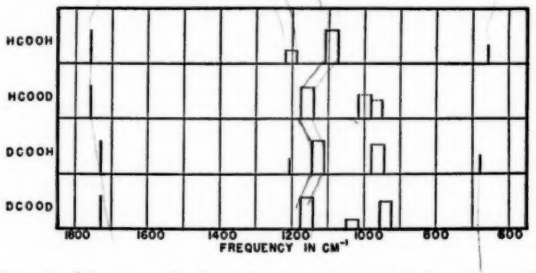

FIG. 3. Line graph for the monomers of formic acid. Heights of lines indicate intensities approximately.

A preliminary experiment was performed on the thermal decomposition of light oxalic acid in vacuum at about 180°C. The resultant HCOOH was tested for water content by comparison of vapor pressure measurements with those made by Coolidge[3] for formic acid-water mixtures. Further, the infra-red spectrum of the light acid showed no absorption band in the region of 1600 cm^{-1} where water absorbs strongly. These tests showed that there was less than 3 percent of H_2O present. The high yield of formic acid obtained substantiates the work of Wobbe and Noyes[4] on the thermal decomposition of oxalic acid. Unfortunately, it was not possible to determine the extent of the deuteration of the formic acids by means of the mass spectrograph. However, the spectra themselves indicate that the CD, OD, and OH groups are at least 95 percent pure. The experimental technique was the same as that employed in previous investigations.[5]

The monomer and dimer spectra of DCOOH and DCOOD are shown in Figs. 1 and 2. Parts of the monomer spectra of HCOOH and HCOOD were restudied and a few corrections and additions are made. In the spectrum of HCOOH ν(C=O) is found at 1760 cm^{-1}, the double band listed at 1093 has minima at 1111 and 1075 cm^{-1}, and there is also a true monomer doublet with minima at 1221 and 1190 cm^{-1}. In the monomer spectrum of HCOOD the following minima were redetermined: 1178, 1142, and 1018 cm^{-1}. Fig. 3 shows the positions of all the bands below 1800 cm^{-1} in the spectra of the four isotopic monomer forms of formic acid. Table I gives the positions and some assignments for the bands in the monomer and dimer spectra of DCOOH and DCOOD.

We are unable to give a consistent interpretation of the bands whose frequencies lie below 1700 cm^{-1}. The apparently irregular shifts that occur in the spectra upon deuterium substitution seem to indicate either accidental degeneracies or strong interactions which are different for the different molecules. The simple triatomic calculation suggested by Bonner and Hofstadter is certainly inadequate to explain the spectra.

It is interesting that practically all the bands in the monomer spectra below 1700 cm^{-1} show a doublet structure with a separation of about 34 cm^{-1} which is roughly the separation to be inferred from the spectrum of the 3ν(OH) band in formic acid at 10,203A studied by Bauer and Badger.[6] It seems difficult to understand why these bands seem to show a persistent doublet structure since any vibrational mode which has an appreciable change in dipole moment parallel to the least moment of inertia axis should exhibit a strong qQ branch. It would seem worth while to study the fundamental bands of the various formic acids under higher resolution.

We wish to express our appreciation to the Research Department of the Calco Chemical Division of American Cyanamid Company for the interest shown in this work.

[3] A. S. Coolidge, J. Am. Chem. Soc. **50**, 2166 (1928).
[4] D. E. Wobbe and W. A. Noyes, Jr., J. Am. Chem. Soc. **48**, 2856 (1926).
[5] R. C. Herman and R. Hofstadter, J. Chem. Phys. **6**, 534 (1938).
[6] S. H. Bauer and R. M. Badger, J. Chem. Phys. **5**, 852 (1937).

Effect of Electric Fields on the Decomposition of Nitrous Oxide by Alpha-Rays

A. D. KOLUMBAN AND H. ESSEX
Department of Chemistry, Syracuse University, Syracuse, New York
(Received February 16, 1940)

Ion yields expressed in molecules of gaseous products uncondensed by liquid air, per ion pair are

30°	no field	4.35
	half-saturation	4.15
	full saturation	4.61
100°	no field	4.75
	half-saturation	4.65
	full saturation	5.76.

If these results are interpreted on the assumption that ions are neutralized at the electrodes without decomposition, then it follows that in the absence of an electric field, 9 percent of the reaction, is initiated by combination of ions at 30°C, and 4 percent of the reaction is so initiated at 100°C. The increase in ion yield at high field strength is probably due to electron collisions with molecules. As this occurs at field strengths at which the current-field strength curve is horizontal, the new reaction is not initiated by ionization. Therefore, as the major part of the energy of alpha-rays remains in the primarily ejected electrons, electron collisions without ionization should initiate part of the reaction occurring in the absence of electric fields.

IN chemical reactions in the presence of ionizing radiations, it is possible to separate that portion of the reaction consequent on ion recombination from that portion of the reaction independent of ion recombination by comparing the rates of the reaction in the absence and presence of electric fields. In the presence of an electric field between metal plates, ions can be removed from the gaseous mixture before recombination takes place and neutralized upon the electrodes without decomposition. If the field strength is sufficient to produce a saturation current all of the ions are removed from the gas phase before recombination. Any reaction still taking place under such conditions must be initiated by other mechanisms than ion recombination.

In this laboratory a method has been worked out for determining the ion yield in a reaction vessel in which the number of ions produced in unit time can be measured directly by the saturation current between metal electrodes and compared with the measured rate of the reaction. This method of determining ion yield is also directly applicable to the determination of the ion yield in electric fields and has been so used in the decomposition of ammonia by alpha-rays by Smith and Essex.[1] In that reaction 40 percent of the reaction was found to be initiated by ion recombination. The same technique has now been applied to the determination of the ion yields in the presence and absence of electric fields in the decomposition of nitrous oxide.

[1] Smith and Essex, J. Chem. Phys. **6**, 188 (1938).

EXPERIMENTAL

The experimental technique of these measurements was essentially the same as that used in the decomposition of ammonia and described in considerable detail in the article cited. The nitrous oxide used was a cylinder-contained product of the Ohio Chemical Company, and stated by them to have a minimum nitrous oxide content of 99.5 percent. It was passed into the reaction system over soda lime and barium oxide to remove water and carbon dioxide and in the reaction system was separated from noncondensible gases by evacuation after freezing out in a trap with liquid air.[2] To insure complete removal of noncondensible gases, the cycle—condensation, evacuation, vaporization, condensation was repeated six times with each sample.

The reaction system is shown in Fig. 1. The cylindrical reaction vessel was provided with

[2] The liquid air used in this investigation was provided by the General Electric Company through the courtesy of Dr. L. M. Willey, to whom the authors express their gratitude.

platinum plate electrodes placed very close (2 mm) to the ends of the cylindrical vessel so that a minimum amount of ionization was produced back of the electrodes where some of the ions might escape inclusion in the saturation current. The radioactive material, mesothorium, was placed in the depression in the bottom of the tube. In one series of runs the reaction system was sealed after removal of the noncondensible gases and the reaction rate measured by the change in the residual pressure after freezing out the nitrous oxide by liquid air in trap I. The number of ions produced in unit time was determined by measuring the saturation current between the electrodes. In making the runs at no field the experiments were continued for a week or more. Saturation current measurements, and pressure measurements on the McLeod gauge after freezing out the nitrous oxide with liquid air were made initially after 24 hr., and after that, at intervals of several days each during the run. Similar technique was employed in making the measurements in a field: but for the measurements in a field except when determining the saturation current, or measuring the residual pressure, a constant potential was applied between the electrodes during the entire run. In order to prevent arcing between the electrodes and the glass walls of the reaction vessel thin copper shields were sealed to the outside of the glass ends of the reaction vessel with nitrocellulose cement in which fine silver filings were mixed. The silver filings effected electrical contact between glass and shield. The shield at the high potential end was electrically connected to the high potential lead. The shield at the low potential end was grounded and provided with a hole through which passed the lead from the electrode to the ion-current measuring galvanometer. In this way, the current through or over the glass was not included in the ion-current. The reaction vessel was enclosed in a constant temperature bath and runs were made at 30°C and 100°C. Pressures were in the neighborhood of atmospheric. Preliminary measurements showed that the error introduced due to desorption of noncondensible gas from the walls was negligible.

In a second series of runs the reaction system was connected through a mercury sealed glass

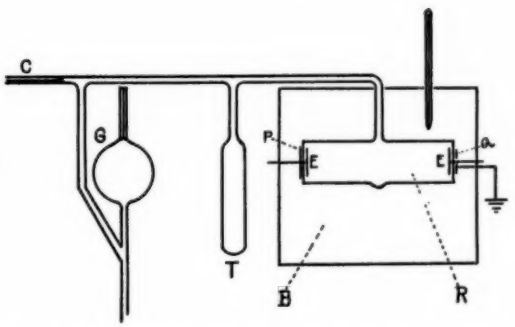

FIG. 1. *B*—Constant temperature air bath, *R*—reaction vessel, *G*—McLeod gauge, *E*—electrodes, *P*—*Q*—thin copper shields to prevent arcing, *T*—trap for condensing out nitrous oxide, *C*—capillary for sealing up system.

stopcock to a mercury vapor vacuum pump backed by an oil pump. In these runs after the residual pressure had reached a value too great to be measured by the McLeod gauge, the N_2O was frozen out in the trap by liquid air, the system evacuated by opening the stopcock, and after closing the stopcock a second run was made. No appreciable difference was observed in the experimental data obtained with the stopcock enclosed, and with the completely sealed apparatus: Therefore the data are not separated in the table of experimental results. With the stopcock enclosed system, pressures slightly greater than atmospheric, were used, to prevent leak in of gases, not condensible by liquid air. Slight outward leak of N_2O is unimportant.

The production of noncondensible gases under the conditions of these experiments, exhibited a considerable induction period lasting at least 24 hours. The current potential curves obtained across the reaction vessel became horizontal above 16,000 volts at 30°C and above 9000 volts at 100°C indicating complete removal of ions, i.e., no combination of ions in the gaseous phase.

The experimental results are presented in Table I. Ion yields are expressed in terms of moles of noncondensible gases produced per ion pair. Partly because of the small amount of decomposition occurring in such a comparatively brief time, the ion yields obtained during the first 24 hours show much greater divergence from each other than the ion yields obtained after 24 hours. In Fig. 2 the average ion yields are plotted against the ratio of the plate current to the saturation current. In Fig. 3 the ion yields

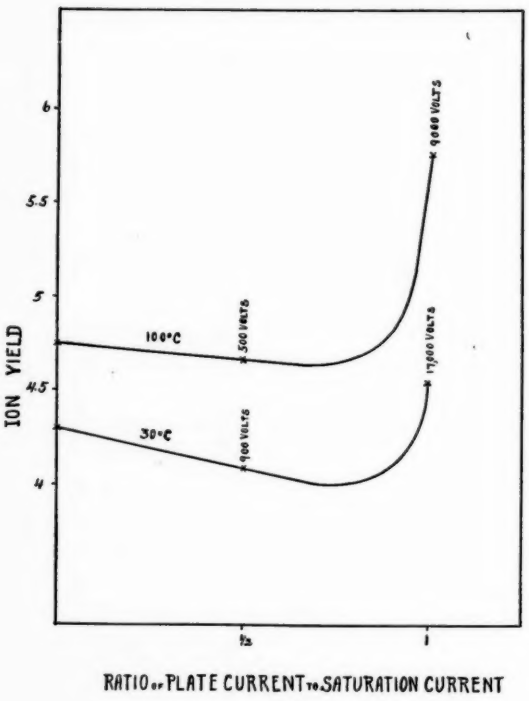

FIG. 2.

and current are plotted against the field strength. Between the experimentally determined points, the curves are given their probable form.

DISCUSSION OF RESULTS

The decomposition of N_2O by alpha-rays has been studied by Wourtzel.[3] The ion yield obtained as recalculated by Mund[4] is 2.7 at 18°C and 4.0 at 315°C.

G. R. Gedye[5] has investigated the N_2O decomposition by cathode rays and obtains an ion yield of 3.9 at 18°C.

There is general agreement among the investigators who have studied the decomposition of N_2O in the presence of alpha-rays and also in the presence of cathode rays that at a particular stage of the reaction the products are nitrogen, nitric oxide and oxygen. The balanced equation for their production is

$$4N_2O \rightarrow 3N_2 + 2NO + O_2 \qquad (1)$$
(O_2 produced partly as O).

In the experiments of other investigators in which the partial pressures of NO and O_2 were considerable, reaction may be expected to occur according to the equation $2NO + O_2 = 2NO_2$. The kinetics of this reaction have been studied by Bodenstein.[6] The reaction is termolecular and

[3] Wourtzel, Le Radium **11**, 289, 332 (1919).
[4] Mund, J. Phys. Chem. **30**, 890 (1926).
[5] Gedye, J. Chem. Soc. **2**, 3016 (1931).
[6] Bodenstein, Zeits. f. physik. Chemie **100**, 68 (1922).

TABLE I. *Ion yields at 30°C.*

Experiment Number	Length of Run in Hours	Pressure in mm	Ion Yield No Field: During First 24 Hours	Ion Yield No Field: From 24 Hours to End of Run	Experiment Number	Length of Run in Hours	Pressure in mm	Ion Yield Half-Saturation: During First 24 Hours	Ion Yield Half-Saturation: From 24 Hours to End of Run	Experiment Number	Length of Run in Hours	Pressure in mm	Ion Yield Full Saturation: During First 24 Hours	Ion Yield Full Saturation: From 24 Hours to End of Run
11	313	515	3.82	4.02	13*A*	127.5	502	3.10	4.14	12*A*	109.5	487	4.31	4.32
11*B*	236	545	3.38	4.42	13*B*-1	240.5	762	3.63	4.24	12*B*	240	764	3.91	4.90
11*C*	214	520	3.06	4.17	13*B*-2	182	760	3.69	4.08					
11*D*	217.5	526	4.53	4.45										
11*E*-1	148.5	770	4.17	4.66										
11*E*-2	244	768	3.85	4.26										
11*E*-3	241	771	3.42	4.45										
Average			3.75	4.35				3.47	4.15				4.11	4.61
					At 100°C									
14	160.5	653	4.50	4.84	15	160.75	676	3.70	4.86	16	169	665	4.52	5.82
14*A*	165	640	4.57	5.16	15*B*	148	807	3.89	4.45	16*A*	145	777	3.91	5.70
14*B*	158	836	3.60	4.56										
14*BB*	148	826	3.89	4.45										
Average			4.14	4.75				3.79	4.65				4.21	5.76

the velocity constant is so small at the temperatures of these measurements, that appreciable combination is not possible at the very low partial pressures of NO and O_2 reached in these experiments. On the other hand, part of the oxygen must originally be produced as atoms and some of these atoms of oxygen may react with NO to give NO_2. Other oxygen atoms will react with each other to give O_2. From the NO_2 produced in this way the following subsequent reactions may be expected to occur

$$2NO_2+2Hg=2HgNO_2(s), \qquad (2)$$

$$2HgNO_2(s)=2HgO+2NO \qquad (3)$$

as in the photochemical decomposition of N_2O.[7]

$HgNO_2$ is a solid and its decomposition is very slow accounting for the induction period observed in our experiments. From the initial and final ion yields (in moles of noncondensible gases formed per ion pair) it is possible to estimate the ion yield in moles of N_2O decomposed per ion pair for comparison of these results with those of Mund.[4] It is apparent from the Eqs. (1), (2) and (3) that if X is the number of moles of NO which react with O to give NO_2, the number of moles of noncondensible gas formed from 4 moles of N_2O in the initial stages of the reaction is

$$3+2-x+1-\frac{x}{2}=6-\frac{3x}{2}$$

and the number of moles of noncondensible gas formed from 4 moles of N_2O after the stationary state or "radioactive" equilibrium is established is

$$3+2+1-\frac{x}{2}=6-\frac{x}{2}.$$

x may therefore be obtained from the experimental data from the relation

$$\frac{6-3x/2}{6-1x/2}=\frac{\text{ion yield in the first 24 hours}}{\text{ion yield after 24 hours}}.$$

At 30° and 100°C these values are

	30°C	100°C
Ion yield first 24 hr.	3.75	4.14
Ion yield after 24 hr.	4.35	4.75

[7] W. A. Noyes, Jr., J. Chem. Phys. **5**, 807 (1937).

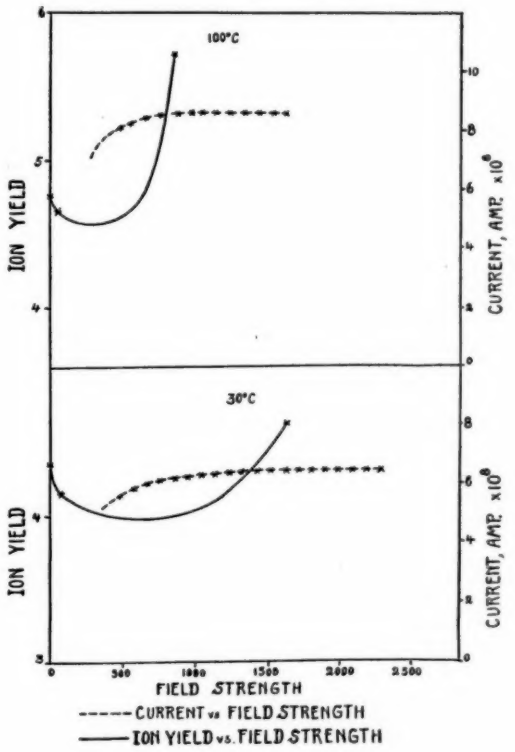

FIG. 3.

At 30°C $x=0.776$ and at 100°C $x=0.723$ from which the ion yield in terms of moles of N_2O decomposed per ion pair is,

$$\text{at } 30°\text{C } \frac{4}{6-0.388}\times 4.35=3.10$$

and

$$\text{at } 100°\text{C } \frac{4}{6-0.362}\times 4.75=3.37.$$

The value 3.10 obtained at 30° may be compared with 2.75, the value at 30° from Mund's calculations from Wourtzel's experimental data. As the intensity of ionization in our experiments was a great deal less than that of Wourtzel, the difference between our ion yield and that of Wourtzel is in agreement with the frequently observed fact that the ion yield in alpha-ray decompositions increases with a decrease in intensity of ionization. In our experiments on the decomposition of ammonia by alpha-rays at low intensities of ionization, the ion yield agreed excellently with the extrapolated ion yield for

this reaction at zero intensity of ionization as calculated from the measurements of Luyckx on the change in the ion yield with intensity of ionization. No data is available in the literature on the decomposition of N_2O at low intensities of ionization, with which the results of this work might be directly compared.

The temperature coefficient of the ion yield is, according to Mund 0.0044 per degree and from these measurements 0.0039 per degree.

The ion yield consequent on recombination of ions is calculated from the ion yield in no field and the ion yield in a field of sufficient strength to produce a plate current equal to half the saturation current by doubling the difference between the ion yield at zero field strength and at half saturation. The results of such a calculation show that at 30° 9.2 percent of the reaction is initiated by combination of ions and 90.8 percent due to other mechanisms and at 100°C 4.2 percent is due to recombination of ions and 95.8 percent to other mechanisms. The ion yields at voltages sufficient to produce saturation can not be used for such calculations because at high voltages decomposition is produced by a new mechanism, probably by collision of electrons with molecules. The amount of decomposition due to this new reaction which is apparent at high field strength can be safely neglected at voltages sufficient to produce half-saturation as these voltages are very low compared with the voltages necessary for saturation, i.e., 900 volts compared with 17,000 volts at 30°C and 500 volts compared with 9000 volts at 100°C.

In Fig. 3 are plotted the curves of ion yield *versus* field strength at 30° and 100°C together with the current-field strength curves at the same temperatures. Comparison of the curves shows that decomposition due to high field strength is apparent far below the field strength necessary for ionization by electron collision. Similar relations are apparent in the work on the alpha-ray decomposition of ammonia.[1]

These facts point definitely to the decomposition of N_2O by electrons having far less than sufficient energy for ionization and therefore to this mechanism in the decomposition of N_2O by alpha-rays in the absence of electric fields, due to ejected electrons.

Ion yields of the observed magnitudes are energetically possible even though no reaction accompanies the recombination of ions. In air the energy of an alpha-particle consumed per ion pair produced is 35 electron volts.[8] The relative ionization in N_2O compared with air is 1.05;[9] from which figures the alpha-ray energy consumed per ion pair in N_2O is $35\times1/1.05=33.3$ ev. Most of the energy lost in the passage of an alpha-particle must be lost in inelastic collisions by the primarily produced electrons. Quantitative data for the fraction of energy lost by inelastic collisions in N_2O are not available but for the passage of low energy electrons through hydrogen, according to Lunt and Meek[10] 92 percent of the energy is so lost. Assuming the same efficiency in N_2O, the energy so lost per ion pair is $33.3\times0.92=30.6$ ev. The most abundant positive ions produced in N_2O by electron collisions are N_2O^+ for which the ionization potential is 12.9.[11] The energy lost per ion pair by other inelastic collisions is therefore $30.6-12.9=17.7$ ev, sufficient to split 10 molecules of N_2O by the mechanism

$$N_2O=N_2+O; \qquad \Delta E=1.7 \text{ ev.}$$

Part of this reaction probably occurs with electron attachment to oxygen

$$N_2O+e=N_2+O^-.$$

Electrons having energies in excess of 1.7 volts are capable of attachment to N_2O in this manner according to Bradbury and Tatel.[12] Formation of negative ions by this mechanism also probably accounts for the increased ion yields at high field strengths.

Studies of the alpha-ray decomposition of nitrous oxide and ammonia at higher field strengths are now being made in this laboratory.

---

[8] Rutherford, Chadwick and Elliss, *Radiations from Radioactive Substances*, p. 80–81.
[9] R. D. Kleeman, Proc. Roy. Soc. **A79**, 220 (1907).
[10] Lunt and Meek, Proc. Roy. Soc. **A157**, 146 (1936).
[11] E. C. G. Stueckelberg and H. D. Smyth, Phys. Rev. **36**, 478 (1930).
[12] Bradbury and Tatel, J. Chem. Phys. **2**, 835 (1934).

Note on the Ultraviolet Absorption Systems of Benzene Vapor

G. NORDHEIM AND H. SPONER, *Department of Physics, Duke University, Durham, North Carolina*

AND

E. TELLER, *Department of Physics, The George Washington University, Washington, D. C.*

(Received March 21, 1940)

An attempt has been made to give a coherent interpretation of the absorption systems of benzene vapor in the far ultraviolet including the Rydberg series. The following assignments are proposed: A forbidden transition of symmetry $^1A_{1g} \rightarrow {}^1B_{1u}$ is suggested for the bands at 2050 to 1850A and an allowed $^1A_{1g} \rightarrow {}^1E^-_u$ transition for the much more intense bands at 1850 to 1650A. The continuous background in the latter region may possibly be due to a transition involving a C−H dissociation. The observed two Rydberg series can both be assigned to allowed transitions of symmetry $^1A_{1g} \rightarrow {}^1E^-_u$.

1. INTERPRETATION OF THE SYSTEMS AT 2000A AND 1750A

THE first absorption region of benzene lies at 2700–2200A. It represents an electronic transition $^1A_{1g} \rightarrow {}^1B_{2u}$ which is forbidden[1] by symmetry and is made allowed when vibrations of type[2] ϵ^+_g are excited. The analysis[3] of the vibrational structure of this absorption system has confirmed these assumptions. The interacting ϵ^+_g vibration is the Raman active vibration of frequency 606 cm^{-1}.

A stronger absorption spectrum has been observed[4] in the region from 2050A to 1850A. It consists of a number of diffuse broad groups showing some structure. The spectrum retained its diffuseness even when the absorption tube was surrounded by dry ice.[5] Below 1850A the bands are overlapped by a still stronger absorption system which has the appearance of a continuous background upon which bands are superimposed, which are much sharper than the bands of the system just mentioned.

The strong intensity of the absorption below 1850A suggests an allowed transition. According to calculations[6] of electronic states an allowed transition is to be expected in this region. The transition can be described by the excitation of a double bond electron of character e^-_g into an e^+_u level.[7] The resulting electronic configuration can be represented by a hole $(e^-_g)^{-1}$ left in the A_{1g} ground level multiplied by the wave function of an e^+_u electron. The product $(e^-_g)^{-1}e^+_u$ yields molecular wave functions of symmetry B_{1u}, B_{2u}, E^-_u. Transitions to the first two levels are forbidden while $A_{1g} \rightarrow (e^-_g)^{-1}e^+_u E^-_u$ is allowed. (All discussed transitions concern singlet terms.) We tentatively interpret the relatively sharp bands below 1850A as this transition. It has been shown[8] that in a degenerate electronic state the symmetrical nuclear configuration does not correspond to a stable equilibrium. This holds for the upper E^-_u state whose degeneracy can be removed by a nuclear displacement of ϵ^+_g symmetry. Hence the equilibrium configuration differs from the symmetrical one by an ϵ^+_g displacement. The deviation from the symmetrical configuration will, however, be small because the single bond electrons which are predominant in determining the shape of the molecule, are left undisturbed in this transition and only one double bond electron is excited. The slight change in equilibrium configuration may account for the somewhat irregular vibrational structure of the $A_{1g} \rightarrow E^-_u$ transition. We are inclined to believe that the apparently continuous absorption which forms the background corresponds to

[1] A. L. Sklar, J. Chem. Phys. **5**, 669 (1937).
[2] Symmetry symbols for vibrations are denoted with small Greek letters.
[3] H. Sponer, G. Nordheim, A. L. Sklar and E. Teller, J. Chem. Phys. **7**, 207 (1939).
[4] E. P. Carr and H. Stücklen, J. Chem. Phys. **6**, 55 (1938).
[5] Personal communication from Dr. H. Stücklen for which we are much indebted.
[6] E. Hückel, Zeits. f. Physik **70**, 204 (1931); Zeits. f. Elektrochem. **43**, 752 (1937); A. L. Sklar, reference 1; M. Goeppert-Mayer and A. L. Sklar, J. Chem. Phys. **6**, 645 (1938).
[7] If the symmetry symbols refer to single electrons, capital letters are replaced by small ones.
[8] A. H. Jahn and E. Teller, Proc. Roy. Soc. Lond. **A161**, 220 (1937).

another electronic transition; namely, to a repulsive state leading to the rupture of one C−H bond.[9]

The absorption region between 2050A and 1850A represents the forbidden transition $A_{1g}\rightarrow(e^-_g)^{-1}e^+_u B_{1u}$. The transition $A_{1g}\rightarrow(e^-_g)^{-1}e^+_u B_{2u}$ has been ascribed to the longest wave-length absorption as mentioned in the beginning of this note. Both transitions are made allowed by vibrations of type ϵ^+_g and the $A_{1g}\rightarrow B_{1u}$ transition also by a β_{2g} vibration.[10] The assignments of the observed absorption systems to the two transitions are based upon calculations[11] of the relative positions of the B_{1u} and B_{2u} levels. The observed occurrence of 965 and 160 progressions in the system $A_{1g}\rightarrow B_{1u}$ may be explained in an analogous way as for the near ultraviolet bands. It is interesting to note that the 965 progression which, as Carr and Stücklen (cf. 4) have done, is best interpreted by an excitation of the totally symmetrical C−C vibration in the upper state, shows unusually strong convergence so that large anharmonicity of this vibration must be assumed. As the transition is forbidden, both a $1\rightarrow 0$ and $0\rightarrow 1$ transition should be observed for the vibration which makes the transition allowed. Apparently only the latter is present and will be one band of the first group. The former will be weaker on account of the Boltzmann factor and the corresponding band, being diffuse, may escape observation. In addition, it may be obscured by the tail of the predissociation observed in the $A_{1g}\rightarrow B_{2u}$ system. On the other hand, the neighborhood of the allowed E^-_u level, and the C−H repulsion curve may very well explain the apparent irregularity of the intensity of the 160 progressions; bands in which excitation of a β_{2g} vibration rather than an ϵ^+_g vibration makes the transition allowed may contribute to the irregular appearance of the system. A more detailed analysis of the spectrum seems impossible at the present moment owing to the diffuseness of the whole system.

That the spectrum at 2050A is much stronger than the 2600A bands can be explained by the fact that the former lies closer to the allowed absorption system at 1770A. The intensity of a forbidden transition is proportional[12] to $(1/\Delta E)^2$ where ΔE is the energy distance to the next allowed level of appropriate symmetry. Calculating the ΔE values from the long wave ends of the systems $A_{1g}\rightarrow E^-_u$, $A_{1g}\rightarrow B_{1u}$, $A_{1g}\rightarrow B_{2u}$, one finds that the $A_{1g}\rightarrow B_{1u}$ transition should be about ten times stronger than the $A_{1g}\rightarrow B_{2u}$ system. The actual ratio can easily be larger because we have used in fact ΔE values for the equilibrium configuration of the nuclei in each state while the hypersurfaces of potential energy may approach closer for vibrating nuclei. This will be of greater relative importance for the higher lying B_{1u} surface. A further contribution may arise if the upper state of the continuum at 1770A is used instead of the E^-_u in calculating the ΔE values. If this continuum extends farther towards the red, then $(1/\Delta E)^2$ will again show a greater increase for B_{1u} than for B_{2u}. The observed intensity ratio is indeed larger[13] than 1 : 10.

The 2050A system may alternatively be ascribed to a forbidden $A_{1g}\rightarrow E^+_g$ transition, since an E^+_g level has been predicted by Sklar (cf. 1) in this energy region on the basis of the Heitler-London approximation method. The above considerations may as well be applied to an $A_{1g}\rightarrow E^+_g$ transition, but the vibration which makes the transition allowed will be ϵ^-_u rather than ϵ^+_g. Moreover, the degeneracy of the E^+_g state may cause a slight asymmetry of the equilibrium configuration and hence a more involved vibrational structure.

[9] It cannot be excluded, however, that the strong apparently continuous region in reality represents the $A_{1g}\rightarrow(e^-_g)^{-1}e^+_u E^-_u$ transition and that the sharp bands are somewhat accidentally superimposed on it belonging to another electronic state which could represent the first member of one of the Rydberg series. This interpretation is favored by Dr. R. S. Mulliken (private communication, see also J. Chem. Phys. **7**, 20 (1939)).

[10] A β_{2g} vibration causes mixing of the B_{1u} state with an A_{2u} state, and an $A_{1g}\rightarrow A_{2u}$ transition is allowed. However, there is no information about the energies of A_{2u} states in benzene, and therefore, it is not possible to estimate the intensity with which β_{2g} vibrations could appear in the $A_{1g}\rightarrow B_{1u}$ system.

[11] M. Goeppert-Mayer and A. L. Sklar, J. Chem. Phys. **6**, 645 (1938). These authors mention already the possibility of assigning the B_{1u} and E^-_u levels to the observed absorptions in the way proposed here.

[12] G. Herzberg and E. Teller, Zeits. f. physik. Chemie **B21**, 410 (1933). See also considerations on intensities by R. S. Mulliken, J. Chem. Phys. **7**, 20, 353 (1939).

[13] According to private communication from Dr. Carol A. Rieke, for which we are greatly indebted, the intensity ratio of about 1 : 1000 calculated by N. Q. Chako, J. Chem. Phys. **2**, 644 (1934) is much too high.

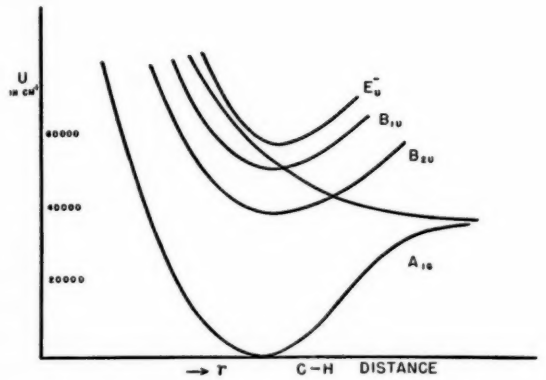

FIG. 1. Schematic potential curves illustrating predissociation and diffuseness in benzene spectra.

2. PREDISSOCIATION AND DIFFUSENESS OF THE BANDS

Predissociation and diffuseness of some of the bands may be explained by the rupture of a C−H bond. In Fig. 1 potential energies of the different levels are drawn as functions of one of the C−H distances denoted by r. The symmetry symbols attached are significant only in the neighborhood of the minima where the C−H distance in question is equal to the other C−H distances. The repulsive curve which we assume to represent the upper state of the continuous absorption at 1770A must have the symmetry E^-_u or A_{2u} in the vicinity of the equilibrium distance in order to give rise to a strong absorption. If we assume that the excitation consists in transferring a C−H bonding electron into an antibonding state, then the transition moment will lie in the molecular plane and the repulsive state must be E^-_u. Such a state can be constructed by superimposing excitation in the different C−H bonds with appropriate phases. If now one C−H distance is increased, the superimposed amplitudes change until, for great r values, the excitation is localized in that C−H bond which is to be broken.

We shall expect predissociation in the transition $A_{1g}\rightarrow B_{2u}$, when the vibrational energy of B_{2u} reaches the intersection with the repulsive curve. Though we know from the spectrum that the vibrational energy is mostly accumulated in the totally symmetrical C-vibration, one may expect that on account of anharmonic forces the energy of oscillation may go over into the stretching of a C−H bond. The diffuseness of the $A_{1g}\rightarrow B_{1u}$ system is readily explained from Fig. 1 where the intersection between the repulsive curve and the B_{1u} curve takes place at much lower vibrational energies. On the other hand, we explain the sharpness of the $A_{1g}\rightarrow E^-_u$ system by placing the E^-_u curve just above the repulsive curve, hereby avoiding intersection. Fig. 1 gives the impression that the maximum of continuous absorption lies at slightly longer waves than the strongest bands of the $A_{1g}\rightarrow E^-_u$ system. Actually the maxima of the continuous and discrete systems seem to coincide. But our figure, taking into account only one degree of freedom, is an extremely poor representation of the polydimensional energy surfaces, and it is difficult to predict the exact location of such maxima within a few hundred wave numbers.

3. INTERPRETATION OF THE RYDBERG SERIES

In the far ultraviolet, very strong sharp absorption bands have been observed and arranged into two Rydberg series.[14] They begin at about 1550A and extend till 1360A. The Rydberg formulae which have been proposed are as follows:

$$\nu = 74{,}495 - R/(n+0.97)^2 \qquad \text{(I)}$$

$$\nu = 74{,}590 - R/(n+0.55)^2 \quad n=3, 4, 5\cdots. \qquad \text{(II)}$$

In these formulae the two ionization limits almost coincide and correspond to a mean value of 9.19 volts. The most recent determination of the ionization potential by the electronic impact method[15] gives 9.8±0.1 volts, a value which represents an upper limit according to the nature of these experiments.

The intensity of both the Rydberg series definitely points to the fact that they are due to allowed transitions (i.e., the upper state must have the symmetry E^-_u or A_{2u}). The members of one series will belong to electronic states of the same symmetry. If we extrapolate series I toward the red, we come into the region of 1600A ($n=2$) and 2100A ($n=1$). In both these regions we observe only diffuse and structureless absorption

[14] W. C. Price and R. W. Wood, J. Chem. Phys. **3**, 439 (1935).

[15] A. Hustrulid, P. Kusch and John T. Tate, Phys. Rev. **54**, 1037 (1938).

which corresponds to the tail ends of the above-mentioned 1850A and 2600A systems, respectively. Therefore, we are led to the conclusion that the system at about 1480A is the first observed member of series (I).

On the other hand, the extrapolation of series (II) leads into the region of the 1770A system observed by Carr and Stücklen and discussed above. Since we have earlier identified this strongest of all absorption systems with an allowed transition $A_{1g}\rightarrow E^-_u$, it seems suggestive to us to assign tentatively series (II) to transitions $A_{1g}\rightarrow(e^-_g)^{-1}(ne^+_u)E^-_u$ with the 1850–1650A system as its first member. That the intensity of the first member[16] is much larger than that of the succeeding ones may be explained by the fact that it takes place much more within the molecular dimensions than the higher members.[17]

Since the other Rydberg series (I) leads to the same ionization state, an (e^-_g) hole has to be expected in the upper states of series (I) as well as of series (II). The intensity of series (I) points also to allowed transitions. The only transitions satisfying both these requirements are $A_{1g}\rightarrow(e^-_g)^{-1}(na_{2u})E^-_u$ and $A_{1g}\rightarrow(e^-_g)^{-1}(ne^-_u)A_{2u}$. The first of these two assignments seems to us more likely. In fact, in $A_{1g}\rightarrow E^-_u$ the degenerate upper states would have a somewhat unsymmetrical nuclear equilibrium configuration, and thus a relatively complicated vibrational structure should be expected. In the $A_{1g}\rightarrow A_{2u}$ transition, on the other hand, the occurrence of only totally symmetrical vibrations would be insufficient to account for the observations of Price, who finds a 960 and 670 energy difference associated with series (I) in addition to smaller energy differences. If these energy differences correspond to a vibrational structure, they would be explained more readily by an $A_{1g}\rightarrow E^-_u$ transition.

But the $A_{1g}\rightarrow(e^-_g)^{-1}(ne^-_u)A_{2u}$ assignment cannot be excluded definitely. If the (e^-_g) hole and the (ne^-_u) electron would be coupled very weakly, the (e^-_g) hole would determine the equilibrium configuration of the nuclei. The degenerate e^-_g orbit would then lead to an unsymmetrical configuration and a complicated vibrational structure, so that the results would be essentially the same as for $A_{1g}\rightarrow E^-_u$. The coupling described in this section obtains, however, only if the separation of the various levels of the $(e^-_g)^{-1}(ne^-_u)$ configuration is less than the splitting of the $(e^-_g)^{-1}$ wave function by the zero point vibrations of the molecule. Analogy with atomic spectra leads us to an estimate of about 0.1 volt for the former quantity in the first member of series (I). On the other hand, the splitting by the zero point vibration will probably be rather smaller than the total width of the vibrational structure which is about 1000 cm^{-1}. Therefore, it is unlikely that $A_{1g}\rightarrow A_{2u}$ could give rise to a sufficiently complicated vibrational pattern.

There is, of course, also the possibility that some of the bands forming the pattern and especially some of the violet companions could be arranged into independent Rydberg series and in this case both transitions $A_{1g}\rightarrow(e^-_g)^{-1}(na_{2u})E^-_u$ and $A_{1g}\rightarrow(e^-_g)^{-1}(ne^-_u)A_{2u}$ could be present. Theoretically this would be the most satisfactory alternative, since it would account for all possible allowed transitions in which the most loosely bound e^-_g electron is excited.

[16] See photograph p. 209 in W. C. Price and D. W. Walsh, Proc. Roy. Soc. Lond. **A174**, 207 (1940).

[17] The same intensity relations hold for atomic Rydberg series where also the first member is more influenced by the extended structure of the atom.

Spectroscopic Measurements of Gaseous CN

II. Thermal Dissociation of Cyanogen*

JOHN U. WHITE†
Department of Physics, University of California, Berkeley, California

(Received January 22, 1940)

Free CN radicals are formed from cyanogen at high temperature. Their absorption spectrum was observed in a furnace at 1500°K. From the lower limit of the absolute absorption coefficient found in Part I of this paper, their partial pressure and hence the equilibrium constant of the dissociation of cyanogen to free radicals are calculated. A lower limit for the heat of the reaction

$$C_2N_2 \rightarrow 2CN \qquad K_{1500°K}=1.1\times10^{-12} \qquad H_0=138.1(\pm1) \text{ kcal.}$$

follows directly. $f=0.1$ is estimated to be the most probable f value for the $^2\Sigma\rightarrow{}^2\Sigma$ transition of CN. The most probable value of the heat of dissociation of cyanogen is calculated from this to be $H_0=146(\pm4)$ kcal. By calculating the partial pressure of CN at about 400°C, the thermal polymerization of cyanogen is explained as the addition of the free radicals formed to cyanogen molecules. From thermodynamic cycles, it is shown that the most probable value of the heat of dissociation of CO is 11.054 volts, and of the heat of vaporization of graphite 169.2 kcal., although 9.797 volts and 140.2 kcal. respectively, for these values cannot be completely eliminated.

INTRODUCTION

THE absolute absorption coefficient of CN, which was found in the preceding paper,[1] gives a quantitative measure for the amount of CN radical present wherever its absorption is observed. In this paper the measure is considered as a lower limit and applied to the CN formed by the thermal dissociation of cyanogen at high temperatures. When the partial pressures of CN and cyanogen are known, the equilibrium constant and free energy of the dissociation can be calculated directly. Lower limits and best values of the thermodynamic quantities are calculated from the absorption coefficient found previously and from a somewhat larger one estimated to be closer to the correct value, respectively.

APPARATUS

The same apparatus was used in this experiment as in the preceding one, with the substitution of a high temperature furnace for the apparatus producing electrical dissociation. The 21-foot grating with the cylindrical lens in the second order was unchanged. Some of the same cyanogen was used. As there was no question of timing, sparks were run in the source as fast as power could be supplied to the condenser. Half a minute, at five sparks a second, was needed to give a good exposure through the absorption cell. The photographic plates and methods of calibration and measurement were identical. The furnace was made from an Alundum tube 70 cm long. The middle 60 cm were wound with 88 turns of carefully spaced Nichrome ribbon, 0.04 ohm per foot, set in Alundum cement. The 5 cm at each end were wound with number 18 wire and connected in a separate circuit. Quartz windows cemented on

TABLE I. *Temperature distribution in furnace.*

DISTANCE FROM CENTER OF FURNACE	ABSOLUTE TEMPERATURE	
3.5 cm	1516°K	Position of thermocouple during exposure
5	1515	
8	1514	
10	1514	
13.5	1518	
17.5	1520	
19.5	1518	
21.5	1512	
23.5	1503	
25	1493	End of absorption cell

* This and the preceding paper are condensed from a thesis submitted in partial fulfillment of the requirements for the degree of Doctor of Philosophy in the Department of Physics.

† Now with the Standard Oil Development Company, Elizabeth, New Jersey.

[1] J. U. White, J. Chem. Phys. **8**, 79 (1940).

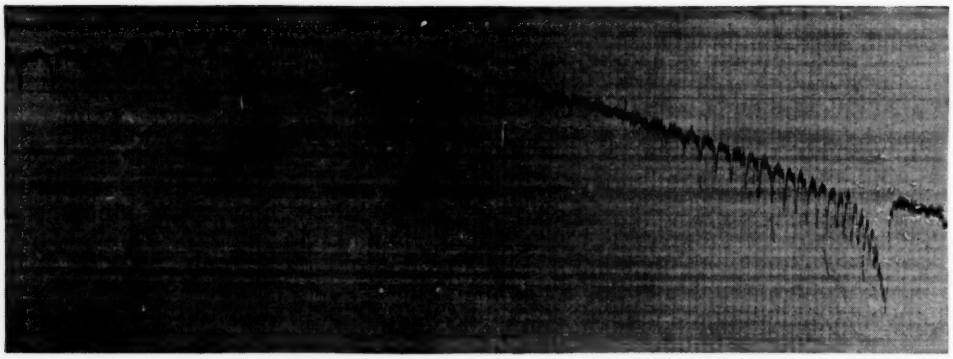

FIG. 1. Microphotometer trace of CN absorption at 1500°K.

the ends of the furnace, in addition to those of the absorption tube, prevented convection, and asbestos cloth served as thermal insulation. The temperature distribution was adjusted by pulling asbestos off the middle of the furnace and draping it over the ends until the set of readings shown in Table I was obtained. Quartz windows were fused on a quartz tube 50 cm long and 2.5 cm in diameter to make the absorption cell. When it was placed in the middle of the furnace, a correction of $-1°$ was needed to reduce the temperature at the position of the thermocouple to the mean for the absorption cell.

The thermocouple was made of platinum and platinum-rhodium wires, and readings were taken with a sensitive galvanometer. The melting and freezing points of samples of pure silver and gold were measured under the same conditions that existed later in the other temperature determinations. The observed differences between the melting and freezing points were 3° and 2° for silver and gold, respectively. The averages were taken as the best values in drawing the calibration curve for the galvanometer.

MEASUREMENTS

After the furnace had been heated to 1100°C and allowed to come to equilibrium, the absorption cell was pumped out and cyanogen admitted to a pressure of about 60 cm. An exposure was taken ten seconds later. The gas was then pumped out, some fresh admitted to $\frac{1}{4}$ the pressure, and another exposure taken. This was repeated until the absorption disappeared. The furnace was then heated to a higher temperature and another set of exposures was taken. This was repeated at intervals of about 30° to the highest temperature, 1515°K. At this point, four exposures at pressures ranging from 64 cm down to 1 cm showed measurable absorption. Three exposures were also taken at about the same pressure at intervals ranging from 10 seconds to 5 minutes after admitting the cyanogen to the cell. The final results show that there was no delay in establishing equilibrium. Only the exposures taken at the highest temperature were worked up. However, a visual comparison with the exposures at other temperatures showed that they would give about the same results if they were used. A microphotometer trace of one of the exposures, showing the high temperature distribution of intensity in the band and the formation of a head, is shown in Fig. 1.

CALCULATIONS

The method of measuring the plates and reducing the measurements to absorption coefficients was exactly the same as that described

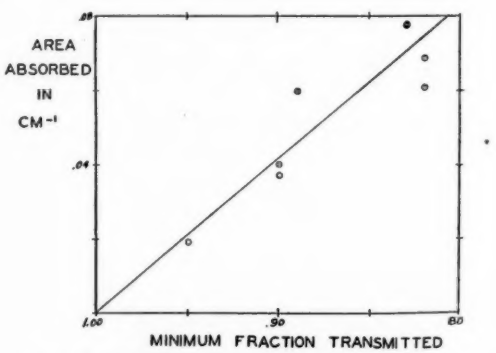

FIG. 2. Relation between area and maximum intensity of the lines.

TABLE II. *Equilibrium constants and partial pressures at 1515°K.*

TIME AFTER ADMITTING CYANOGEN	PRESSURE CYANOGEN	*P.P.* CN	K
10 seconds	669 mm	$680(\pm 200)\times 10^{-6}$ mm	$9.40(\pm 7)\times 10^{-13}$
1 minute	616	670	9.8
5 minutes	655	710	10.1
10 seconds	176	410	12.9
10 seconds	44.5	200	12.3
10 seconds	12.0	100	11.4

before.[1] The areas of 20 different lines were measured on large scale microphotometer traces to obtain the new relation between area and maximum absorption. It is shown in Fig. 2. A new set of curves relating the amount of light absorbed by each line to the absorption coefficient of its stronger component was calculated for 1500°K. It is shown in Fig. 3 with scales both of A/I_0s and of the observed minimum of the fraction transmitted. Values of a were determined from it for each line and then $\sum_K B$ was calculated for each exposure. If we recall that it was shown in Part I of this paper that an upper limit for the partial pressure of CN at 300°K is

$$P_{CN}=\frac{0.0035}{x}\sum_K B,$$

and multiply by the ratio of the two temperatures, then

$$P_{CN_{1515°K}}=\frac{0.0147}{x}\sum_K B.$$

RESULTS

The partial pressures of CN calculated for the different observed intensities of absorption are tabulated in Table II. The pressure of cyanogen and the corresponding equilibrium constants are also shown. The probable errors indicate the absolute uncertainty including that in the f value used. The consistency of the readings shows that their relative errors compared to each other are much smaller. The extent of the agreement of the first three values in the table shows the fluctuations to be expected between the different readings and indicates that there is no trouble from delay in reaching equilibrium. However, the variation with pressure is larger than can be accounted for by photometric errors. I have no explanation for this, but point out that in any case its effect on the results is small. The value of $K=1.1(\pm 0.7)\times 10^{-12}$ in atmospheres was taken as the best value. At 1515°K a lower limit for the free energy of the dissociation $C_2N_2\rightarrow 2CN$, is

$$\Delta F=-RT\ln K=82.9 \text{ kcal.}$$

The entropies of C_2N_2 and CN were next calculated in the usual way.[2,3] The vibration frequencies and moment of inertia of CN are well known, those of C_2N_2 were taken from the paper of Stevenson[4] with the exception of δ_2. His value of 230 cm^{-1} was raised to 240 cm^{-1}, on the suggestion of Professor W. F. Giauque, to make the calculated entropy agree better with the thermal value that he and Ruhrwein obtained.[5] When these frequencies are substituted in the table given by Gordon and Barnes and the proper calculations are made, the molal entropy of CN is found to be 60.6 E.U. at 1500°K. That of C_2N_2 is 84.9 E.U. As the nuclear spin does not change in a chemical

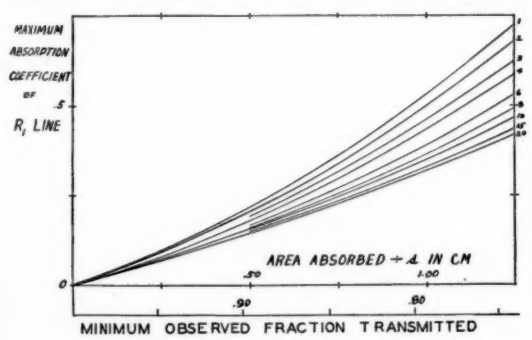

FIG. 3. Relation between absorption coefficient and amount of light absorbed.

[2] W. F. Giauque, J. Am. Chem. Soc. **52**, 4808 (1930).
[3] A. R. Gordon and C. Barnes, J. Chem. Phys. **1**, 297 (1933).
[4] D. P. Stevenson, J. Chem. Phys. **7**, 171 (1939).
[5] R. A. Ruhrwein and W. F. Giauque, J. Am. Chem. Soc. **61**, 2940 (1939).

TABLE III. *Appearance potentials, excitation potentials, and relative abundances of particles present in the discharge.*

PARTICLE	APPEARANCE POTENTIAL	RELATIVE ABUNDANCE	EXCITATION POTENTIAL
$C_2N_2^+$	14.1 volts	3.4	
C_2N^+	21.3	0.7	
C_2^+	18.6	0.2	
CN^+	19.8	0.1	
CN	6.3		3.2, 1.3 volts
A^+	15.5		
A			11.5
C+N from CN	6.4		

reaction, it has been neglected in these calculations. The entropy change in the dissociation is $\Delta S=36.3$ E.U., from which we can reduce the free energy to 1500°.

$$\Delta F_{1500^\circ}=82.3(\pm 1.5) \text{ kcal.}$$

The heat of dissociation of C_2N_2 into CN is, therefore,

$$\Delta H_{1500^\circ}=\Delta F+T\Delta S$$
$$=136.8(\pm 1.5) \text{ kcal.}$$

This is reduced to ΔH at absolute zero by adding the difference in the heat capacities of the reactants and products. If we assume rotation to be classical and the heats of the vibration terms to be given by the Einstein formula, the correction is +1.3 kcal. Then $\Delta H_0=138.1$ kcal. In other units ΔH_0 is 6.00 electron volts. Since this calculation is based on an upper limit to the concentration of CN found previously, it only yields a lower limit to the heat of dissociation. To decide how close the actual value is to this limit, we must consider the method of determining it.

DEGREE OF DISSOCIATION OF CYANOGEN IN THE ELECTRIC DISCHARGE

We must now discuss the assumption of complete dissociation of the cyanogen in the electric discharge at great dilution, which was made in Part I of this paper.[1] The first evidence comes from a study of the mechanism of the discharge. From Table III, which is reproduced from Part I, it is evident that at the start of a discharge in a mixture of cyanogen and argon the process requiring least energy is the formation of CN radicals, thereafter it is their excitation. The low excitation potentials of CN explain why only its spectrum was seen in emission. In the case where there is very little cyanogen present one would expect it to be almost completely dissociated, which would be indicated by a linear relation between the amount of cyanogen present and the intensity of CN absorption. This has been found. The amount of cyanogen needed to supply the ions postulated in the section on reaction kinetics is less than one percent of the total amount present at the greatest dilution when any rates were measured.

Since the publication of Part I,[1] it has been pointed out to the author that as soon as some CN radicals have been formed, their dissociation to carbon and nitrogen is energetically about as easy as the dissociation of the remaining cyanogen to form more radicals. Therefore, even when the cyanogen present has been very largely dissociated, the number of radicals actually present is less than it would be if there were no secondary dissociation by an amount depending on the relative collision cross sections of C_2N_2 and CN. Lacking experimental knowledge of these cross sections, we can only assume from their energy requirements that they are about equal. In that case, a calculation of the reaction rates shows that the maximum concentration of CN attained is $1/e$ of that predicted for no secondary dissociation. As the measurements were probably not made exactly at the time of maximum concentration, there is a further, but unknown correction to be applied in the same direction.

We are guided by three other considerations in deciding how much allowance to make for this. The first is rigorous and sets a lower limit to the concentration of CN that could have been present. Dispersion theory states that for any molecule the sum of the f values for all the transitions out of a given state is one. Therefore, in the case of the greatest possible error the concentration of CN cannot be less than 0.026 of the calculated value, because in that case the f value for that one transition would be greater than unity. Since CN has other transitions, the lower limit must be somewhat higher than this. The second check lies in the comparison of the f value with that calculated by Mulliken[6] from theoretical considerations. His value, which is of the order of 0.1, indicates that not all the CN

[6] R. S. Mulliken, private communication with the author.

that could have been formed was observed in the present experiment. The third is that the observed dissociation energy lies slightly on the short wave side of the beginning of the absorption spectrum of cyanogen. From a study of the photopolymerization of cyanogen Hogness and Liu-Sheng T'sai[7] have found that it is polymerized appreciably by the light from a hydrogen tube transmitted through air. To get an appreciable effect, light of wave-lengths considerably longer than 1850A must be effective. Their conclusion from their measurements, that the first step in polymerization is dissociation to free radicals, is confirmed by the calculations made in the section on thermal polymerization.

In view of these facts it appears that the f value of $0.026(\pm 0.006)$ calculated previously is too low. It remains as an experimentally observed lower limit, but the best value is probably three or four times as large. Correspondingly, the heat of dissociation given above should be taken as an accurate lower limit. $f=0.1(\pm 0.05)$ is used in calculating the most probable value. Since this method of calculation is insensitive to variations in the f value, this change only increases H_0 by 8 kcal. to make the most probable value $\Delta H_0=146(\pm 4)$ kcal., or in other units $\Delta H_0=6.33(\pm 0.17)$ volts.

Comparison with Previous Work

Kistiakowsky and Gershinowitz[8] found $\Delta H=77$ kcal. by measuring the variation of K with temperature on a quartz spectrograph. It is the purpose of this paragraph to show that their incomplete resolution and neglect of pressure broadening effects may introduce large enough errors to account for the difference. Their fundamental measurement was the comparison of the intensities of absorption of the band head at λ3883 for different temperatures and partial pressures of cyanogen. Effectively they measured K in arbitrary units and substituted in the van't Hoff equation. For example, if K and K' correspond to the temperatures of T and T' respectively,

$$\frac{d\ln K}{dT}=\frac{\ln K-\ln K'}{T-T'}=\frac{\Delta H}{RT^2}.$$

If the value of K' defines the arbitrary units in which it is expressed, all the error in the determination must appear in K. The error in K needed to produce the observed difference in ΔH is found by differentiating and dividing by the original equation. If we use the lower limit found for ΔH,

$$\frac{\delta\ln K}{\ln K/K'}=\frac{\delta\Delta H}{H}=\frac{137-77}{137}=0.44.$$

Then

$$\delta K/K=0.44\ln K/K'.$$

For $T-T'=46°$, which is larger than most of their temperature differences, $K/K'=4$. Since $K=[CN]^2/[C_2N_2]$, and $[C_2N_2]$ is accurately measurable,

$$\tfrac{1}{2}\delta K/K=\delta[CN]/[CN]=0.30.$$

Thus, an error of only 30 percent in estimating the equality of two absorption lines would account for the discrepancy. Their measurements were all made at atmospheric pressure, in a furnace about a meter long, using a spectrograph of medium resolving power. From the present work with very high resolving power I have calculated that the absorption had to become very strong before they could observe it at all. All their measurements lie in the region where the centers of the lines are almost completely absorbed out. There the amount of light absorbed changes slowly with the concentration of the absorbing molecules but is very sensitive to broadening of the lines. If the CN band lines are broader in an atmosphere of cyanogen than in one of nitrogen, it is understandable that halving the partial pressure of cyanogen and substituting nitrogen for it might decrease the width of the lines by 30 percent. This would explain the difference between their results and mine.

Chemical Applications

Thermal polymerization

The change of free energy with temperature of any reaction at atmospheric pressure is given by

[7] T. R. Hogness and Liu-Sheng T'sai, J. Am. Chem. Soc. **54**, 123 (1932).
[8] G. B. Kistiakowsky and H. Gershinowitz, J. Chem. Phys. **1**, 432 (1933).

TABLE IV. *Possible heats of dissociation of* CO *and* CN *and heats of vaporization of graphite on the basis of predissociations observed in the* CO *spectrum.*

DISSOCIATION PRODUCTS OF CO AT 11.054 VOLTS		D(CO)		L	D(CN)	
CARBON	OXYGEN	VOLTS	KCAL.	KCAL.	VOLTS	KCAL.
^3P	^3P	11.054	254.8	169.2	6.38(±0.13)	147(±3)
^1D	^3P	9.797	225.8	140.2	5.12	118
^3P	^1D	9.097	209.7	124.1	4.42	102
^1S	^3P	8.384	193.3	107.7	3.71	85
^1D	^1D	7.840	180.7	95.1	3.17	73
^3P	^1S	6.886	158.7	73.1	2.21	51
^5S	^3P	6.738	155.3	69.7	2.06	47

the partial differential equation

$$(\delta\Delta F/\delta T)_p = -\Delta S.$$

The entropy change in the dissociation of cyanogen has, as explained above, been calculated as a function of temperature. When an approximation, valid in the neighborhood of 1200°K is made for the vibrational entropy change, the following expression is obtained:

$$\Delta S = 4.56 + 7/2R \ln T - 0.013T.$$

Substituting this in the equation above and integrating at constant pressure, an expression is obtained for ΔF. The constant is evaluated by using the known free energy change at 1500°F. From the values of ΔF around 400°C, the order of magnitude of the partial pressure and density of CN radicals is calculated. At 375°C, there is 1/30 of a radical per cc, at 425°C, 3, and at 475°C, 300. If each one formed adds immediately to a cyanogen molecule, the polymerization process should begin to become appreciable somewhere in this temperature range. Actually, it is observed to start slightly above 400°C, which is in satisfactory agreement with the calculations made above. This is further evidence that the first step in polymerization is the formation of free radicals and that at temperatures where polymerization occurs, free radicals of CN may add to cyanogen directly instead of recombining with each other.

HEAT OF VAPORIZATION OF GRAPHITE AND HEAT OF DISSOCIATION OF CO

To show the application of the present work to the determination of these two quantities, it is necessary to give an outline of the other relevant data. Herzberg[9] has given a very clear and detailed treatment of the problem in his review of this field, from which the important points in the following discussion are taken. By two thermodynamic cycles involving data that was incontestible, except for the heat of dissociation of cyanogen to two CN radicals, he obtained two relations between L, the heat of vaporization of graphite, D(CO), and D(CN). After the one involving D(CN) has been changed to correspond to the new value for cyanogen, they are:

$$L = \mathrm{D(CO)} - 85.6(\pm 0.5) \text{ kcal.}$$
$$\mathrm{D(CN)} = \mathrm{D(CO)} - 108(\pm 3) \text{ kcal.}$$

Thus, if any one of these three quantities can be determined, the other two follow directly. The most accurate information is that based on the predissociations observed in the CO spectrum. As Herzberg has pointed out, the predissociation limit at 11.054 volts is an extremely accurate value for a possible heat of dissociation. Unfortunately it is not necessarily the correct value. The data only tells us that the heat of dissociation has this value if the dissociation products are not excited, otherwise it is this value minus the excitation energy of the products. As the position of the low lying levels of carbon and oxygen are well known, it is possible to calculate the dissociation energies corresponding to all the permissible combinations of products. Herzberg's table of all these quantities compatible with the known vibration levels of CO is reproduced in Table IV with the changes necessitated by the new cyanogen value. The values of L and D(CN) corresponding to each possibility are also given. Unfortunately there is not enough evidence known from the CO spectrum to determine

[9] G. Herzberg, Chem. Rev. **20**, 145 (1937).

which possibility is the correct one. The selection must be made from supplementary data about CN or L.

The heat of dissociation of CN has not been determined accurately. However, the vibration levels of the lowest $^2\Sigma$ and $^2\Pi$ states have been observed directly up to 3.4 volts and those of the $^2\Pi$ have been clearly followed by using the perturbations up to 4.2 volts. As all the evidence indicates that these two states dissociate to the same products, the heat of dissociation must be larger than this. A Birge-Sponer extrapolation of the levels gives around 7 volts for the heat of dissociation of the normal state, which is almost certain to be too high. It would, however, be rather difficult to reconcile it and the known levels with a value less than 5.5 volts.

If CN dissociates to normal atoms, $C(^3P)+N(^4S)$, the highest possibility of Table IV is the only acceptable one, although the next is so close to the arbitrary limit we have set that it cannot be completely excluded. If CN goes to the first permitted combination of excited atoms, 1.35 volts above the ground state, the second, third, and fourth possibilities are acceptable. The high excitation energy of all the other combinations of products makes them incompatible with the known vibration levels of CO. The possible energies for the two pairs of products just mentioned can be further restricted by considering the dissociation energies allowed the $B^2\Sigma$ state of CN on the basis of the possible dissociation products remaining for it. In the first case the highest value gives a very reasonable heat of dissociation for the excited state, but the next highest is too low. This corroborates the conclusions drawn from the ground state and further decreases the likelihood of dissociation to normal atoms at 5.12 volts. In the second case, the third and fourth highest values are only compatible with the dissociation of the excited state to combinations of products two and three pairs above the lowest possible. The usual rule that a state dissociates to the lowest permissible pair of products indicates that these two possibilities are unlikely compared to the second. By the same rule, dissociation to excited atoms at 5.12 volts is less likely than to normal ones at 6.38 volts.

The effect of errors in the f value on these arguments should be considered. The greatest errors possible, corresponding to $f=1$ and $f=0.026$ increase and decrease $\Delta H_{0C_2N_2}$ by 0.60 and 0.33 volt, respectively, which would decrease or increase the values of D(CN) by half as much. The estimated probable error is 0.13 volt. All the possibilities mentioned above are permissible throughout this range except the third, which is impossible for the smaller f values. Dissociation to the first combination of normal atoms is always the most acceptable. In summarizing, we may say that if CN dissociates to normal atoms, the most reasonable value is 6.38 volts, and if it dissociates to excited atoms, 5.12 volts is the best one. As Sponer[10] and Mulliken[11] both give CN normal dissociation products, the most likely possibility is D(CN) = 6.38 volts, D(CO) = 11.054 volts, $L=169.2$ kcal.

This value of L is in excellent agreement with the thermal measurement of 177 kcal. made by Marshall and Norton[12] and with almost all the other evaporation method values. It does not agree with 150 kcal., the only equilibrium rather than dynamic value.[13] The discrepancy between these has been ascribed to experimental error and to a real difference between the equilibrium and dynamic vapor pressures. While the value chosen as most likely on the basis of the present work indicates that it is experimental error, the fact that the second choice gives a value of $L=140.2$ kcal. prevents us from making a positive selection between these two.

The author is indebted for helpful discussions and criticisms to Professor F. A. Jenkins, at whose suggestion the problem was undertaken, and to Professor G. K. Rollefson.

---

[10] H. Sponer, *Molekulspecktren*, p. 39.
[11] R. S. Mulliken, Rev. Mod. Phys. **4**, 48 (1932).
[12] A. L. Marshall and F. I. Norton, J. Am. Chem. Soc. **55**, 431 (1933).
[13] H. Kohn and M. Guckel, Zeits. f. Physik **27**, 305 (1925).

The Photolysis of Methylethyl Ketone

WALTER J. MOORE, JR. AND HUGH S. TAYLOR
Frick Chemical Laboratory, Princeton University, Princeton, New Jersey
(Received March 14, 1940)

The nature of the products from the photochemical decomposition of methylethyl ketone at temperatures from 90 to 200° has been re-examined. In contrast with earlier results, the formation of ethane, propane, and butane parallels the frequency of the corresponding free radical collisions. At the higher temperatures, however, production of ethane and especially of methane becomes predominant. The influences on the product distribution of secondary reactions, the lifetimes of the free radical collision complexes, and the activation energies and entropies, are considered.

THE photochemical decomposition of methylethyl ketone has previously been investigated by Norrish and Appleyard[1] using radiation in the near ultraviolet absorption region around 3000A, and more recently by Ells and Noyes[2] who worked in the region around 1850A. Both these investigations suggested that equivalent amounts of ethane, propane, and butane occurred in the reaction products, together with an amount of methane which increased markedly with increasing temperature. This result was indeed surprising, since if the hydrocarbons were formed by interaction of free radicals produced in the primary process, one would expect the ratio ethane : propane : butane to be approximately 1 : 2 : 1. The present experiments were undertaken to check this anomalous result, using a method of analysis for hydrocarbons which had proved reliable in previous studies of free radical reactions.[3]

Experimental Details

The photolyses were carried out in a static system identical with that used for our studies of metal alkyl decompositions.[3] Ketone at forty mm pressure was irradiated with the unfiltered output of a high pressure arc of the mercury-in-quartz type, operating hot at 55 volts and 3.5 amp. d.c., until about fifty percent was decomposed. The methylethyl ketone used was a product of the Eastman Kodak Company, purified by treatment with anhydrous copper sulfate, and careful fractional distillation. A fraction boiling within a tenth of a degree at around 79.5° was retained; its refractive index was $n_D^{15}=1.38118$, compared with a reported value for the pure compound[4] of $n_D^{15}=1.38140$.

The products, amounting to about five cc of gas, were analyzed as follows:

1. A fraction pumped off from liquid air was burned over cupric oxide at 310°, converting carbon monoxide to dioxide, from which methane could be pumped off at liquid-air temperature; the carbon dioxide was pumped off at −78°, and any residual vapor was assumed to be water.

2. A fraction pumped off at −138° (m.p. of ethyl chloride) was hydrogenated on nickel at 100° to determine ethylene, then cracked over nickel at 310° to methane, thus giving the average carbon content of the fraction. This fraction is made up of C_2 and C_3 hydrocarbons.

3. A fraction at −78°, consisting of C_3 and C_4 hydrocarbons, was similarly analyzed.

Experimental Results

The observations were extended over a temperature range of from 90 to 200°. At the lowest temperature there was observed a small amount of diketone formation, evidenced by the appearance of a yellow oil and the typical odor of diketones in the reaction vessel. At the higher temperatures, however, no diketone formation was detected. Tests for acetaldehyde with Schiff's reagent were negative. There was evidently some polymer formation at all temperatures, and after pumping off products volatile at −78°, an odor resembling that of mesityl

[1] Norrish and Appleyard, J. Chem. Soc. 874 (1934).
[2] Ells and Noyes, J. Am. Chem. Soc. **60**, 2031 (1938).
[3] Moore and Taylor, J. Chem. Phys. **8**, 396 (1940).
[4] J. Timmermans and F. Martin, J. chim. phys. **25**, 411 (1928).

oxide was distinctly noticeable; there was insufficient residue, however, to make possible the identification of the responsible compound or compounds.

The results of the analyses of the volatile products are given in Table I.

We note that at the lower temperatures considerably more propane is formed than either ethane or butane, but that at 200° the formation of methane and ethane is of primary importance.

TABLE I. *Percentage composition of photolysis products of* MeEtCO.

TEMP. °C	90	110	155	200
H_2	0.4	0.1	0.3	0.0
CO	47.5	49.0	47.0	48.5
CH_4	3.4	4.4	9.0	18.0
C_2H_4	2.2	0.5	1.7	3.0
C_2H_6	11.5	13.0	14.5	12.5
C_3H_8	19.1	20.0	18.6	11.0
C_4H_{10}	13.2	13.0	9.0	7.0
C_4H_8	1.5	—	0.0	—

GENERAL DISCUSSION

If, as a first approximation, we disregard the reactions of acetyl and propionyl radicals possibly arising in the primary process, the reactions with which we are concerned are as follows:

$$CH_3+CH_3=C_2H_6, \quad (1a)$$

$$CH_3+C_2H_5=C_3H_8, \quad (1b)$$

$$C_2H_5+C_2H_5=C_4H_{10}, \quad (1c)$$

$$CH_3+CH_3COC_2H_5=CH_4+CH_3COC_2H_4, \quad (2a)$$

$$C_2H_5+CH_3COC_2H_5=C_2H_6+CH_3COC_2H_4. \quad (2b)$$

At 110° the hydrocarbon products probably arise principally from the interactions of free radicals. The ratio of the numbers of collisions of types 1a : 1b : 1c is roughly 1.00 : 1.74 : 0.83, while the observed formation of ethane, propane, and butane are in the ratio 1.00 : 1.54 : 1.00. Assuming equal activation energies for the reactions (1), there are two other factors which may influence the relative recombination rates of the free radicals.

The lifetime of the quasi-molecule formed in the free radical collisions will increase from (1a) to (1c). The entropy of activation should decrease in going from (1a) to (1c), since it is less for reactions between more complex radicals.[5] A proper evaluation of these factors would perhaps suffice to explain the observed deviations from the purely kinetic theory ratios.

In addition, and especially at higher temperatures, the secondary reactions (2) will be of importance, leading to the formation of methane and ethane at the expense of the other hydrocarbons. A detailed kinetic analysis of these reactions is difficult and not very informative, since we can already follow qualitatively the effect of the decreased radical concentrations in decreasing the amount of recombination of radicals as compared with secondary reaction with ketone molecules.

It is interesting to note that methane is formed from methylethyl ketone considerably more easily than from acetone.[6] This difference may most reasonably be ascribed to the lowered energy of activation for the reaction of a methyl radical with $-C_2H_5$ to form C_2H_4, as compared with the reaction with $-CH_3$ to form CH_2.

It appears also that methyl radicals are more effective in polymerizing ethylene than are ethyl radicals, since much greater amounts of ethylene remain in the photochemical decomposition of diethyl ketone than are found with methylethyl ketone.[2,7] This is in accord with the results of experiments by Yeddanapalli and Jungers[8] on the relative efficiencies in ethylene polymerization of methyl and ethyl radicals prepared by reaction of the corresponding iodides with mercury vapor.

The formation of an oxygen-containing polymer from such fragments as $CH_3COC_2H_4$ would also account for the small amount of ethylene formation, this possibility being also suggested by the characteristic odor of the nonvolatile photolysis products.

[5] Bawn, Trans. Faraday Soc. **31**, 1536 (1935).

[6] Taylor and Rosenblum, J. Chem. Phys. **6**, 119 (1938).
[7] Noyes and Ells, J. Am. Chem. Soc. **61**, 2492 (1939).
[8] J. C. Jungers and L. M. Yeddanapalli, Trans. Faraday Soc. **36**, 483 (1940).

The Thermal Reaction Between Hydrogen and Oxygen

I. Comparison of Experiments and Theory

O. OLDENBERG AND H. S. SOMMERS, JR.
Research Laboratory of Physics, Harvard University, Cambridge, Massachusetts
(Received March 8, 1940)

The present theory of the slow thermal reaction between hydrogen and oxygen, while satisfactorily describing the existence of the various explosion limits, fails to describe the following features: the sudden transition from the slowest reaction to the explosion ("second explosion limit"), and some effects of the vessel size and of a KCl film on the rate and the second explosion limit. Conclusions regarding the theory are discussed.

I. PROBLEM

FOR certain spectrographic investigations which we shall report on in a subsequent paper, it is desirable to produce the maximum steady reaction rate of the thermal reaction of hydrogen and oxygen. As our work requires a large reaction vessel and pressures near atmospheric, the danger of a violent explosion prompted us first to study the explosion limits in smaller containers.

Hinshelwood and his co-workers[1] have described this reaction by means of the pressure-temperature diagram of Fig. 1. Explosion occurs for any combination of pressure and temperature located on the peninsula of the diagram; above and below this peninsula a steady reaction takes place. (On the scale of Fig. 1, the "Continuous Reaction" below the "First Limit" of the explosion peninsula does not show up.)

(Hinshelwood, investigating the explosion peninsula, called its borderlines "upper" and "lower" explosion limits. In our discussion the name "upper" limit would be misleading, since our attention is focused on the range of the steady reaction between this "upper" and the still higher "third" limit (Fig. 1). Therefore we shall use the term "second" instead of the conventional "upper" explosion limit.)

While older theories restricted themselves to rather vague outlines of the part played by the gas phase and the surface reactions, recently a detailed reaction scheme has been worked out by Kassel and Storch, and Lewis and von Elbe.[2] This theory accounts for a great many striking features of the reaction, in particular the various explosion limits and the steady reaction between the second and the third limit. In our experimental work we found many results explained by the theory, but also other results which we failed to reconcile with it. It is the purpose of the present paper to discuss whether this theory may need some modification.

II. THE PRESENT STATE OF THE THEORY[3]

There is general agreement that the reaction above the second explosion limit, at sufficiently high temperatures, is a chain reaction and that the walls play a part in breaking the chains. This hypothesis is necessary in order to explain the fact that the rate increases with the vessel size or with the addition of a foreign gas, which is expected to slow down the diffusion of the chain carriers to the walls.

[1] See the book by C. N. Hinshelwood and A. T. Williamson, *The Reaction between Hydrogen and Oxygen* (Oxford, Clarendon Press, 1934).

[2] L. S. Kassel and H. H. Storch, J. Am. Chem. Soc. **57**, 672 (1935); L. S. Kassel, Chem. Rev. **21**, 331 (1937); B. Lewis and G. von Elbe, J. Am. Chem. Soc. **59**, 656 (1937); B. Lewis and G. von Elbe, *Combustion, Flames and Explosions of Gases* (Cambridge University Press, 1938). See the recent textbook of H. J. Schumacher, *Chemische Gasreactionen* (Dresden and Leipzig, Theodor Steinkopff, 1938), p. 462. In some respect the most recent form of the theory, carried through in full detail by Lewis and von Elbe, differs from the earlier form, summarized by Kassel in Chem. Rev.; Kassel assumes that the chains ordinarily start on the walls with but a few originating in the gas phase, while Lewis and von Elbe find that the starting of most chains at the walls is incompatible with their scheme (book, p. 68).

[3] A detailed discussion of the theory is given in the book of Lewis and von Elbe, reference 2. In order to avoid confusion we apply the same numbers to the single reactions.

The detail of the theory is based on Semenoff's[4] conception of branching chains whose breaking *exceeds* the branching in the steady reaction and just *equals* the branching at the *explosion limits*. This is accomplished by the following chain:

$$OH+H_2 \rightarrow H_2O+H, \quad I$$
$$H+O_2 \rightarrow OH+O, \quad II$$
$$O+H_2 \rightarrow OH+H. \quad III$$

Since the *branching* reactions II and III are of the first order in the chain carriers, the *breaking* reaction is, to a certain extent, restricted by the theorem of Kassel and Storch.[2] This states that branched chain explosions can occur only if chain branching and chain breaking processes are of the same order with respect to the chain carriers. This requirement is fulfilled by the breaking reaction:

$$H+O_2+M \rightarrow HO_2+M. \quad VI$$

However, VI actually breaks the chain only if the radical HO_2 which is formed by VI is sure to be destroyed at the wall:

$$HO_2+\text{wall} \rightarrow \text{destruction}. \quad XII$$

The chain breaking reaction VI requires triple collisions. Therefore it becomes increasingly rare with decreasing pressure. This failure of chain breaking at low pressures explains the second explosion limit on the low pressure side of the steady reaction.

On the other hand, it is observed that at higher pressures the rate of the steady reaction increases with the pressure so strongly that for a certain high pressure limit another type of explosion results (third explosion limit). In order to explain this it is assumed that at higher pressure VI is not absolutely chain breaking, but that instead HO_2 has a chance to continue the chain by

$$HO_2+H_2 \rightarrow H_2O+OH. \quad X$$

X must be supposed to have a high energy of activation so that it comes into play only after numerous collisions but is ineffective at low pressures because of too rapid a diffusion of HO_2 to the wall. (The alternative continuation of the chain by $HO_2+H_2 \rightarrow H_2O_2+H$ is disregarded only because it would not materially affect the final result.)

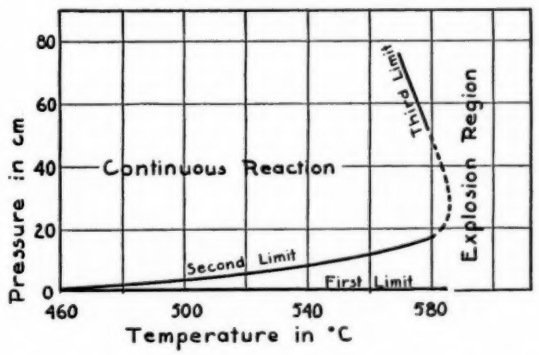

FIG. 1. Explosion limits of reaction of $2H_2+O_2$. First and second limits after Hinshelwood. Dotted section never investigated.

The chain is started by the thermal dissociation of H_2 in the gas phase

$$H_2+M \rightarrow H+H+M. \quad XIII$$

This set of reactions successfully describes a very complicated behavior; the steady reaction at varying pressure bordered *on both sides* by explosions.

By means of a detailed computation Lewis and von Elbe explain the shape of the curve of the second explosion limit (Fig. 1) and the effect of varying the partial pressures of H_2, O_2, and inert gases.[5]

In a letter to the editor,[6] we reported measurements of the third explosion limit, which also are in substantial agreement with the predictions given by the present theory.

III. DIFFICULTIES

While this theory explains the facts presented in the preceding section, it leads to some difficulties[7] with regard to other experiments which

[4] N. Semenoff, *Chemical Kinetics and Chain Reactions* (Oxford, Clarendon Press, 1935).

[5] Lewis and von Elbe identify the shape of this curve with the temperature dependence of reaction II (book, pp. 32 and 35). So they attribute an energy of activation of 24.2 to 26.0 kcal. per mole to this reaction. This agrees sufficiently well with the value of 32 kcal. per mole derived by Kantorowa and Nalbandjan on the basis of entirely different experiments (Physik. Zeits. Sowjetunion **4**, 758 (1933)).

[6] O. Oldenberg and H. S. Sommers, Jr., J. Chem. Phys. **7**, 279 (1939).

[7] As an outstanding difficulty Lewis and von Elbe (book, p. 68; J. Chem. Phys. **7**, 711, footnote 10 (1939)) mention the surprisingly strong effect of a silver surface in suppressing the reaction. Recently they succeeded in

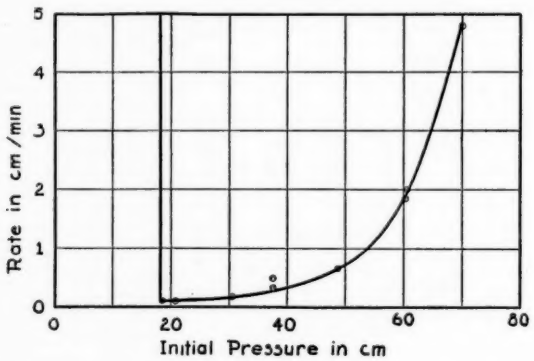

FIG. 2. Rate *versus* pressure. Approach to second explosion limit. Pyrex vessel coated with KCl. $T=568°C$.

will be discussed in the present section. Our disagreement with the theory is largely based on recent experiments which were not available to its authors.

A. The rate-pressure curve

An effect difficult to interpret is manifest in the rate-pressure curve (constant temperature, varying initial pressure, the rate measured either at the beginning of the reaction or, instead, after the inhibition period). Schematically such a curve was given by Thompson and Hinshelwood.[8] It shows a gradual decrease of rate with diminishing pressure to a very low value, suddenly terminated by the explosion (second explosion limit). As the abruptness of this change is very striking we checked it in greater detail. (We shall describe our experimental arrangement in a paper on the third explosion limit, to be published. For low pressure the mixture $2H_2+O_2$ cannot be directly admitted into an evacuated vessel because it would explode during admission; in order to prevent this a total of about 50 cm was admitted, beginning with H_2, and then quickly pumped out to the desired pressure.) The resulting rate-pressure curve is given in Fig. 2. The minimum rate was only 0.1 cm/min. The experiments were made in a KCl-covered Pyrex vessel, 14 cm long, 4.5 cm wide, at 568°C.

The same behavior was observed, without accurate measurements, in very many experiments with clean Pyrex as well as Pyrex covered with KCl: at a certain range of low pressures the reaction is very slow indeed, the more so the lower the pressure, while at a pressure slightly lower still, below a sharply defined limit, the second limit, explosion occurs.

This second explosion limit is reproducible, within a mm, in a large group of successive experiments in the same vessel. In some types of vessel it may depend on the rate of manipulation (see Section III *D*2). There is no conspicuous induction period;[9] as soon as gradual pumping brings the pressure to the limit, explosion occurs; if in another experiment the pumping is stopped a millimeter above the limit, an exceedingly slow reaction follows which never goes over into an explosion.

The explosion at the second limit is certainly not caused by heating, as it takes place after a minute change of pressure from another condition at which the rate is exceedingly low and, therefore, the heat production negligible. The sudden change of rate is explained, *in general terms*, by Semenoff's[4] theory of branching chains as follows. The explosion occurs as soon as the branching exceeds the breaking in one chain. If we assume the breaking to be caused by triple collisions, the average length of the individual chain increases with decreasing pressure until finally one of the chains gets out of control and leads to the explosion of the second limit. This picture, in which the explosion is attributed to the development of an individual chain, could be compatible with an over-all yield decreasing with decreasing pressure right above this limit (Fig. 2) only if we assume that the other factor affecting the over-all yield—the number of chains per sec.—decreases very strongly with the pressure.

While this *general* picture of the second explosion limit may seem satisfactory, the *specific* picture of the chain reaction given in the present theory must furnish such chains (number per sec., continuation, branching, breaking) as a function of the pressure as just described in the general picture. In the theory, the rate dH_2O/dt

explaining this effect themselves by the presence of silver in the vapor phase, exceeding the regular vapor pressure, so that this difficulty has been removed.

[8] H. W. Thompson and C. N. Hinshelwood, Proc. Roy. Soc. London, **A122**, 610 (1929).

[9] A very brief induction period of 0.1 sec. was discovered by A. Kowalsky (Physik. Zeits. Sowjetunion **1**, 595 (1932); **4**, 723 (1933)) with the help of a photographically recorded membrane manometer.

is expressed by a complicated equation (66 in the book by Lewis and von Elbe).[10] It is claimed that for any combination of partial pressures of hydrogen, oxygen, and a foreign gas, this equation represents the rate, in particular, in the various limiting cases in which the rate may approach infinity, that is, the explosion limits. For the second explosion limit this equation is simplified by neglecting the chain continuation through the radical HO_2, that is, discarding the reaction X: $HO_2+H_2 \rightarrow H_2O+OH$. The reason for discarding this reaction is that if HO_2 should be able to continue the chains, the second explosion limit would depend upon the vessel size. This would be contradictory to the observations of Hinshelwood. Another obvious simplification of the general formula is given by the fact that we are dealing with $2H_2+O_2$ without foreign gases (total concentration $M=2H_2+O_2$).

The explosion limits are derived from the equation for the rate by the requirement that the rate become infinite. As a matter of fact, the rate is derived from the theory as a smooth function of the pressure curving up, as expected, on both sides toward the vertical (Fig. 3). The minimum rate (caused by the counteraction of increasing chain length and decreasing number of chains) is derived from the same formula; it occurs at a pressure *twice as high* as the second explosion.[11] Hence the theoretical curve does not contain the sharp kink given by the experiments at a low value of the rate near the minimum of the curve (dotted line of Fig. 3).

To this argument the objection has been made that the left wing of the curve discussed (left of the dotted line) represents *unstable states*. This means that the curve accounts only for the initial reaction rate of the mixture; by the progress of the reaction the partial pressure of the reactive mixture decreases, so that the rate increases until the explosion occurs.

This intrepretation of the present theory seems to us not valid. First of all, the initial rate for a pressure slightly above the second explosion limit is so very low that even a considerable increase of rate would not affect the stability. A reliable criterion for the stability, however, is derived from the general equation for the reaction rate $d(H_2O)/dt$ (Eq. (66) in the book). This equation is supposed to express the rate for any concentrations of H_2, O_2, and a foreign gas (the latter in this case would represent the H_2O gradually developed by the reaction). But now, in contrast to the preceding application of the same formula, we want to discuss the progress of the reaction (not only the initial rate for which $M=2H_2+O_2$). Therefore, the variables H_2, O_2, and M are connected by the obvious relation expressing the gradual decrease of M by the reaction, $2H_2O$ replacing $2H_2+O_2$. Furthermore, dealing with the second explosion limit, we neglect reaction X (see above).

The result of a simple computation is that for the initial pressure which belongs to the minimum of the curve in Fig. 1, the rate not only remains finite throughout, but actually fails to increase during the reaction. This result of the theory contrasts with the experiment in which the explosion occurs right in the beginning of the reaction for conditions very close to those of an exceedingly slow reaction. Hence the theoretical formula does not lead to the abrupt change which is so striking in the experiments.[12]

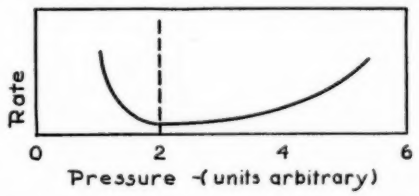

FIG. 3. Rate *versus* pressure. The solid line represents the theory of Lewis and von Elbe. The broken line indicates the pressure where the second explosion actually occurs.

[10] Although Lewis and von Elbe state it as their immediate aim to discuss experiments from 560°C upward, any explanation of the second explosion limit would be unsatisfactory which would fail to apply to the *whole* temperature range in which this type of explosion occurs, that is, down to 450°C. According to Hinshelwood and Thompson, the high order gas reaction comes into prominence already from 520–530°C; this applies to a conventional vessel size.

[11] This minimum is computed with the same approximation, neglecting reaction X. It is true that this must be applied only to the second explosion limit, not necessarily to higher pressures. But since the theory claims to represent the real curve in which minimum and second explosion limit nearly coincide, no such distinction must be made. Moreover, it is obvious that by discarding the approximation we may obtain a shifted position of the minimum, but by no means the sharp kink in the curve as it is actually observed.

[12] So far we have considered only the case of chain initiation in the gas phase, which is the case principally treated by Lewis and von Elbe. These authors also consider chain initiation at the wall (their Eq. (82)).

Another possibility for reconciling the theory with the abrupt transition from a very low rate to the explosion is as follows: In the theory, the chains get longer under decreasing pressure because the breaking requires triple collisions. It may happen that an individual very long chain develops a considerable amount of heat *within a small volume* and so causes the explosion. Such a local concentration of one chain can occur only if all steps of the chain take place without many intervening collisions, which would cause diffusion of the carriers and distribution of the heat over a wider volume. Hence a high heat of activation of one or the other step would militate against such local origin of the second explosion. The heat of activation of II is supposed to be high (30,000 cal./mole, see Section II). For such a high value, local heating is incompatible with the fact that the second explosion can be traced down to temperatures as low as 450°C where the consecutive steps of the chain would not be expected to follow each other without very many intervening collisions. The result is that we are unable to reconcile the present theory (chain breaking by formation in triple collisions of the radical HO_2) with the abruptness observed in the change from the lowest rates to the explosion.

This argument is directed against the *specific* picture of the reaction discussed in Section II. One still may hope to preserve the picture of the chain proper, that is, its continuation, breaking, and branching, and only mend the theory by introducing another starting process which would decrease very rapidly with the pressure. Although it may be mathematically possible to invent such a pressure function, it seems safe to guess that it would not represent a reasonable process of chains starting in the gas phase.

B. Effects of vessel size on second explosion limit and rate

Another difficulty arises from the effect of the vessel size on the *second explosion limit* and the *rate*. The second explosion limit is observed to be independent of the vessel size.[13] Theoretically, this leads to the conclusion that, under the conditions of the second explosion limit, reaction X (continuation of the chain by HO_2) is rare as compared to XII (destruction of HO_2 at the wall). Apart from the mathematical reasoning given by Lewis and von Elbe (book, p. 42), the exclusion of reaction X under the conditions of the second explosion limit may be understood as follows: According to the theory, the explosion is essentially a process in the gas phase. The only wall effect appearing in the reaction scheme (Section II) is the destruction at the wall of the HO_2 radicals. The observation that the second explosion limit is independent of the vessel size leads to the conclusion that the HO_2 is *certain* to be destroyed at the wall, irrespective of whether it travels a longer or shorter distance before it reaches the wall. Hence any chance for HO_2 to continue the chain must be relatively rare, that is, reaction X must be negligible under the conditions of pressure and temperature characteristic of the second explosion limit.

This explanation, however, necessarily involves an effect of the vessel size on the *rate* as is seen by the following argument. We understand that under the conditions of the second explosion limit the triple collision VI is absolutely chain breaking, since reaction X is excluded, independent of the vessel size. Hence the reaction X must be excluded as well at a pressure only very slightly higher, that is, in the region of the steady reaction, just above the second explosion limit. Hence the rate of this reaction must be independent of the vessel size, the wall having only the effect of destroying *each* HO_2 formed by VI. This theoretical conclusion is surprising, as experimentally the vessel size is known to affect the rate of the reaction strongly.

One may try to explain the discrepancy by the fact that *rates* are generally measured at pressures considerably higher than the *second explosion limit*. Such higher pressures obviously increase the chance for the continuation of the chain by X and so may explain the effect of vessel size on the rate. This explanation, however, does not agree with the numerical values, as is evident from the following comparison.

But after a thorough mathematical treatment they reject this hypothesis (p. 68) for several reasons. Anyway, it is of interest that this modification of their theory (although not so easily treated mathematically) does not lead either to the striking sharp kink near the minimum pressure which is actually observed.

[13] G. H. Grant and C. N. Hinshelwood, Proc. Roy. Soc. London **A141**, 31, Table III (1933).

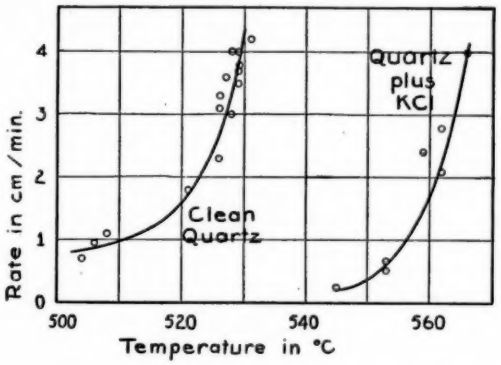

FIG. 4. Rate *versus* temperature. Quartz vessel clean and coated with KCl.

Grant and Hinshelwood found the second explosion limit to be 125 mm (at 552°C for 1 : 1 mixture), independent of the size, in silica bulbs up to 7.5 cm diameter. At a slightly higher pressure, say 130 mm, a steady reaction takes place, the rate of which, if the theory is correct, must also be independent of the vessel size (HO_2 being 100 percent destroyed at the wall). Unfortunately no data are available obtained under these conditions, but nevertheless the following extension of the argument indicates a disagreement between experiment and theory. For higher pressures a correspondingly smaller vessel will give the HO_2 the same 100 percent chance of being destroyed at the wall, and so lead to the prediction of a rate independent of the vessel size. (The relation between the two cases—low pressure, large vessel and high pressure, small vessel—results from the idea that the probability of an HO_2 radical being created at random in the volume and diffusing to the wall depends only on the total number of intervening collisions; it is independent of whether at low pressures these collisions spread over a long distance or at high pressures are concentrated within a small distance.) The result is that, for example, at a pressure of 300 mm the rate ought to be independent of the vessel size for bulbs with a diameter of at least $7.5 \times 125/300 = 3.1$ cm. This conclusion fails to agree with the rates given by Hinshelwood and Williamson. Silica bulbs of diameters 1.7 and 3.2 cm (identical lengths, $p = 30$ cm, 560°C) showed rates as widely different as 0.18 and 0.50. We conclude that the effect of the vessel size on the rate is pronounced in a range analogous to that in which the corresponding effect of the vessel size on the second explosion limit vanishes. This observed fact is contradictory to the theory. On this point, more extensive measurements are planned.

C. Effects of KCl surface

The effect of a KCl surface on the thermal reaction has to be explained by the theory from various points of view.

(*1*) *Effect of (KCl) on the rate.*—As discovered by Pease,[14] KCl covering the walls reduces the rate by a large factor. The experimental results, however, show some inconsistency, as Hinshelwood and Williamson[15] briefly report that KCl in quartz (as distinguished from Pyrex) loses its effect of reducing the rate. Lewis and von Elbe offer the plausible assumption that the experiments in quartz were performed at *higher temperatures* than those in Pyrex. They argue that under this condition the wall loses its effect on the rate, since the reaction takes place completely in the gas phase. This argument leads in particular to the hypothesis that chains *start* in the volume, at least at high temperatures. (Chain *breaking* may be the same in quartz and KCl.)

In order to find the reason for this inconsistency, we performed such experiments in Pyrex as well as quartz vessels. In a group of experiments with quartz we found a very pronounced effect of KCl. We varied the temperature over as wide a range as is permissible, just avoiding the explosion (60 cm pressure). This limited the temperature to about 538° in clean quartz. The comparison between quartz clean and quartz covered with KCl is given in Fig. 4. The effect of KCl at a certain temperature would be given by the ratio of the ordinates. In another quartz vessel, however, the rates were so much more erratic that the effect of KCl may be almost obscured when comparing extreme values. There is an additional effect which may help explain the failure of Hinshelwood and Williamson to find an effect of KCl applied to quartz; Prettre[16] found that "fused quartz changes by

[14] R. N. Pease, J. Am. Chem. Soc. **52**, 5106 (1930).
[15] C. N. Hinshelwood and A. T. Williamson, book, p. 50. See the book by Lewis and von Elbe, p. 50.
[16] M. Prettre, Mémorial des Poudres **27**, 255 (1937).

contact with KCl so that the effect of the KCl cover rapidly disappears." But our main objection to the argument just mentioned of Lewis and von Elbe is still another. The experiments of Hinshelwood and Williamson, comparing clean quartz and quartz with KCl cover, were certainly not performed at higher temperatures than those in Pyrex, because in any case the third explosion limit is below the softening point of Pyrex. For *Pyrex* and *Pyrex with KCl* the same relation between the curves holds as given in Fig. 4, up to the third explosion.

While these experiments remove one argument for the starting of the chains in the gas phase, they put the burden on the theory of explaining the high effect of KCl on the rate. Such a strong reduction of the rate by the wall is not easy to explain on the basis of the theory of Lewis and von Elbe. In this theory the wall affects the rate only by destroying chain carriers. It is assumed that the carrier HO_2, when colliding with Pyrex, is destroyed with nearly 100 percent efficiency (see Section II *B*). Thus, there is no margin left for another material to have a still higher destroying effect on HO_2. Therefore, we may assume that KCl has the power of destroying another chain carrier, O, OH, or H. O atoms do not have a very long life,[17] and therefore have not much chance of diffusing to the walls because of the rather low heat of activation of III.

If OH were the carrier with a life so long that it might be destroyed at the wall, a very large concentration of OH would be built up (in Pyrex still larger than in KCl), since each reaction II and III would produce one OH which would diffuse to the walls. This disagrees with our complete failure to detect any OH by its absorption spectrum in a layer as deep as 90 cm.[18] There remains H as the chain carrier that may be destroyed at KCl walls. This seems to be an exceedingly implausible picture, assuming that each link of the chain lives so long that the carrier H has an excellent chance to diffuse to the surface, where it may be destroyed if the surface consists of KCl, and may survive if it consists of glass. (This assumption, which cannot be completely excluded, would contradict the remark of Lewis and von Elbe (book, p. 40) that "a chain carrier spends most of its life as HO_2." But this statement seems to be unessential to their theory.)

(*2*) *Effect of the surface on the second explosion limit.*—Lewis and von Elbe base their discussion on the idea that only gas phase reactions need be considered for the theory of the second explosion limit, since it is practically unaffected by the walls. This had been observed for Pyrex, quartz, and porcelain. It is not confirmed by our results on the second explosion limit, comparing clean Pyrex with Pyrex coated with KCl (diameter 2.4″); coating raised the second explosion limit materially. Furthermore, the speed of manipulation had some effect. We determined such an effect in our KCl covered vessel by the following procedure: First, the explosion limit was determined to be 18.2 cm. Next, an initial mixture of 52 cm pressure was rapidly evacuated to 18.4 cm and then let stand. A very slow reaction took place. After six minutes we continued the pumping until the explosion occurred. Although during the waiting period the progress of the reaction was slow (only 4 percent of the mixture reacting) the second explosion limit was lowered from 18 to 12 cm. In general, the longer the period of waiting, the lower is the pressure of the second explosion limit. The amount of the water produced during the waiting period is so small that the present theory (attributing to H_2O only the part of an inert molecule) would not explain such an effect. Similar experiments performed in a clean Pyrex vessel also indicated significant effects of the rate of manipulation.

(*3*) *Effects of KCl on the rate and the second explosion limit.*—In the present theory, the effect of KCl, strongly reducing the rate, must be explained by the great power of KCl to break chains by destroying some type of chain carrier. This leads to the prediction that KCl should make the mixture far less explosive. Instead, the opposite is observed. As published in a letter to the editor,[6] KCl makes the explosion peninsula expand into the territory which, in clean Pyrex (diameter 2.4″, 540°C), would be occupied by the nonexplosive reaction. It seems difficult to reconcile this observation with the theory.

One may try to explain the fact that KCl

[17] P. Harteck and U. Kopsch, Zeits. f. physik. Chemie **B12**, 327 (1931).

[18] O. Oldenberg and H. S. Sommers, Jr., to be published.

strongly reduces the rate by a slow reaction of KCl with the glass walls so that the K is gradually built into the glass and Cl_2 is liberated, which in the gas phase may cause the effects described. That this explanation is wrong follows from the fact that the effect of Cl_2 on the *second explosion limit* is known to be the opposite; it reduces the size of the explosion peninsula. Furthermore, the effect of Cl_2 on the *rate*, although it is of the same type as the effect of KCl, is very much less pronounced.[19] We conclude that the liberation of Cl_2 is not responsible for the effects discussed with KCl covering the walls.

The vapor pressure of KCl is so small that such effects cannot be explained by the presence of its vapor. At 540°C this pressure is only 0.00028 mm.[20] This gives a mean free path of such a magnitude that collisions with a vapor molecule are not more probable than collisions with the wall. Furthermore, in a quiescent gas, when only an exceedingly slow reaction is going on, one cannot very well expect the vapor pressure of KCl to build up to a value far exceeding the equilibrium value.[21]

IV. Conclusions

The great successes of the present theory make it highly desirable to modify it as little as possible. Nevertheless, we did not succeed in our attempts to adapt it to the experimental results discussed in the preceding section. The following brief argument is intended only as a preliminary account of conclusions which, obviously, must be checked by more experimental work.

The main difficulties are summarized as follows: (1) the theory fails to describe the sharp kink in the rate-pressure curve; (2) the vessel size has no effect on the second explosion limit, but a strong effect on the rate in a pressure range where, according to the theory, it is not expected; (3) for the surface covered with KCl the effect on the rate (slowing down the reaction) would theoretically lead to an effect on the second explosion limit (reducing the tendency toward explosion) which contradicts the facts.

A. The second explosion limit

In the search for another theory one may be guided by the following consideration which would make a *surface* effect responsible, or partly responsible, for the second explosion limit. It is known that in the thermal hydrogen-oxygen combination two processes are superimposed, a gas phase reaction and a surface reaction. The gas phase reaction has a very high temperature coefficient, the surface reaction a low one.[1] Consequently, at high temperatures the gas phase reaction is much faster; on the other hand, "at temperatures below, or not much above 500°C, the reaction takes place almost entirely on the walls of the containing vessel" (Hinshelwood and Williamson). The second explosion limit has been reported by Thompson and Hinshelwood for temperatures as low as 450° where the gas phase reaction has almost completely vanished. Hence it is plausible to attribute this limit to the surface reaction.

According to Garstrang and Hinshelwood,[22] it is true that the *surface* reaction does not vary with the pressure in the required manner, showing no sign of increasing as the pressure drops from higher values toward the explosion limit. But this does not force us to attribute the second explosion limit to the *volume* reaction, as this reaction does not show such an effect either.[23]

Furthermore, it seems difficult to mend the present theory—attributing the second explosion to a *volume* effect—by assuming more involved steps in the volume reaction. The reason is that the treatment of Kassel and Storch seems to exhaust the possible volume reactions.

The main argument of Lewis and von Elbe for attributing this limit to a volume reaction had been the fact that it seemed practically unaffected by the walls. This argument is invalidated by the observation that KCl covering

[19] Hinshelwood and Williamson, book, p. 76.
[20] Joseph E. Mayer, J. Chem. Phys. **6**, 301 (1938).
[21] The situation is different in the experiment on a silver vessel. There, according to Lewis and von Elbe, a vapor pressure of Ag exceeding the thermal value builds up. It cannot be caused by the thermal reaction of $2H_2+O_2$ knocking out silver atoms, because in a silver vessel this reaction is infinitely slow. Presumably it is due to the oxidation of silver at 550°C.

[22] W. L. Garstrang and C. N. Hinshelwood, Proc. Roy. Soc. **A130**, 642 (1931).
[23] Alyea's (J. Am. Chem. Soc. **53**, 1324 (1931)) detailed scheme for the explosion as originating from the surface has been disproved by Garstrang and Hinshelwood (Proc. Roy. Soc. **A134**, 1 (1931)).

the walls materially changes this limit.[24] (With KCl the vessel size has a considerable effect on the limit, the larger size favoring the explosion. This suggests that the "second explosion" is not a straight surface phenomenon, for then it would be entirely unaffected by the vessel size. These observations will be discussed in a subsequent paper.)

Grant and Hinshelwood[13] presented some arguments for the theory that a process *in the volume* is responsible for the "second explosion." The present discussion, however, makes us believe more in an earlier argument of Thompson and Hinshelwood[8] which leads them to the "hypothesis of two simultaneously operating mechanisms."

The interpretation of the second explosion as caused, or partly caused, by the surface would straighten out the difficulties mentioned above: (1) the sharp kink of the rate-pressure curve would be understood by the thesis that, for a certain low pressure, a gas phase chain reaction is interfered with by some foreign substance coming from the surface; (2) the second explosion limit would lose its objectionable correlation with the rate as a function of vessel size; (3) the fact that KCl slows down the volume reaction would not lead any longer to a conclusion regarding the second explosion, because this would be attributed to the surface.

It is admitted that by attributing the second explosion limit to a surface effect we do not explain this explosion as satisfactorily as it apparently is done by the present theory; instead we shift difficulties to something the details of which remain unknown.

B. The chain reaction

How would this step modify the present theory? The change would be profound—far more so than we should wish. In the present theory, the complicated part played by the hypothetical radical HO_2 is largely introduced for the very purpose of explaining the second explosion limit. Once we attribute this limit to another process, there is not much reason left for introducing HO_2 and attributing a considerable chemical stability to it (ability to diffuse to the walls) at temperatures as high as 580°. Then the Bonhoeffer-Haber reaction may seem simpler and, therefore, preferable. In recent papers, Prettre[25] investigated the order of the thermal reaction and found that it agreed well with the Bonhoeffer-Haber scheme.

One difficulty is caused by the very powerful quenching a KCl surface exerts on the rate. This observation seems to be hard to explain by a gas phase reaction *starting in the gas phase*, so that for the surface no other effect on the chain would be left but breaking it. It may be preferable—in contrast to Prettre's hypothesis—to assume that the chains start at the surface. (This will be accessible to an experimental test.) Chains starting at the surface have also been assumed by Neumark, Kulashina and Poljakow[26] on the basis of other evidence. The theory of Lewis and von Elbe, however, cannot simply be modified by assuming that the chains start at the surface (instead of reaction XIII). The reason is that this modification would not describe the facts concerning vessel size and rare gases.[27]

Since new experiments are suggested by the present discussion, it seems futile to elaborate the theory any further before the experiments are carried out. The experimental work is being continued.

---

[24] O. Oldenberg and H. S. Sommers, Jr., reference 6. See also G. H. Grant and C. N. Hinshelwood, reference 13.

[25] M. Prettre, J. Chim. Phys. **33**, 189 (1936).

[26] E. Y. Neumark, L. P. Kulashina and M. V. Poljakow, Acta Physicochim, U. R. S. S. IX, 733 (1938).

[27] Lewis and von Elbe, book, p. 68.

Theoretical Isotherms for Adsorption on a Square Lattice

LEWI TONKS
General Electric Company, Schenectady, New York

(Received February 17, 1940)

A method which is not self-consistent has been used by J. K. Roberts to calculate the adsorption isotherm of adatoms, which are larger than the spacing of the adsorption sites on the substrate so that each adatom excludes all others from neighboring sites. It consists in completely formulating the internal statistics of a sample of the film surface and allowing for the effect of the rest of the film by introducing one or more "environmental" parameters as undetermined functions. These are determined by the requirement that each site of the sample shall be an average site. The failure of this method is traceable to the fact that these functions, when determined, are found to vary with surface concentration in a manner inconsistent with the physical requirements. The same difficulty is found to be latent in Peierls' treatment of adsorption with interaction between adatoms and in Bethe's treatment of superlattices. The adsorption isotherms for two cases with no interaction between neighbor adatoms are here calculated by another method. The one case is that of Roberts, the other that in which 9 sites are excluded by each adatom. The method requires separate treatment of dilute (small θ) and concentrated (θ nearly unity) films. At each extreme it involves successive approximations. For the dilute film' the number of free sites is determined as a function of the number of adatoms by enumerating the number of ways that adatoms occur (1) without overlapping of exclusion patterns, (2) with the exclusion patterns of only two adatoms overlapping, etc. This yields the adsorption isotherm. For the concentrated film, the interactions of the free sites themselves are treated in an analogous but necessarily somewhat different manner to give the adsorption isotherm near $\theta=1$. Some fairing of the relations to bridge the intermediate values of θ is necessary. The results are: for the 5-site exclusion pattern

$$\theta=2Ap[1-(5/2)\theta+(3/2)\theta^2+3/4\theta^3], \quad 0\leqq\theta\leqq 0.5$$
$$\theta=Ap[1-\theta-3(1-\theta)^3+5(1-\theta)^4], \quad 0.5\leqq\theta\leqq 1$$

and for the 9-site exclusion pattern

$$\theta=4Ap[1-(9/4)\theta+\theta^2], \quad \theta \text{ near zero}$$
$$\theta=2Ap(1-\theta)^2, \quad \theta \text{ near unity.}$$

These cases are compared with the limiting cases, first the 1-site exclusion pattern and second the infinity-site pattern which is the same case as adsorption on a siteless surface.

1. INTRODUCTION

IN conjunction with more general investigations by Langmuir[1] on the behavior of monatomic films of adatoms on an underlying crystal lattice, I undertook an investigation of the statistics of simple cases in which the adatoms were located on sites on the substrate and were large enough to prevent adsorption on neighboring sites. This was in 1936.

Since then several similar investigations have appeared[2,3] which found their inspiration in Bethe's treatment of the order-disorder problem[4] and are based on the use of a partition function. Such treatments have the appearance of deriving the adsorption isotherm of a surface film to a good approximation over the whole range form $\theta=0$ to $\theta=1$. On the other hand, I found it necessary, with my method, to treat the sparsely populated and the densely populated films as two separate cases, and to fill an intervening gap by "intelligent" guessing. The calculation became rapidly more complicated as higher orders of approximation were sought, and, I fear, leads at best to semiconvergent series.

But the difference between my results and those achieved by the newer method has led to a critical examination of the situation which exposes fundamental inconsistencies in the latter when it is applied to a case where the number of sites exceeds the number of close-packed adatoms.

In the following, I shall first analyze the newer method so as to exhibit its paradoxes, and second describe and apply the older more rigorous method.

[1] J. Chem. Soc. (London), April or May, 1940.

[2] R. Peierls, Proc. Camb. Phil. Soc. **32**, 471 (1936) first applied the general method to surface films. He was concerned with the case where the density of the close-packed film is equal to the density of sites, and the interaction energy between neighbors is negative.

[3] J. S. Wang, Proc. Roy. Soc. **A161**, 127 (1937) and J. K. Roberts, Proc. Camb. Phil. Soc. **34**, 577 (1938). J. S. W. treats the case where the interaction energy is positive, and hence can lead to exclusion—see curve *a* of his Fig. 2. J. K. R. treats exclusion plus interaction between permitted neighbors. The method used by these investigators will be designated as the PWR method.

[4] H. A. Bethe, Proc. Roy. Soc. **A150**, 552 (1935).

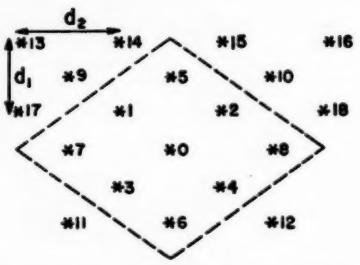

FIG. 1. Site arrangement of Roberts. Tonks' sample of film is outlined by the dashed lines.

2. THE PEIERLS-WANG-ROBERTS (PWR) METHOD

This method consists in choosing a small section of the adsorbing surface as a sample and writing down its partition function, taking account of the effect of the unanalyzed environment by undetermined functions as parameters. These are fixed by the condition that every site of the sample shall be an average site, that is, that the probability that it is occupied by an adatom is θ, the average coverage.

The model in which Roberts[3] was interested involves an adatom whose exclusion pattern covers the adjacent sites. Thus an adatom at site 0 on the 110 crystal face shown in Fig. 1 would prevent adsorption on 1, 2, 3 or 4, that is, it has an exclusion pattern which covers these 4 sites. In addition, adatoms forming a pair, as, for instance, two on 0 and 5 or 0 and 6 or 2 and 4, but not 0 and 7 or 0 and 8 (because they are further apart) have an interaction energy V. The adsorbed layer is in equilibrium with the gas, the adsorption energy per atom being χ.

As the sample area the seven sites, 0–6, were chosen. The partition function consists of a sum of terms of the type

$$g\eta^{p}\zeta_1^{n_1}\zeta_2^{n_2}\xi^{n_0+n_1+n_2}, \tag{1}$$

one for each of the possible configurations of the sample area. ξ is identified with the partition function B of the gas[3] per molecule, the adsorption energy χ, and the partition function[5] $v(T)$ for the adsorbed states

$$\xi=v(T)e^{\chi/kT}/B, \quad B=\left(\frac{2\pi mkT}{h^2}\right)^{\frac{1}{2}}\frac{kT}{p}b_g(T); \tag{2}$$

[5] R. H. Fowler, Proc. Camb. Phil. Soc. **31**, 260 (1935).

n_0, n_1, n_2 are, respectively, the number of adatoms in the central site (0 or 1), the first ring consisting of sites 1–4, or the second ring consisting of sites 5 and 6;

$$\eta=e^{V/kT};$$

and p is the number of interacting pairs in the configuration. ζ_1 and ζ_2 are the environmental parameters which can be looked upon as corresponding, respectively, to energies V_1 or V_2 of interaction between ring 1 or ring 2 and the surrounding film. g is the multiplicity of the configuration.

In order to maintain uniformity with Langmuir's notation. θ_R will be used for the PWR θ, and θ will here denote the fraction relative to close-packing that the surface is covered. It is apparent that

$$\theta=2\theta_R. \tag{3}$$

By formulating successively the probability of occupancy of the central site, a ring 1 site, or a ring 2 site in terms of the probabilities in the partition function, and then setting them each equal to θ_R, three equations result. From these ζ_1 and ζ_2 can be eliminated, leaving a relation between θ and ξ which, in effect, constitutes the adsorption isotherm by virtue of Eq. (2). Roberts has plotted such isotherms up to $\xi=400$ for $\eta=0.01$, 0.1, 1.0 to cover a range of interaction energies.

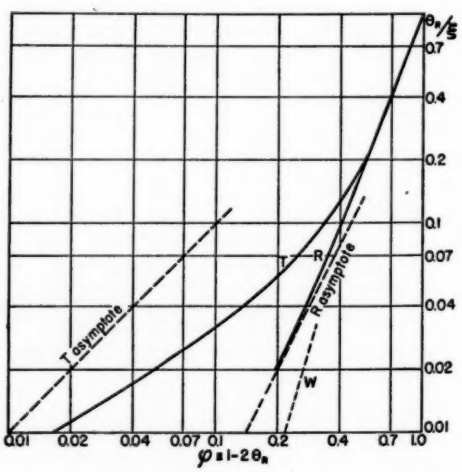

FIG. 2. Adsorption isotherm characteristics calculated by Roberts' method with zero pair interaction energy. R is for Roberts' sample of film. T is for Tonks' sample of film.

Henceforward we confine our attention to the case where the pair interaction energy is zero. Then $\eta=1$ and by Roberts' Eqs. (9) and (2),

$$\zeta_1=\zeta_2(\equiv\zeta).$$

At high values of ξ (high gas pressure, low temperature) it is easily found that asymptotically:

$$\zeta=\xi^{-\frac{1}{2}},\quad \theta_R=\tfrac{1}{2},\quad \theta=1$$

$$\varphi\equiv 1-\theta\equiv 1-2\theta_R=\frac{1}{\xi\zeta}=\xi^{-\frac{1}{2}}$$

whence, in the limit as $\theta\to 1$,

$$\theta/(2\xi)\to\varphi^2/2. \tag{4}$$

By a general line of reasoning it can be shown that for isothermal changes in the adsorbed film[6]

$$\theta=(2Ap)\theta_f, \tag{5}$$

where A is a constant, p the gas pressure, and θ_f the fraction of the total number of sites which are free to adsorb. When no sites are covered by adatoms on adjacent sites, it is evident that $\theta_f=1-\theta$ and we have Langmuir's adsorption isotherm. From Eq. (5) it thus appears that in general $\theta/(2Ap)$ is the fraction of "free" sites, and A is fixed by the requirement that at $\theta=0$, $\theta/(2Ap)$ shall be unity.

Now in Eq. (4), ξ is proportional to p and $\theta/2\xi$ is unity at $\theta=0$ as can be verified from Roberts' equations. Accordingly $\theta/2\xi$ is the $\theta/(2Ap)$ of the previous paragraph. Thus Eq. (4) becomes

$$\theta_f=\varphi^2/2. \tag{6}$$

This equation appears as "R asymptote" in Fig. 2. Hence the analysis yields the result that for an almost complete film the relative number of free sites is proportional to the square of the film's incompleteness.

TABLE I. *Component partition functions of sample area.*

n_1	P_{n_1}	P_{n_1}
0	$(\xi+1)(y+1)^4$	$=P_0$
1	$4x(y+1)^2$	$=P_1$
2 (adj.)	$4x^2(y+1)$	$=P_{2a}$
2 (opp.)	$2x^2$	$=P_{2o}$
3	$4x^3$	$=P_3$
4	x^4	$=P_4$

[6] See Eq. (41) of reference 1.

TABLE II. *Calculation of isotherm according to Roberts using Tonks' sample.*

y	0.1	1.0	3.0	10	30
x	0.1089	1.500	5.355	21.30	77.4
ξ	0.1189	2.033	6.357	16.92	40.86
$2\theta_R$	0.155	0.572	0.78	0.92	0.98
ζ_1	0.91	0.74	0.84	1.26	1.90
ζ_2	0.84	0.49	0.47	0.59	0.73

Once pair interaction energy has been abandoned, however, the choice of the 7-site sample appears somewhat arbitrary. The sites 0, 1, 2, 3, 4, 7, 8 are in every way equivalent to 0, 1, 2, 3, 4, 5, 6 and one should reasonably expect a more exact result if all the sites 0–8 were included in the sample.* This result should not differ significantly from Eq. (6).

The following procedure to handle this case, is, I think, somewhat less unwieldy than Roberts'. With him the "environmental" energies V_1 and V_2 are combined with the "site" energy to give the parameters

$$x=e^{V+V_1/kT}B^{-1},\quad y=e^{V+V_2/kT}B^{-1}.$$

The x and y are his ϵ_1 and ϵ_2. The partition function for the sample can now be formulated from a table each row of which contains the partition function for one possible configuration of the first ring (Table I). For the probabilities of finding the central site occupied, or a given first ring site occupied, or a given second ring site occupied, we then have:

$$\theta_R=\frac{\xi\partial(\Sigma P_{n_1})/\partial\xi}{\Sigma P_{n_1}}=\frac{(x/4)\partial(\Sigma P_{n_1})/\partial x}{\Sigma P_{n_1}}$$

$$=\frac{(y/4)\partial(\Sigma P_{n_1})/\partial y}{\Sigma P_{n_1}}.$$

The last two equalities lead to two relations,

Note added in proof.*—This analysis has recently been made by Roberts in an article (Proc. Camb. Phil. Soc. **36 (1), 53 (1940)) which reached the author after the present paper was submitted for publication. In that article the nature of the failure of the statistical method is not analyzed, but Roberts resorts to an empirical method to handle values of θ_R greater than 0.25. He does not seem to recognize that this technique does not lead to true equilibrium conditions (reference 1).

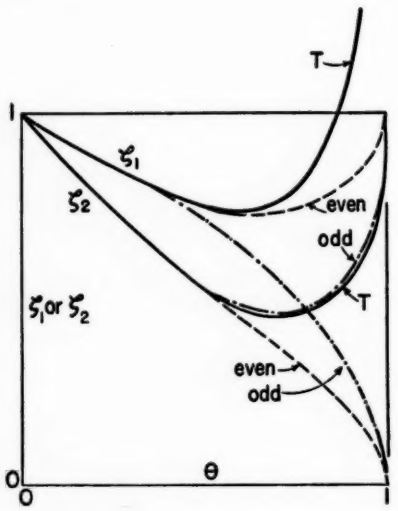

FIG. 3. Behavior of environmental parameters ζ_1 and ζ_2: (1) Qualitatively according to physical considerations, curves marked "odd" and "even." (2) As given by Roberts' method, curves marked T.

one between x and y:

$$x(1+x)^3-y(1+y)^4+xy(x-3y-xy-2xy^3)=0,$$

and the other for ξ in terms of x and y:

$$\xi=y[1+x(2+x+2y)(1+y)^{-3}].$$

Then from the first equality:

$$\frac{\theta_R}{1-\theta_R}=\frac{\xi(1+y)^4}{(1+y)^4+(1+x)^4-1+4xy(2+x+y)}.$$

Choosing a set of values of y, these equations were solved in order for x, ξ and θ_R, and the result is tabulated in Table II, and represented in Fig. 2 as Curve T. For the larger values of x it was necessary to use an expansion valid for this region which, in the limit, gives

$$\theta_f=\varphi.$$

Comparing this with Eq. (6) we are thus presented with the anomaly that an additional step toward closer approximation leads to a highly divergent result!

The nature of the trouble can be seen from the course of ζ_1 and ζ_2 which are also tabulated in Table II. The only influence of the environment on the sample lies in the possibility that the exclusion pattern of an external adatom covers a sample site. Accordingly this influence is always unfavorable to ring 1 and ring 2 occupancy.

The behavior of Bethe's ϵ is a guide to the reasonable behavior of the ζ's. He found that ϵ (comparable with ζ) was double-valued. The value lying between unity and infinity corresponds to a predominantly "right" environment, the value between unity and zero corresponds to a predominantly "wrong" environment. The situation here is similar. A complete film will occupy either the 0, 5, 6, 7, 8, 9, 10, 11, 12 etc. sites or it will occupy the 1, 2, 3, 4, 13, 14, 15, 16, 17, 18, etc. sites. In Langmuir's terminology it will either be an *even* film, which we can arbitrarily identify with the former, or an *odd* film. Thus in place of "right" and "wrong" we have "odd" and "even." It is apparent that ζ_1 for an odd film decreases to zero with increasing θ. On the other hand, ζ_2 finally increases to unity because the odd environment excludes ring 2 sites less and less. Accordingly we should expect the situation shown qualitatively by the $\zeta_{1\,\mathrm{odd}}$ and $\zeta_{2\,\mathrm{odd}}$ curves of Fig. 3. For an even film the situation would be approximately reversed, as shown by the $\zeta_{1\,\mathrm{even}}$ and $\zeta_{2\,\mathrm{even}}$ curves in the same figure. Therefore, any solution which is valid for the whole range of θ must have two pairs of values for the ζ's, which behave in accordance with the foregoing analysis. It follows that the equality of ζ_1 and ζ_2 found by Roberts proves the incorrectness of the method, as does the variation which the newer calculation gives for the ζ's. These values are plotted in Fig. 3.

It seemed possible that if a large enough sample were taken so that the environment did not directly affect sites whose probability of occupancy was set equal to θ, then a valid result might be obtained. I tried this with a square sample of 13 sites (0–12 in Fig. 1). The equations were

$$\theta=\text{Prob. for site 0}=\text{Prob. for site 1.}$$

This meant that only one parameter could be introduced. Noting that site 5 could be covered from the outside in two ways, whereas 9 could be covered in three, I chose

$$\zeta_{\mathrm{corner}}=(\zeta_{\mathrm{medium}})^{\frac{3}{2}}.$$

This, I think now, was not a good guess, but the attempt has convinced me that the method is

unworkable, for the nature of the equations is such that with finite ζ's, ξ cannot approach infinity. It remains possible that by replacing ζ with some function of ξ or θ the method might be salvaged.

The environmental parameter does not lead to these difficulties in the range where Bethe's[4] results are of interest; namely, in the neighborhood of the transition to complete disorder. His two successive approximations do not give diverging results, and, as has been discussed, the variations of ϵ' and $1/\epsilon'$, the two possible values of ϵ, are consistent with the physical requirements. But as complete order is approached ϵ' goes to infinity. However, the most favorable environmental effect will occur when all the environmental neighbors, approximately $Z/2$ in number, are right. This means that the largest physically attainable value of ϵ' is of the order $x^{Z/2}$. A similar argument applies to $1/\epsilon'$. This is a limitation of the theory where the ordering tendency is high—just the range where the adsorbed film behavior is being analyzed.

Peierls[2] has dealt with an adsorbed film without encountering the present difficulties. He considers adatoms whose exclusion pattern includes only the site which the adatom occupies. It is interesting to note what happens when an exclusion pattern covering nearest neighbors, which is latent in Peierl's treatment, is accentuated. This can be brought about by putting his interaction energy, $-V$, equal to $+\infty$. Then η, his Eq. (4), becomes zero, and solving

$$\epsilon=\zeta\xi$$

and his Eq. (10) with $\eta=0$:

$$\xi=\epsilon(1+\epsilon)^{Z-1}$$

simultaneously for ζ for large ξ we have

$$\zeta=\xi^{-(Z-1)/Z}\rightarrow 0.$$

This is absurd, because, by assumption the central sample site is an average site so that a valid method would yield a second value of ζ which approaches unity.

Wang has brought out the latent difficulty in P's equations by applying them to the case where η is small. So doing simply gives another in the set of divergent results. A replot of Curve *a* of W's Fig. 2 ($\eta=5.53\times10^{-4}$) above $\xi=20$ onto the coordinates of the present Fig. 2 gives the curve W.

Faced with these failures to solve the problem before us by Bethe's ingenious stratagem, it is pertinent to examine the older method.

3. Calculation of Adsorption Isotherms—Assumptions and Nomenclature

The cases which will be discussed are some of those listed by Langmuir.[1] A square array of sites on a substrate is assumed, each one of which can hold an adatom with a certain energy of attachment. The adatoms are supposed to have a diameter d_a, the sites to be a distance d_s apart. Thus depending on the ratio d_a/d_s, one adatom will prevent any other atom from occupying a total of 1, 5, 9, 13, 21 etc. sites. Any such array of sites constitutes an *exclusion pattern* and any site in the array is *excluded*. The central site is *occupied* and the rest of the excluded sites are *covered*. Any site which is not excluded is *free*.

There is the further assumption that there is no interaction energy between adatoms (save that which maintains the exclusion pattern).

We now define: E=number of sites in the exclusion pattern, σ_s=number of sites per unit area, σ_E=number of excluded sites per unit area, σ_f=number of free sites per unit area, σ_1=number of adatoms per unit area when close-packed,

$$\gamma=\sigma_s/\sigma_1, \tag{7}$$

σ=number of adatoms per unit area,

$$\theta_f=\sigma_f/\sigma_s, \tag{8}$$

and, as before,

$$\theta=\sigma/\sigma_1. \tag{9}$$

The method to be used depends upon Eq. (5), used here in the form

$$\theta=\gamma A p\theta_f. \tag{10}$$

The procedure will be to calculate θ_f in terms of θ, or what amounts to the same thing, σ_f in terms of σ.

Incidentally, from the previous discussion we see that

$$A=\xi/p \tag{10.5}$$

with ξ given by Eq. (2).

4. Adsorption Isotherm for $E=5$, $\gamma=2$ for Low Concentration

This is the case the treatment of which by Roberts has already been discussed. Each adatom excludes its own and the four neighboring sites. The lattice need not be square but can, within a certain range of side ratio, be face-centered rectangular. If the sides of the elementary rectangle are d_1 and d_2, $d_1<d_2$, the range of adatom diameter within which the present case applies is

$$\tfrac{1}{2}(d_1^2+d_2^2)^{\frac{1}{2}}<d_a<d_1.$$

The limiting proportion for the rectangle occurs when the range for d_a vanishes, i.e., when

$$d_2/d_1=3^{\frac{1}{2}}.$$

For the square array,

$$d_1=d_2=2^{\frac{1}{2}}d_s,$$

so that the range of d_a is

$$d_s<d_a<2^{\frac{1}{2}}d_s.$$

For convenience we shall think invariably in terms of a unit area of surface.

We shall be repeatedly interested in the probability that a given site is occupied. Evidently this is σ times the chance that it is occupied by a particular adatom, which is $1/\sigma_s$. This chance has been lessened by the fact that there is some probability that the particular site lies within an exclusion pattern. If it is known that this is not the case, that is, that the site is not excluded by any of the $\sigma-1$ other adatoms, then the probability of finding the particular adatom on it is $1/\sigma_f$. The relation between the two at low concentrations, i.e., when $\sigma\ll\sigma_1$, is apparent from the fact that each adatom excludes 5 sites so that

$$\sigma_f=\sigma_s-5\sigma. \tag{11}$$

This cannot be the general relation for σ_f, for it assumes that every adatom excludes 5 sites, none of which are excluded by any other adatom. Whenever two (or more) exclusion patterns overlap σ_f is greater than the Eq. (11) value. Thus the problem of calculating σ_f is that of enumerating the ways in which exclusion patterns can occur, singly and overlapping, and the frequency of each configuration so that the excluded areas contributed by all of them may be summed for subtraction from σ_s.

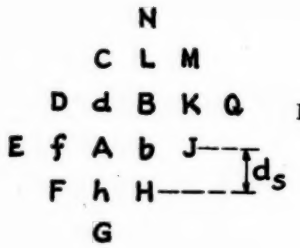

Fig. 4. Sites on adsorbing field.

The calculation can be made by successive approximations. The first is given by Eq. (11). The smaller σ the better an approximation it is, for the smaller relatively is the number of overlapping patterns which it neglects. The next approximation considers the *doublets*, that is, the pairs of adatoms whose exclusion patterns overlap; and the third takes *triplets*, three adatoms which have a continuous exclusion pattern, into account. Since each doublet contains two singlets, and each triplet contains 3 singlets and two or three doublets, there is a possibility of overcounting. To avoid this, only those adatoms can be counted as singlets, whose exclusion patterns are isolated from other exclusion patterns, so that it is known that they are not parts of doublets, triplets, etc. These will be called *isolated singlets*. Similarly, only *isolated doublets* will be counted.

In this connection it becomes necessary to calculate the probability of finding an adatom at a site when something is known about neighboring sites. For instance, given an adatom at A, Fig. 4, what is the probability of finding one at B? It is greater than σ/σ_s because B certainly is not covered by an adatom located at either b or d, and it is less than σ/σ_f because it may be covered by an adatom at L or K.

Consider the probability that a particular atom, X, is located at B. It is $1/\sigma_s$. But alternatively it is the probability that B, b, d, L and K are unoccupied by any other atom and that X is on the otherwise free site A, namely,

$$\frac{1}{\sigma_f}\left(1-\frac{\sigma}{\sigma_s}\right)^5.$$

Since every adatom can have the role of X, we have then two expressions, necessarily equal,

for the probability of finding a site occupied:

$$\frac{\sigma}{\sigma_s}=\frac{\sigma}{\sigma_f}\left(1-\frac{\sigma}{\sigma_s}\right)^5. \tag{12}$$

This equation is identical with Eq. (11) to the first-order approximation, which is as far as either of them are valid. Formulated in terms of X, the right member of Eq. (12) appears reasonable enough, but considered in terms of the probability of finding an adatom in general at B, it appears somewhat paradoxical, for it is the product of the six probabilities that b, d, L, K and B are unoccupied and that B as a free site is occupied.

The original question can now be answered. The probability of finding an adatom at B when one is already at A is the probability that L, K and B are unoccupied and that B is occupied as a free site, that is,

$$\left(1-\frac{\sigma}{\sigma_s}\right)^3\sigma/\sigma_f.$$

Since the approximation we shall make is to take triplets into account, the relative number of which is of the order σ^3, all probabilities must be correct to terms of this order.

We first consider isolated singlets, an adatom at A is isolated if B, C, D, E, F, G, H, J, are all unoccupied. On this basis the number of isolated singlets would be

$$\sigma\left(1-\frac{\sigma}{\sigma_s}\right)^8=\sigma\left(1-8\frac{\sigma}{\sigma_s}\right).$$

This is valid only to σ^2, that is, as far as it has been expanded. To justify another term in the expansion the σ/σ_s needs correction. The rule already established is applied to occupancy of B. The probability of an adatom at B is

$$(1-\sigma/\sigma_s)^3\sigma/\sigma_f$$

rather than σ/σ_s since we know that b and d are unoccupied. For C, since of its neighbors only d is certainly unoccupied, the probability is

$$(1-\sigma/\sigma_s)^4\sigma/\sigma_f.$$

The probability that B and C and the other 6 sites are all unoccupied is then

$$[1-(\sigma/\sigma_f)(1-\sigma/\sigma_s)^3]^4[1-(\sigma/\sigma_f)(1-\sigma/\sigma_s)^4]^4.$$

Since the final approximation does not distinguish between σ_s and σ_f, σ_f can be substituted for σ_s. Putting

$$\psi=\sigma/\sigma_f=\theta/\gamma\theta_f \tag{13}$$

for convenience and noting that there are σ adatoms like A, the total number of isolated singlets is seen to be

$$\sigma[1-\psi(1-\psi)^3]^4[1-\psi(1-\psi)^4]^4,$$

each excluding 5 sites.

There are two types of doublet, the d type represented by adatoms at A and B, and the s type by adatoms at A and J.

In the former case, the occurrence of an adatom at B, as we have already seen, is governed by the probability $\psi(1-\psi)^3$. For this doublet to be isolated requires further the unoccupancy of sites N, C, D, E, F, G, H, J, Q, M, ten in number, introducing the probability factor $(1-\psi)^{10}$. Other d doublets involving A are AD, AF, and AH. The last two will be counted with sites F and H, respectively, the first requires a multiplicity factor 2 in the probability. Thus the number of d doublets is

$$2\sigma\psi(1-\psi)^{13} \text{ each excluding 8 sites.}$$

Similar reasoning for s doublets gives

$$2\sigma\psi(1-\psi)^{16} \text{ each excluding 9 sites.}$$

Of triplets there are 5 types, all shown in Fig. 5. Their common probability factor is ψ^2. This is to the required degree of approximation as it stands. The number of type a with multiplicity 2 is $2\sigma\psi^2$ excluding 13 sites each.

The information for all five types is given in Table III. From this it appears that the whole number of cells excluded by triplets is

$$240\sigma\psi^2.$$

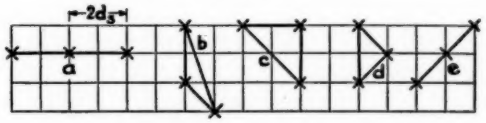

FIG. 5. Triplets—arrangements of three atoms having overlapping exclusion patterns.

TABLE III. *Types of triplets and their characteristics.*

TYPE	NUMBER OF EXCLUDED SITES	MULTIPLICITY	TOTAL EXCLUSION FOR TYPE
a	13	2	26
b	12	8	96
c	13	4	52
d	11	4	44
e	11	2	22
Total Multiplicity		20	
Total Exclusion, all Types			240

By way of a check on the method used here to calculate the occurrences of the various configurations, we note that the sum of the isolated singlets plus twice the isolated doublets plus thrice the triplets should equal σ identically through terms in ψ^2. It does.

The sum of the excluded sites from (5), (6), (7) and (8) plus the free sites is equal to the total number σ_s:

$$\sigma_s=\sigma_f+5\sigma[1-\psi(1-\psi)^3]^4[1-\psi(1-\psi)^4]^4 +16\sigma\psi(1-\psi)^{13}+18\sigma\psi(1-\psi)^{16}+240\sigma\psi^2. \quad (14)$$

Dividing Eq. (14) through by σ_f, expanding the right member through ψ^3, and noting Eqs. (7), (8) and (9), we find

$$\theta_f^{-1}=1+5\theta/\gamma\theta_f)-6[\theta/\gamma\theta_f)]^2+24[\theta/\gamma\theta_f)]^3. \quad (15)$$

Formally, the problem is now solved, for this gives the required functional relation between θ and θ_f which, with Eq. (10) establishes the relation between p and θ.

To express θ_f in terms of θ we assume the result with undetermined coefficients:

$$\theta_f=1+\alpha\theta+\beta\theta^2+\delta\theta^3$$

and fix them by substitution in Eq. (15). As a result

$$\theta_f=1-\tfrac{5}{2}\theta+\tfrac{3}{2}\theta^2+\tfrac{3}{4}\theta^3. \quad (16)$$

Thus for the adsorption isotherm we have

$$\theta=2Ap[1-\tfrac{5}{2}\theta+\tfrac{3}{2}\theta^2+\tfrac{3}{4}\theta^3]. \quad (17)$$

Curve A_1 in Fig. 6 is a plot of θ_f against $1-\theta$ down to $1-\theta=0.5$.

The whole treatment is dependent upon treating ψ as a small quantity. Eq. (14) is seen to contain powers of $(1-\psi)$ up to the 16th. In expanding to

$$1-16\psi+120\psi^2-560\psi^3$$

all terms but the first two were necessarily neglected. Rigorously this limits the present result to values of ψ of the order of $\frac{1}{32}$ or less, so that θ is limited to less than $\frac{1}{16}$ by Eq. (13). This is a severe restriction inherent in the method which would make further approximations along the present line futile. The fact that the coefficients 6 and 24 in Eq. (15) are differences between much larger numbers suggests, however, that this limitation may be more severe than necessary. Besides, the succession of coefficients in Eq. (17) points even more strongly in the same direction. It is for this reason that the curve has been carried down to $\theta_f=0.22$ at $\theta=0.5$.

5. ADSORPTION ISOTHERM FOR $E=5$, $\gamma=2$ HIGH CONCENTRATION

In order that full coverage of the field should occur, that is, that $\sigma=\sigma_1=\sigma_s/2$, it is necessary that all adatoms lie in one of the two possible but identical lattices. Langmuir[1] discusses how the coexistence of both leads to long time effects in reaching a true equilibrium. In the present analysis I confine my attention to a nearly complete film, which requires that it be predominantly of one type, let us say the even one.

At first every adatom which evaporates from a complete lattice leaves only one free site behind it. But when four adjacent adatoms in a square have evaporated, case 4*a* of Fig. 8, it is seen that there are five free sites; for the central site is uncovered when the last of the four corner sites loses its adatom. It is thus possible that σ_f exceeds $\sigma_1-\sigma$. On the other hand, an atom condensing into the central site, case 3*a* of Fig. 8 (forming a single adatom in the odd lattice) excludes four other previously free sites. Thus σ_f can be less than $\sigma_1-\sigma$. In general this will be the case because there is a strong tendency to form the odd lattice as σ decreases.

We shall denote the deficiency in σ_f by σ_d thus:

$$\sigma_d=\sigma_1-\sigma-\sigma_f \quad (18)$$

and shall then calculate σ_d in terms of the other quantities in Eq. (18). Finally, by eliminating σ_d, σ_f can be expressed as a function of $(1-\theta)$.

This problem could probably be approached in the same way as the dilute film except that we consider free sites rather than adatoms as distributed over the surface. There is, however, the essential difference that the adatoms are conserved, whereas the number of free sites depends upon the configuration of the film. θ fixes σ, but the same θ can yield many values of σ_f.

We shall again in this case deal in isolated configurations in order to avoid overlapping and multiple counting. To assure isolation it is necessary and sufficient that the configuration shall be bounded by a single close-packed line of even adatoms. See Fig. 8. The omission of a corner adatom would permit another configuration to have a covered site in common, the omission of a side boundary atom would allow a common free site. As before we can use the terms singlets, doublets, etc. but now they apply to free sites.

Since the equilibrium condition of the surface is independent of the mechanism of evaporation and condensation, provided they are not inconsistent, the analysis can be based on the assumption that n adatoms evaporate at random from the occupied sites per element of time, and that the same number condense at random on free sites. The probability of evaporation P_e of a given adatom is, therefore,

$$P_e=n/\sigma=n\sigma_1/\theta \tag{19}$$

and the probability P_c that condensation occurs on a given free site is

$$P_c=n/\sigma_f. \tag{20}$$

Consider a sample area of the surface containing a certain number of sites which are grouped around site S, and denote the configuration of the adatoms as type α. Let the total number of α configurations which exist on the surface in equilibrium be σ_α. We suppose that the evaporation of any one of ρ_α adatoms from α will give a new configuration β, whose total occurrence is σ_β, and likewise that the condensation of an adatom into any one of ρ_β free sites in β will give an α configuration.

Accordingly, the rate $\alpha\rightarrow\beta$ will be

$$P_e\rho_\alpha\sigma_\alpha$$

and the rate $\beta\rightarrow\alpha$ will be

$$P_c\rho_\beta\sigma_\beta.$$

The principle of detailed balancing requires that these rates be equal, whence, using Eqs. (19) and (20),

$$\sigma_\beta=\sigma_\alpha(\rho_\alpha/\rho_\beta)\theta^{-1}(\sigma_f/\sigma_1). \tag{21}$$

This relation enables us to calculate successively more complicated configurations. It is convenient to put

$$\sigma_f/\sigma_1=2\theta_f=\varphi_f. \tag{22}$$

Let the α and β configurations be those of Fig. 7*A*. The multiplicity of α is unity. The probability that the 9 lattices points shall be simultaneously filled is θ^9, and the number of sites which could be S is σ_1. Accordingly,

$$\sigma_\alpha=1\times\theta^9\times\sigma_1=\sigma\theta^8.$$

Also,

$$\rho_\alpha=1, \quad \rho_\beta=1.$$

Therefore by Eqs. (21) and (22)

$$\sigma_\beta=\theta^8\sigma_f=\sigma_1\theta^8\varphi_f$$

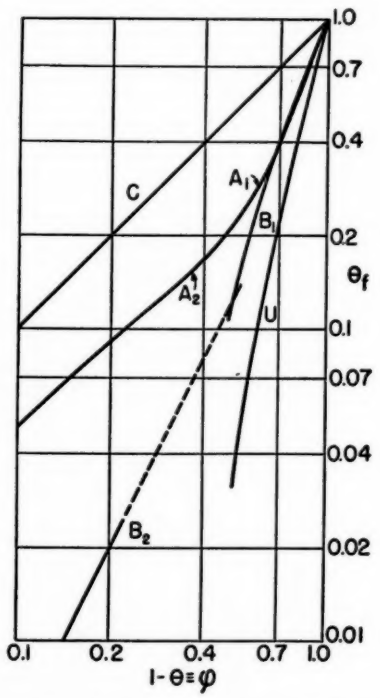

FIG. 6. Various adsorption isotherm characteristics. A_1, $\gamma=2$, Eq. (17), $\theta<0.5$. A_2, $\gamma=2$, Eq. (29), $\theta>0.5$. B_1, B_2, larger adatoms, $\gamma=4$, Eqs. (32) and (31). *C*. Smaller adatoms, $\gamma=1$. Eq. (33). *U*. Adatoms on a uniform field.

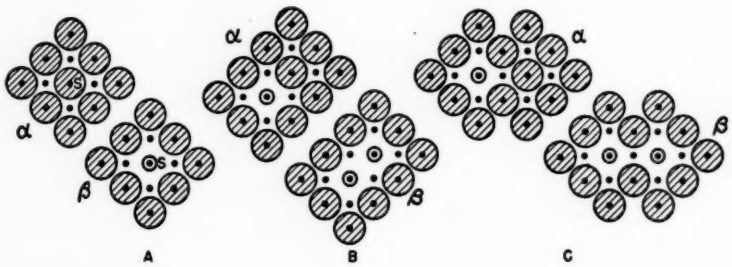

FIG. 7. Surface configurations involving isolated free sites. Dots show sites, small circles show free sites, large circles show adatoms.

and this is the number of isolated free sites, to be denoted by σ_{f1},

$$\sigma_{f1}=\sigma_1\theta^8\varphi_f. \tag{23}$$

For isolated doublets, d type, we have the α and β configurations of Fig. 7B. Evidently σ_α is directly related to σ_{f1} with a multiplicity of 4:

$$\sigma_\alpha=4\sigma_{f1}\theta^3=4\sigma_1\theta^{11}\varphi_f.$$

Also,

$$\rho_\alpha=1, \quad \rho_\beta=2.$$

Therefore

$$\sigma_{f2d}=2\sigma_1\theta^{10}\varphi_f{}^2. \tag{24}$$

Likewise, for isolated doublets, s type, the α and β configurations are shown by Fig. 7c and

$$\sigma_{f2s}=2\sigma_1\theta^{12}\varphi_f{}^2. \tag{25}$$

The general rule for the occurrence of these configurations is that

$$\sigma=A\sigma_1\theta^{\Sigma}\varphi_f{}^{\Sigma_1-\Sigma}, \tag{26}$$

where A is the multiplicity, Σ the number of adatoms in the configuration, and Σ_1 the number of even sites.

The validity of this method of calculating has been verified for first, second and third orders by adding the number of free sites due to isolated singlets, isolated doublets and triplets using Eqs. (23), (24) and (25) and 5 similar expressions for the triplets, and checking that the sum is equal to σ_f through terms in $\sigma_f{}^3$. Beyond this the configurations for quadruplets etc. are so many in number as to make wider verification unpractical. That already carried out is sufficient to demonstrate the soundness of the counting method.

Accordingly, from here on we confine ourselves to configurations which contribute to σ_d. The first that we consider is that of 4a of Fig. 8 where 4 adjacent free sites in a square yield a fifth free site in the odd lattice. That the rule already stated in Eq. (26) applies in this and future cases will be assumed; in any case it can be confirmed by the method of Eq. (21).

Using a subscript for σ from the representations of Fig. 8,

$$\sigma_{4a}=\sigma_1\theta^{12}\varphi_f{}^4.$$

For each occurrence 4a contributes an amount Σ_d to σ_D:

$$\Sigma_d=\Sigma_1-\Sigma-\Sigma_f,$$

Σ_f being the number of free sites. This expression for the individual configuration is strictly analogous to Eq. (18) for the film as a whole.

Since

$$\Sigma_f=5 \quad \text{and} \quad \Sigma_1-\Sigma=4,$$

it follows that

$$\Sigma_d=-1 \text{ for } 4a.$$

TABLE IV. *Configurations in incomplete film.*

SYMBOL	MULTIPLICITY A	$\Sigma_1-\Sigma$	NO. OF SITES Σ_1	NO. OF ADATOMS Σ	FREE SITES Σ_f	$\Sigma_1-\Sigma-\Sigma_f$ Σ_d	$A\Sigma_d$	CONTRIBUTION TO σ_d
ALL CASES	FOR WHICH	<3	YIELD			0	0	0
3a	1	3	16	13	0	3	3	$3\sigma_1\theta^{13}\varphi_f{}^3$
4a	1	4	16	12	5	−1	−1	$-\sigma_1\theta^{12}\varphi_f{}^4$
4b	8	4	19	15	1	3	24	$24\theta^{15}\varphi_f{}^4$
4c	4	4	21	17	1	3	12	$12\theta^{17}\varphi_f{}^4$
4d	2	4	20	16	0	4	8	$8\theta^{16}\varphi_f{}^4$

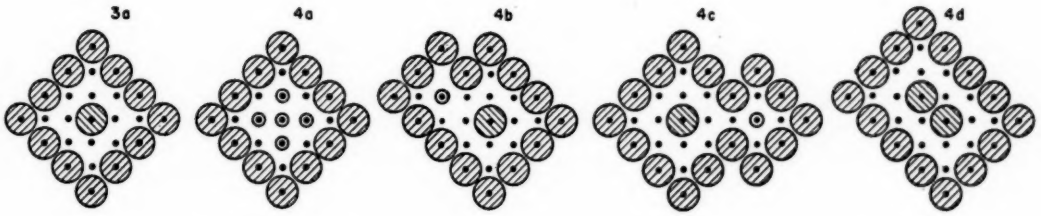

FIG. 8. Configurations contributing to deficiency of free sites to order of approximation φ_f^4. The cross-hatching distinguishes the adatoms in the odd from those in the even film.

In Fig. 8 all of the configurations for which $\Sigma_1-\Sigma$ is 3 or 4 and which contribute to Σ_d are shown and the information regarding them is tabulated in Table IV.

The successive approximations consist in counting configurations whose σ's contain successively higher powers of φ_f. At this point all those for which its exponent, $\Sigma_1-\Sigma$, is less than 5 have been counted. Breaking off the process here, and adding the contributions to σ_d we have

$$\sigma_d=\sigma_1\varphi_f^3[3\theta^{13}+(-\theta^{12}+12\theta^{17}+24\theta^{15}+8\theta^{16})\varphi_f].$$

From Eq. (18)

$$\sigma_d=\sigma_1(1-\theta-\varphi_f)$$

and σ_d can be eliminated. We now replace θ by $1-\varphi$, φ small. The bracketed expression is valid to the order φ or φ_f of small quantities. Accordingly θ^{13} is expanded to $1-13\varphi$ whereas θ^{12}, θ^{15}, θ^{16} and θ^{17}, being multiplied by φ_f, are each replaced by unity. We then have

$$\varphi_f=\varphi-\varphi_f^3[3(1-13\varphi)+43\varphi_f]. \qquad (27)$$

It is worth noting that this equation will give the relation between φ and φ_f more accurately to higher values of φ than would the series expansion for φ_f in terms of φ. This is because the exactness of the φ_f^3 coefficient of the bracket would be lost in the transformation. Eq. (27) solved for φ is

$$\varphi=\varphi_f\frac{1+3\varphi_f^2+43\varphi_f^3}{1+39\varphi_f^3}.$$

Table V gives a few pairs of values of φ and φ_f. Values of θ_f are also included. This checks well with Eq. (16) at $\phi=0.5$.

A series for θ_f in terms of φ which gives even better agreement with Eq. (16) at $\varphi=0.5$ and reproduces Table V in the range below $\varphi=0.5$ is

$$\theta_f=\tfrac{1}{2}(\varphi-3\varphi^3+5\varphi^4). \qquad (28)$$

Some values of θ_f calculated by this formula are listed in the table under the symbol θ_{f28}.

Thus the isotherm

$$\theta=A_p[1-\theta-3(1-\theta)^3+5(1-\theta)^4] \qquad (29)$$

can be adopted for the range

$$1\geqq\theta\geqq0.5.$$

This is plotted as curve A_2 in Fig. 6.

To carry the approximation another step would be difficult, although not impossible, for 30 different configurations would have to be taken into consideration.

6. Isotherms of Adatoms of Other Sizes

For larger adatoms the same methods that were used here for low values of θ can again be applied, but near $\theta=1$ new complications arise. For instance, in the next range of atom size, $2^{\frac{1}{2}}d_s<d_a<2d_s$, four different close-packed lattices (instead of the previous two) become possible; and ten pseudo-close-packed lattices for which $\theta=0.8$ can be found. All the adatoms in the latter are related to each other by the knight's move in chess. As the atom size increases, such alternatives multiply; so that the range of φ becomes ever smaller within which a fairly simple analysis can be applied which is based on

TABLE V.

φ	0.103	0.223	0.355	0.483	0.725
φ_f	0.1	0.2	0.3	0.4	0.6
θ_f	0.05	0.1	0.15	0.2	0.3
θ_{f28}	0.0501	0.101	0.150	0.208	

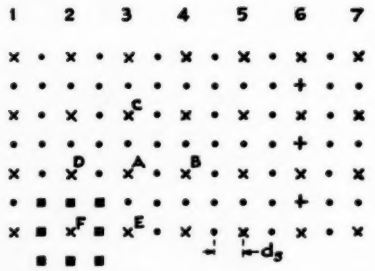

FIG. 9. Close-packed film of adatoms (crosses) excluding 9 cells each. Solid squares show exclusion pattern, vertical crosses show alternative filling of sites.

the single ultimate lattice that must exist for θ to be unity.

There is probably still some significance to a low φ analysis for this case, particularly as it has certain features not found with the smaller adatoms.

A regular close-packed arrangement of the adatoms is shown in Fig. 9. The exclusion pattern of a single adatom, F, is shown by the black squares. Each adatom excludes 9 sites. One-quarter of the sites are occupied so that $\gamma=4$. Evidently all the adatoms in any number of columns can be displaced one site without violating any exclusion conditions. For example, in column 6 of the figure the atoms could occupy the positions indicated by the vertical crosses. Alternatively, any number of rows could shift in the same way. But the displacement of either, rows or columns, locks the adatoms against displacements at right angles.

The possibility of such shifts is important, because it means that for θ almost unity the number of free sites varies with $(1-\theta)^2$ instead of $1-\theta$. This can be seen as follows: Suppose that from the completely covered surface the adatom at A evaporates. The free site A can then be excluded by the inward motion by one site of B and D, singly or both, or by C and E similarly, followed by any number of other adatoms in the particular row or column. This number is limited only by the locking already mentioned, which can occur when other adatoms besides A have evaporated. As a result, the single free site can be split in many ways into two gaps each $3d_c$ long in a line of adatoms whose normal spacing is $2d_c$.

Each such gap in an adatom row represents a deficiency of $\frac{1}{2}$ atom below saturation. Hence

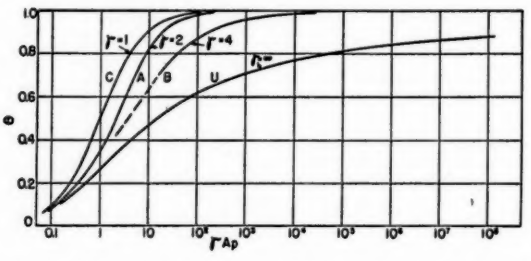

FIG. 10. Adsorption isotherms. Designations as in Fig. 6.

their total, s, numbers

$$s=2(\sigma_1-\sigma). \tag{30}$$

With a number of free sites the interlocking becomes much more complicated, because one-site shifts in the direction of both rows and columns become possible. As a result, single gaps are to be found in a chain terminated at both ends by locking. (The pseudo-close-packed $\theta=0.8$ lattices which have already been mentioned represent the ultimate in this direction.) This means that the problem is one of finding the number of adjacencies of two such gaps to form a free site on a surface rather than in a row.

We note that each gap is a gap with respect to a row or column but not both. In this sense it is polarized. Only two similarly polarized gaps can combine to give a free cell. Since half the gaps are polarized horizontally, half vertically, we have to consider the combinations of only $s/2$ gaps at a time. Each of the $s/2$ horizontal gaps finds either another one of the $s/2$ horizontal gaps or one of the σ adatoms adjacent to it on the right. Thus the chance that it finds another gap is $\frac{1}{2}s/(\sigma+s/2)$, and for all $s/2$ gaps there are $\frac{1}{4}s^2/(\sigma+s/2)$ gap pairs (without duplication) and hence that number of free sites. Including the vertical gaps,

$$\sigma_f=\tfrac{1}{2}s^2(\sigma+s/2).$$

Elimination of s with Eq. (30) gives

$$\sigma_f=2\sigma_1(1-\theta)^2,$$

whence the isotherm Eq. (10) takes the form[7]

$$\theta=4Ap(1-\theta)^2/2, \quad \theta \text{ near unity.} \tag{31}$$

The analysis of the dilute film taking isolated

[7] The difference in coefficient of Ap between Eqs. (31) and (32) here and Eqs. (50) and (51) of reference 1 arises from a difference in convention regarding A. Here A is defined by Eq. (10.5).

singlets and the three possible types of doublet into account by the method already outlined gives[7]

$$\theta = 4Ap(1-2.25\theta+\theta^2), \quad \theta \text{ near zero.} \quad (32)$$

In Fig. 6 curves B_1 and B_2 are plots of θ_f in these equations.

Two other θ_f plots have been added to Fig. 6 in order to fill out the picture of the change in the isotherm as γ increases. Curve C is θ_f for $\gamma=1$ in which case each adatom excludes only the site it occupies, and for which the isotherm is

$$\theta = Ap(1-\theta) \quad (33)$$

over the whole range. Curve U is for adsorption on a uniform field,[8] corresponding to $\gamma=\infty$.

The isotherms have been plotted in an unusual way in order to exhibit their behavior the better with respect to the extremes of concentration. In Fig. 10 these same isotherms have been plotted in the usual fashion θ against pressure.

In conclusion, I want to thank Dr. Langmuir for having proposed this investigation and for consulting with me during its progress.

[8] L. Tonks, Phys. Rev. **50**, 955 (1936), Eq. (28); or Eq. (35) of reference 1.

JUNE, 1940 JOURNAL OF CHEMICAL PHYSICS VOLUME 8

Potential Function of Acetylene Molecule. II

TA-YOU WU
Department of Physics, National South-West Associated University, Kun-ming, China

(Received January 26, 1940)

From a study of the interaction between the vibration and the rotation, the convergence factor of the rotational lines of the vibration-rotational bands of C_2H_2 is obtained as a function of the various vibrational quantum numbers and the constants in the first-order anharmonic potential. A tentative calculation of the first- and second-order anharmonic potentials is carried out for the C_2H_2 molecule on the basis of the classification of the absorption bands given in Part I.

INTRODUCTION

IN Part I of this paper,[1] the coefficients $\nu_1, \cdots \nu_5$, $x_{11}, \cdots x_{45}$ in the vibrational energy expression of C_2H_2 have been obtained in terms of the constants in the first- and the second-order anharmonic potentials. It was found that there are 30 unknown constants $\omega_1, \cdots \omega_5$, $a, \cdots k$, $\beta_1, \cdots \beta_{15}$ in the most general quadratic, cubic and quartic potentials that are consistent with the geometrical symmetry of the molecule while there are only 22 relations connecting these constants and the quantities $\nu_1, \cdots \nu_5$, $x_{11}, \cdots x_{45}$. In the following, an attempt is made to obtain five more relations between these constants and the convergence factors of the vibration-rotational bands from an analysis of the interactions between the vibrational and the rotational motions of the molecule, and to obtain an estimate of the potential constants.

[1] T. Y. Wu and A. T. Kiang. J. Chem. Phys. **7**, 178 (1939), referred to hereafter as I.

INTERACTION BETWEEN VIBRATION AND ROTATION

The general theory of the energy of a vibrating-rotating molecule has been given by Wilson and Howard,[2] and for a linear Y–X–X–Y molecule in particular by Sayvetz.[3] The kinetic energy part of the Hamiltonian is

$$\begin{aligned}\tfrac{1}{2}\sqrt{\mu}\sum_k p_k \frac{1}{\sqrt{\mu}} p_k + \tfrac{1}{2}\sqrt{\mu}\sum_{\alpha,\beta}\Lambda_\alpha \frac{\mu_{\alpha\beta}}{\sqrt{\mu}}\Lambda_\beta \\ + \tfrac{1}{2}\sum_{\alpha,\beta}\mu_{\alpha\beta}M_\alpha M_\beta - \sum_{\alpha,\beta}\mu_{\alpha\beta}M_\alpha\Lambda_\beta \\ - \tfrac{1}{2}\sqrt{\mu}\sum_{\alpha,\beta}M_\alpha\left(\Lambda_\beta\frac{\mu_{\alpha\beta}}{\sqrt{\mu}}\right), \quad (23)\end{aligned}$$

in which M_x, M_y, M_z are the components of the total angular momentum, Λ_x, Λ_y, Λ_z are the components of the angular momentum arising from

[2] E. B. Wilson, Jr., and J. B. Howard, J. Chem. Phys. **4**, 260 (1936).
[3] A. Sayvetz, J. Chem. Phys. **7**, 383 (1939).

the vibrational motions, along the x, y, z axes of a coordinate system rotating with the molecule, and the p's are the momenta conjugate to the normal coordinates. The first term represents the kinetic energy of vibration and has been treated in I. The second term represents the energy of interaction between the parallel and the perpendicular vibrations and has been given by Sayvetz.[3] These two terms give rise to energies which are functions of the vibrational quantum numbers alone and hence do not affect the rotational structure of the individual bands. The third term represents the energy of rotation of the molecule with moments of inertia $1/\mu_{xx}$, $1/\mu_{yy}$ etc. which are functions of the normal coordinates. The last two terms involving the products of the M's and the Λ's represents the coupling between the vibrational and the rotational motions of the molecule. Here we shall be chiefly concerned with these last three terms of the Hamiltonian (23).

With the notations of I with the exception of R_1 and R_2 which are now defined as $(\mu_1)^{\frac{1}{2}}$ and $(\mu_2)^{\frac{1}{2}}$ times, respectively, the R_1 and R_2 in I, where

$$\mu_1=\frac{2mM}{(M+m)}, \quad \mu_2=\frac{2mM(a+b)^2}{Mb^2+m(2a+b)^2},$$
$$a=r(C-H), \quad b=r(C-C),$$

it can be shown that the Λ's are given by

$$\begin{aligned}
\Lambda_x &= c_{13}(\mu_1)^{\frac{1}{2}}(y_4p_3-Q_3p_{y_4})+s(y_5p_1-Q_1p_{y_5})+t(y_5p_2-Q_2p_{y_5}),\\
\Lambda_y &= -c_{13}(\mu_1)^{\frac{1}{2}}(x_4p_3-Q_3p_{x_4})-s(x_5p_1-Q_1p_{x_5})-t(x_5p_2-Q_2p_{x_5}),\\
\Lambda_z &= (x_4p_{y_4}-y_4p_{x_4})-(x_5p_{y_5}-y_5p_{x_5}),
\end{aligned} \tag{24}$$

where

$$s=\frac{(bc_{11}-ac_{21})(\mu_2)^{\frac{1}{2}}}{a+b}, \quad t=\frac{(bc_{12}-ac_{22})(\mu_2)^{\frac{1}{2}}}{a+b}, \quad s^2+t^2=1, \quad c_{13}^2\mu_1=1 \tag{25}$$

and x_4 is the x component of R_1, etc.

To obtain the moments and products of inertia as functions of the normal coordinates, it is necessary to picture the perpendicular vibrations as involving changes in the bond angles alone, the bond distances remaining unchanged during these vibrations. Denoting by φ_1 and φ_2 the angles which R_1 and R_2 make, respectively, with the x axis, we obtain

$$\left.\begin{matrix}A\\B\end{matrix}\right\}=I_0\Bigg[1+\alpha Q_1+\beta Q_2+\gamma Q_1^2+\delta Q_2^2+\frac{1}{I_0}Q_3^2-\frac{m(2a+b)}{\mu_1 aI_0}R_1^2+\frac{R_1^2}{I_0}\cdot\begin{cases}\sin^2\varphi_1\\ \cos^2\varphi_1\end{cases}$$
$$-\frac{Mb+m(2a+b)}{2Mb}\cdot\frac{(2a+b)}{aI_0}R_2^2+\frac{R_2^2}{I_0}\cdot\begin{cases}\sin^2\varphi_2\\ \cos^2\varphi_2\end{cases}\Bigg],$$

$$C=R_1^2+R_2^2, \quad D=R_1^2\sin\varphi_1\cos\varphi_1+R_2^2\sin\varphi_2\cos\varphi_2,$$

$$\left.\begin{matrix}E\\F\end{matrix}\right\}=Q_3R_1\cdot\begin{cases}\sin\varphi_1\\ \cos\varphi_1\end{cases}+(sQ_1+tQ_2)R_2\begin{cases}\sin\varphi_2\\ \cos\varphi_2\end{cases},$$

where

$$\begin{aligned}
\alpha I_0 &= 2m(2a+b)c_{11}+[Mb+m(2a+b)]c_{21},\\
\beta I_0 &= 2m(2a+b)c_{12}+[Mb+m(2a+b)]c_{22},\\
\gamma I_0 &= 2mc_{11}(c_{11}+c_{21})+\tfrac{1}{2}(M+m)c_{21}^2,\\
\delta I_0 &= 2mc_{12}(c_{12}+c_{22})+\tfrac{1}{2}(M+m)c_{22}^2,
\end{aligned} \tag{26}$$

and $I_0=\frac{1}{2}[Mb^2+m(2a+b)^2]$ is the equilibrium value of the moment of inertia. Calculation gives for the coefficients μ's in (23)

$$\mu_{xx}=1/A', \quad \mu_{yy}=1/B', \quad \mu_{xy}\sim 0, \quad \mu_{yz}=\mu_{zz}=0, \quad M_z-\Lambda_z=0,$$

where

$$A'=B'=I_0\Big[1+\alpha Q_1+\beta Q_2+\Big(\gamma-\frac{s^2}{I_0}\Big)Q_1^2+\Big(\delta-\frac{t^2}{I_0}\Big)Q_2^2-\frac{2st}{I_0}Q_1Q_2 - \frac{m(2a+b)}{\mu_1 aI_0}R_1^2-\frac{Mb+m(2a+b)}{2Mb}\cdot\frac{(2a+b)}{aI_0}R_2^2\Big]. \quad (27)$$

The contributions to the energy from the terms $\Lambda_\alpha(\mu_{\alpha\beta}/\sqrt{\mu})\Lambda_\beta$ are, up to the second approximation of I,

$$\frac{h^2}{8\pi^2 I_0}[(\omega_3,\omega_4)(v_3+\tfrac{1}{2})(v_4+1)+s^2(v_1+\tfrac{1}{2})(v_5+1)(\omega_1,\omega_5)+t^2(v_2+\tfrac{1}{2})(v_5+1)(\omega_2,\omega_5)-2], \quad (28)$$

where

$$(\omega_i,\omega_j)\equiv(\omega_i/\omega_j+\omega_j/\omega_i). \quad (29)$$

The effect of these contributions can be taken account of in the energy expressions (17) and (18) in I simply making the following replacements, with $B_0=h/8\pi^2 I_0 c$,

$$\beta_9\rightarrow\beta_9+s^2B_0c(\omega_1,\omega_5)\,;\quad \beta_{12}\rightarrow\beta_{12}+t^2B_0c(\omega_2,\omega_5)\,;\quad \beta_{13}\rightarrow\beta_{13}+B_0c(\omega_3,\omega_4). \quad (30)$$

The term $\Sigma\mu_{\alpha\beta}M_\alpha M_\beta$ gives, in a first approximation in which the μ_{zz}, μ_{yy} are given the equilibrium values, the energy of rotation of a rigid rotator

$$(h^2/8\pi^2 I_0)[J(J+1)-(l_1+l_2)^2].$$

The interactions between the vibration and the rotation of the molecule appear in the next approximation. First, taking into account the variations of μ_{zz}, μ_{yy} with the normal coordinates gives the energy change

$$\Delta E_{\text{rot}}=-\frac{h^2}{8\pi^2 I_0}[J(J+1)-(l_1+l_2)^2]\Big[\alpha Q_1+\beta Q_2+\Big(\gamma-\alpha^2-\frac{s^2}{I_0}\Big)Q_1^2+\Big(\delta-\beta^2-\frac{t^2}{I_0}\Big)Q_2^2 -2\Big(\alpha\beta+\frac{st}{I_0}\Big)Q_1Q_2-\frac{2a+b}{aI_0}\Big(\frac{m}{\mu_1}R_1^2+\frac{Mb+m(2a+b)}{2Mb}R_2^2\Big)\Big]. \quad (31)$$

The quadratic terms introduce energy changes that can be calculated by means of the perturbation theory. The linear terms in Q_1 and Q_2 change the equilibrium separations of the atoms by amounts determined by the equations $\partial V/\partial Q_1=\partial V/\partial Q_2=0$ where

$$V=\tfrac{1}{2}\sum_1^3\lambda_iQ_i^2+\Delta E_{\text{rot}},$$

namely,

$$\overline{\Delta Q_1}=\frac{\alpha}{\lambda_1}\frac{h^2}{8\pi^2 I_0}[J(J+1)-(l_1+l_2)^2],\quad \overline{\Delta Q_2}=\frac{\beta}{\lambda_2}\frac{h^2}{8\pi^2 I_0}[J(J+1)-(l_1+l_2)^2].$$

These stretchings necessitate a transformation to the new normal coordinates Q^*_1 and Q^*_2 defined by

$$Q^*_1=Q_1-\overline{\Delta Q_1},\quad Q^*_2=Q_2-\overline{\Delta Q_2}. \quad (32)$$

As a consequence of this transformation, the first-order potential (14) in I contributes the following terms which are quadratic in the normal coordinates

$$\Delta V=\frac{h^2}{8\pi^2 I}[J(J+1)-(l_1+l_2)^2]\Big[\Big(3k_a\frac{\alpha}{\lambda_1}+k_c\frac{\beta}{\lambda_2}\Big)Q^{*2}_1+\Big(3k_b\frac{\beta}{\lambda_2}+k_d\frac{\alpha}{\lambda_1}\Big)Q^{*2}_2+2\Big(k_c\frac{\alpha}{\lambda_1}+k_d\frac{\beta}{\lambda_2}\Big)Q^*_1Q^*_2 +\Big(k_e\frac{\alpha}{\lambda_1}+k_i\frac{\beta}{\lambda_2}\Big)Q^{*2}_3+\Big(k_f\frac{\alpha}{\lambda_1}+k_j\frac{\beta}{\lambda_2}\Big)\sigma^2+\Big(k_g\frac{\alpha}{\lambda_1}+k_k\frac{\beta}{\lambda_2}\Big)\rho^2\Big], \quad (33)$$

in which

$$k_a=8\pi^3\omega_1(\omega_1/h)^{\frac{1}{2}}a,\quad k_b=8\pi^3\omega_2(\omega_2/h)^{\frac{1}{2}}b,\quad k_c=8\pi^3\omega_1(\omega_2/h)^{\frac{1}{2}}c,\quad k_d=8\pi^3\omega_2(\omega_1/h)^{\frac{1}{2}}d,$$
$$k_e=8\pi^3\omega_3(\omega_1/h)^{\frac{1}{2}}e,\quad k_f=8\pi^3\omega_4\mu_1(\omega_1/h)^{\frac{1}{2}}f,\quad k_g=8\pi^3\omega_5\mu_2(\omega_1/h)^{\frac{1}{2}}g, \tag{34}$$
$$k_i=8\pi^3\omega_3(\omega_2/h)^{\frac{1}{2}}i,\quad k_j=8\pi^3\omega_4\mu_1(\omega_2/h)^{\frac{1}{2}}j,\quad k_k=8\pi^3\omega_5\mu_2(\omega_2/h)^{\frac{1}{2}}k.$$

Next we have to consider the contributions from the last two terms in (23). The last term vanishes since $\mu_{xx}/(\mu)^{\frac{1}{2}}=\mu_{yy}/(\mu)^{\frac{1}{2}}=1$ and the operator Λ operates only on quantities within the parentheses. The diagonal matrix elements of $M_\alpha\Lambda_\alpha$ also vanish; but in the next approximation, the nondiagonal elements contribute the following energy change

$$\Delta E=\frac{1}{I_0^2}\sum_{V'R'}{}'\frac{(VR|M_x\Lambda_x+M_y\Lambda_y|V'R')(V'R'|M_x\Lambda_x+M_y\Lambda_y|VR)}{E_V{}^0-E_{V'}{}^0}$$
$$=\frac{h^2}{8\pi^2I_0}[J(J+1)-(l_1+l_2)^2]\left[\frac{2(v_3+\frac{1}{2})-(v_4+1)}{\omega_3-\omega_4}+s^2\frac{2(v_1+\frac{1}{2})-(v_5+1)}{\omega_1-\omega_5}+t^2\frac{2(v_2+\frac{1}{2})-(v_5+1)}{\omega_2-\omega_5}\right]\frac{h}{8\pi^2I_0}$$
$$+\text{terms independent of } J. \tag{35}$$

In obtaining these second-order contributions, the rotational energy has been neglected in comparison with the vibrational energy in the denominator and use is made of the relation $\Sigma_{R'}(R|M_x|R')\times(R'|M_x|R)=(R|M_x{}^2|R)$, etc. The total energy change is, on adding (31), (33) and (35),

$$\Delta E=\frac{h^2}{8\pi^2I_0}[J(J+1)-(l_1+l_2)^2][\sum_1^3(v_i+\tfrac{1}{2})\alpha_i+\sum_4^5(v_i+1)\alpha_i], \tag{36}$$

where

$$\alpha_1=\left(\alpha^2+\frac{s^2}{I_0}-\gamma+3k_a\frac{\alpha}{\lambda_1}+k_c\frac{\beta}{\lambda_2}\right)\frac{h}{4\pi^2\omega_1}+\frac{s^2h}{4\pi^2I_0(\omega_1-\omega_5)},$$
$$\alpha_2=\left(\beta^2+\frac{t^2}{I_0}-\delta+3k_b\frac{\beta}{\lambda_2}+k_d\frac{\alpha}{\lambda_1}\right)\frac{h}{4\pi^2\omega_1}+\frac{t^2h}{4\pi^2I_0(\omega_2-\omega_5)},$$
$$\alpha_3=\left(k_e\frac{\alpha}{\lambda_1}+k_i\frac{\beta}{\lambda_2}\right)\frac{h}{4\pi^2\omega_3}+\frac{h}{4\pi^2I_0(\omega_3-\omega_4)}, \tag{37}$$
$$\alpha_4=\left(\frac{m}{\mu_1}\frac{2a+b}{aI_0}+k_f\frac{\alpha}{\lambda_1\mu_1}+k_j\frac{\beta}{\lambda_2\mu_1}\right)\frac{h}{4\pi^2\omega_4}-\frac{h}{8\pi^2I_0(\omega_3-\omega_4)},$$
$$\alpha_5=\left(\frac{Mb+m(2a+b)}{2Mb}\cdot\frac{2a+b}{aI_0}+k_g\frac{\alpha}{\lambda_1\mu_2}+k_k\frac{\beta}{\lambda_2\mu_2}\right)\frac{h}{4\pi^2\omega_5}-\frac{h}{8\pi^2I_0}\left(\frac{s^2}{\omega_1-\omega_5}+\frac{t^2}{\omega_2-\omega_5}\right).$$

The frequencies of the vibration-rotational lines arising from transitions from the normal vibrational state to a state v_1, v_2, v_3, v_4, l_1, v_5, l_2 are given by

$$\nu=\nu_{\text{vib}}\pm B_0[2+\sum_1^3(v_i+1)\alpha_i+\sum_4^5(v_i+2)\alpha_i]N+B_0(\sum_1^5v_i\alpha_i)N^2, \tag{38}$$

where ν_{vib} is determined by (17) in I together with (30). The α's can be determined empirically from five properly chosen and accurately analyzed bands. Eqs. (37) then furnish five more relations for the determination of the potential constants in (14) in I.

TABLE I.

According to I v_1	v_2	v_3	cm^{-1}	B_1 obs.	B_1-B_0 obs.	B_1 calc.
0	0	0		1.1764		
0	2	1	9640	1.1585	−0.0179	*
1	2	1	11600	1.1526	−0.0238	*
1	0	3	11783	1.1514	−0.0250	1.1618
0	3	1	12676	1.1510	−0.0254	*
2	2	1	13532	1.147	−0.0294	1.1467
0	4	1	15600	1.1435	−0.0329	1.1435
0	5	1	18430	1.1358	−0.0406	1.1360
1	4	1	17519	1.1386	−0.0378	1.1376

CALCULATION OF POTENTIAL CONSTANTS

The transformation coefficients c's and the quantities α, $\beta\cdots$, k_a, $\cdots k_k$ can be calculated from the zeroth-order frequencies and potential constants in I.

$$\begin{gathered}c_{11}=1.125,\quad c_{12}=5.57,\quad c_{13}=-5.70,\quad c_{21}=2.81,\\ c_{22}=-1.53\times10^{11};\quad s^2=0.037,\quad t^2=0.963;\\ \alpha=4.06\times10^{19},\quad \beta=0.689\times10^{19};\\ \gamma=4.25\times10^{38},\quad \delta=4.25\times10^{38};\\ k_a=4.3\times10^{46}a,\qquad k_b=10.3\times10^{46}b,\\ k_c=5.8\times10^{46}c,\qquad k_d=7.7\times10^{46}d,\\ k_e=7.35\times10^{46}e,\qquad k_f=1.56\times10^{46}\mu_1 f,\\ k_g=1.30\times10^{46}\mu_2 g,\qquad k_i=9.8\times10^{46}i,\\ k_j=2.07\times10^{46}\mu_1 j,\qquad k_k=1.74\times10^{46}\mu_2 k,\end{gathered}\tag{39}$$

where the a, b, $\cdots k$ are in cm^{-1} and the other quantities in c.g.s. units.

To obtain the α's, consider first those bands involving only the parallel fundamentals $\nu_1(\nu_0)$, $\nu_2(\nu_5)$, $\nu_3(\nu_a)$. The values of B_1 for the upper vibrational states are known from the analyses of Funke and Lindholm.[4] Table I gives eight such bands. Of these, the B_1's of the 9640, 11,600, 12,676 cm^{-1} bands are probably most accurately known. From them we obtain[5]

$$\alpha_1B_0=-0.0059,\qquad \alpha_2B_0=-0.0075,\qquad \alpha_3B_0=-0.0029.\tag{40}$$

The B_1's of the other bands calculated with these values are given in Table I. Except for the 11,783-cm^{-1} band, the agreement between the calculated and the observed values is satisfactory.

From the bands $\nu_1+2\nu_2+\nu_3+2\nu_5=12{,}711\ cm^{-1}$, $B_1=1.156$ and $2\nu_1+2\nu_2+\nu_3+2\nu_5=14{,}597\ cm^{-1}$, $B_1=1.151$ and the values in (40), we obtain the average value[5]

$$\alpha_4B_0=0.00193.\tag{41}$$

With the values in (40) and (41) and the following bands

$\nu_1+2\nu_2+\nu_4+\ \nu_5=\ 9906\ cm^{-1}$,	$B_0=1.162$
$\nu_1+3\nu_2+\nu_4+\ \nu_5=13{,}033$	1.1501
$\nu_1+2\nu_3+\nu_4+\ \nu_5=\ 9745$	1.166
$2\nu_1+2\nu_3+\nu_4+\ \nu_5=11{,}663$	1.156
$3\nu_1+\ \nu_2+\nu_4+3\nu_5=11{,}586$	1.1584
$3\nu_1+\ \nu_2+\nu_4+5\nu_5=12{,}632$	1.1643

we obtain the average value[5]

$$\alpha_5B_0=0.00245.\tag{42}$$

The agreement between the calculated and the observed B_1's for bands involving the perpendicular fundamentals is not as satisfactory as in the case of those bands involving the parallel fundamentals alone. This may be due to the uncertainty in the assignments of some of the bands or to the lower accuracy with which the B's are determined.

Substituting the values in (39)–(42) into (37) gives

$$\begin{gathered}0.363\,a+0.0090\,c=-30.6\\ 0.048\,b+0.216\,d=-46.1\\ 0.206\,e+0.0152\,i=-20.6\\ 0.437\,f+0.0321\,j=-\ 4.06\\ 0.366\,g+0.0272\,k=-\ 8.34.\end{gathered}\tag{43}$$

Eqs. (18) in I and (43) are still not sufficient for

TABLE II. *Anharmonic potential constants of* C_2H_2 *in* cm^{-1}.

$a\leqq-82$	$c\sim\begin{cases}-110\\35\end{cases}$	for	$\beta_1=0$ $=1.5$
$b\leqq-200$	$d\leqq-167$	for	$0<\beta_2<5$
$e\leqq-85$	$i\sim\begin{cases}-168\\-237\\-312\end{cases}$	for	$\beta_3=\begin{cases}0\\2\\5\end{cases}$
$f\leqq-11$	$j\sim\begin{cases}10\\33\\58\end{cases}$	for	$\beta_{12}=\begin{cases}0\\-1\\-2\end{cases}$
$g\leqq-25$	$k\sim\begin{cases}26\\200\end{cases}$	for	$\beta_5=\begin{cases}7\\8\end{cases}$
$\beta_6\leqq\ 54$	$\beta_7\leqq\ 8$		$\beta_8\leqq\ 10$
$\beta_9\leqq-23$	$\beta_{10}\leqq-117$		$\beta_{11}\leqq-10$
$\beta_{12}\leqq-17.5$	$\beta_{14}\leqq-18$		$\beta_{15}\leqq-13$

[4] G. W. Funke, Zeits. f. Physik **104**, 169 (1937); Funke and Lindholm, *ibid.* **106**, 518 (1937).

[5] These values of the α's can be compared with the empirically chosen values $\alpha_1B_0=\alpha_2B_0=\alpha_3B_0=-0.0051$, $\alpha_4B_0=\alpha_5B_0=0.0020$ of Funke and Lindholm, reference 4.

the evaluation of the potential constants in (14) and (15) in I. However, by making certain reasonable assumptions about some of them, a rough estimate[6] can be made of the others as shown in Table II. These values are admittedly very rough, but any accurate calculation will not be possible without additional empirical data. The order of magnitude of these constants shows that the effect of anharmonicity is not quite negligible in C_2H_2. This is in fact what we would expect from the small mass of the hydrogen atoms in the molecule.

The writer is grateful to Professor D. M. Dennison, of the University of Michigan, for his interest and advice concerning these calculations.

TABLE III. *Classification of* C_2H_2 *bands.*

	CALC.	OBS.		CALC.	OBS.
ν_a	3288*	3288	ν_0	1993*	1973
ν_s	3372*	3372	δ_s	612*	612
$\nu_a+\nu_s$	6548	6500	δ_a	729*	729
$\nu_a+2\nu_s$	9835*	9835	$2\nu_a+\nu_s+\delta_a$	10364*	10364
$3\nu_a$	9640*	9640	$\nu_a+2\nu_s+\delta_s$	10411	10413
$3\nu_a+\nu_s$	12676*	12675	?		9906
$5\nu_a$	15600*	15600	?		13003
$5\nu_a+\nu_s$	18414	18430	$2\nu_a+\nu_0+\delta_a+\delta_s$	9743*	9745
$\nu_a+\nu_0$	5257	5250	$2\nu_a+2\nu_0+\delta_a+\delta_s$	11667	11663
$\nu_a+\nu_s+\nu_0$	8512	8450	$3\nu_a+\nu_0+2\delta_s$	12709	12711
$\nu_a+2\nu_s+\nu_0$	11794	11783	$3\nu_a+2\nu_0+2\delta_s$	14607	14597
$3\nu_a+\nu_0$	11600*	11600	$\nu_0+\delta_a+\delta_s$	3288	3294
$3\nu_a+\nu_s+\nu_0$	14627	14617	$\nu_a+\nu_s+\nu_0+2\delta_s$	9665*	9668
$5\nu_a+\nu_0$	17551	17519	$\nu_a+\nu_s+2\nu_0+2\delta_s$	11567*	11570
$3\nu_a+2\nu_0$	13534*	13532	?		9366
$\nu_a+\delta_s$	3884	3882	$\nu_a+\nu_s+\nu_0+\delta_s$	9081	9085
$\nu_s+\delta_a$	4092*	4092	$3\nu_a+\nu_s+\nu_0+\delta_s$	15162	15081
$\nu_0+\delta_a$	2706	2702	$5\nu_a+\nu_0+\delta_s$	18066	18088
$\delta_a+\delta_s$	1328.6*	1328.6	$2\nu_a+\nu_0+\delta_a$	9193	9177
$\nu_s+\delta_a+\delta_s$	4681	4690	$\nu_a+3\nu_0$	9114	9151
$3\nu_a+\delta_s-\delta_s$	9592	9603	$\nu_s+3\nu_0+\delta_a+3\delta_s$	11587*	11586
$3\nu_a+\nu_s+\delta_s-\delta_s$	12618*	12618	$\nu_s+3\nu_0+\delta_a+5\delta_s$	12734	12732
$\nu_a+2\nu_s+\delta_s-\delta_s$	9799	9801	$3\nu_a+\nu_s+\delta_s$	13230	13230
$5\nu_a+\delta_s-\delta_s$	15521*	15521			

[6] The way in which we arrive at these values is as follows. From the second equation in (43) and the equation for x_{22}, we obtain b and d for a few small values of β_2. It is found that b and d are not very sensitive to β_2. From the first equation in (43) and the equation for x_{11}, it is found that there are no real solutions for a and c unless $\beta_1<1.575$, and then c is very sensitive to the value of β_1 while a is not. In a similar manner, e, i, f, j, g, k are estimated, it turning out that $\beta_5>20/3$ for g and k to be real. While the values of e, f, g are not very sensitive and their values in Table II may be taken as correct within 10 cm^{-1}, the values of i, j, k are very sensitive to the values of the β's assumed and are hence quite uncertain.

TABLE IV.

$\nu_1=1987$	$x_{11}=-13$	$x_{12}=-5$	$x_{24}=-9.3$
$\nu_2=3358$	$x_{22}=13.6$	$x_{13}=-5$	$x_{25}=-10$
$\nu_3=3318$	$x_{33}=-28$	$x_{14}=4$	$x_{34}=-5$
$\nu_4+\nu_{44}=729$	$x_{55}=9$	$x_{15}=-17$	$x_{35}=-16$
$\nu_5=603$	$x_{333}=-2.3$	$x_{23}=-112$	$x_{45}=-13$
	$x_{555}=-0.55$		

TABLE V.

v_1	v_2	v_3	cm^{-1}	B_1 OBS.	B_1 CALC.
0	0	3	9640	1.1585	*
1	0	3	11,600	1.1526	*
1	2	1	11,783	1.1514	1.1502
0	1	3	12,676	1.1510	*
2	0	3	13,532	1.147	1.1427
0	0	5	15,600	1.1435	1.1465
0	1	5	18,430	1.1358	1.1392
1	0	5	17,519	1.1386	1.1406

APPENDIX

In I, it was stated that with the values of the coefficients $\nu_1, \cdots\nu_5$, $x_{11}, \cdots x_{45}$ given by Herzberg and Spink,[7] the agreement between the calculated and the observed frequencies is not satisfactory. However, by modifying the assignments of those bands involving the perpendicular fundamentals, it is possible to obtain good agreement for all except 5 or 6 bands, as shown in Table III. The bands marked with * are those employed in the calculation of the coefficients $\nu_1, \cdots\nu_5$, $x_{11}, \cdots x_{45}$ which are given in Table IV. It is seen that the agreement between the observed and the calculated frequencies is good except in the case of the 6500, 8450, 15,081 and 9151-cm^{-1} bands. The discrepancy in the case of the 6500-cm^{-1} band, namely, *ca.* 50 cm^{-1}, must, however, be regarded as a serious weakness of the classification, since the agreement is expected to be best for such a simple combination band. Also the two parallel type bands at 9906 and 13,033 cm^{-1} and the perpendicular band at 9366 cm^{-1} do not find reasonable assignments in accordance with the selection rules. Another reason for our preferring our classification given in I to the above modified Herzberg-Spink system is the following: According to the latter classification, the convergence factors of the bands in Table I now become as shown in Table V. It is seen that the agreement between the calculated and the observed B_1's is not as satisfactory as that obtained in Table I. It seems that to decide among the various classifications for the C_2H_2 bands that have been proposed, further experimental work, preferably on C_2D_2, is necessary.

[7] G. Herzberg and J. W. T. Spink, Zeits. f. Physik **91**, 386 (1934).

The Nature of the Ions Emitted by Heated Filaments and Salts

B. TOUBES AND G. K. ROLLEFSON
University of California, Berkeley, California

(Received April 1, 1940)

It has been found that positive ions are emitted by filaments of tungsten, tantalum, and molybdenum when heated to temperatures near the melting points. Sodium and potassium ions were found in addition to those of the filament metal. When alkali halides were heated to 800–1000°C on platinum they emitted the singly charged ions of the corresponding alkali metal. No negative ions were found and no ions were obtained from the chlorides of calcium, magnesium, strontium, barium, or zinc.

THE emission of positive ions has been studied by several experimenters. The early work is summarized by Richardson[1] and a later summary has been given by Jones.[2] The most detailed studies using a mass spectrograph to identify the ions have been by Wahlin[3] and by Barnes.[4] They have established that in addition to the ions of sodium and potassium which had been observed earlier, ions of the filament material are emitted. We have made some observations on the variation in intensity of the alkali ions and ions of the filament metal with time and also on the nature of the ions produced by heating a number of salts.

The apparatus used was essentially the same as described by Hogness and Lunn.[5] The magnetic field was calibrated by measuring the change in resistance of a bismuth spiral. It was found that starting from zero current in the magnet coils, the current-field curve was quite reproducible.

In order to prevent contamination by fluxes, the filaments were not brazed or welded to the electrodes but were clamped between heavy tungsten leads in the following way. Each lead was made of two heavy tungsten rods ground flat on one side. These were brazed two inches above the ends with flat sides together. The filament could then be inserted by springing the ends apart and these, when released, held the filament tightly clamped.

The ratio for the charge to mass of the ions was determined by keeping the magnetic field constant, varying the accelerating potential applied to the ions, and noting the electrometer deflections. The peaks in the curve obtained by plotting the electrometer deflections against the accelerating voltages give the values of e/m by application of the formula $e/m=2V/H^2R^2$ in which H is the magnetic field, R the radius of curvature of the path of the ions in the field, and V the accelerating potential applied before extrance of the ion into the magnetic field. The resolution of the apparatus for ion currents of the strength obtained was not sufficient for the separation of the isotopes but was adequate for the determination of the nature of the ions.

Positive ions were obtained from tungsten, tantalum, and molybdenum filaments when these were heated to temperatures slightly below their melting points. All of the ions were found to be singly charged. Sodium and potassium ions were obtained from all of the filaments in addition to the ion of the filament metal. The tungsten filaments also gave some thorium ions. The intensity of emission of the heavy metal ions was constant at a constant temperature for any given filament or like filaments. The sodium and potassium ion currents, however, showed a falling off as time progressed so long as the ions were removed by application of a potential. When a filament, from which the emission had decayed so far as to be unmeasurable, was heated over night at a lower temperature without the application of a potential the current regained nearly its initial value. The rate of decay varied with the different metals. By selecting filament tempera-

[1] O. W. Richardson, *Emission of Electricity by Hot Bodies* (Longmans, Green, 1921).
[2] T. J. Jones, *Thermionic Emission* (Methuen and Company, London, 1936).
[3] Wahlin, Phys. Rev. **34**, 164 (1929); **35**, 653 (1930); **45**, 886 (1934).
[4] Barnes, Phys. Rev. **42**, 487, 492 (1932).
[5] Hogness and Lunn, Proc. Nat. Acad. Sci. **10**, 398 (1924).

ture such that the intensity of the ionic current was the same, it was found that the times required for the emission to fall to its half-value were ten, fifteen, and one hundred and forty minutes for molybdenum, tantalum, and tungsten, respectively. These half-time values cannot be interpreted in any simple manner since it was found that the decay of the emission did not follow any simple rate law. It is probable that the decay is due to an exhaustion of the sodium and potassium on the surface of the filament. The diffusion of more alkali atoms from the interior of the filament is too slow to supply a measurable current.

A large number of experiments were tried with salts heated on a platinum spiral to temperatures of 800 to 1000°C. It was found that the alkali halides gave the corresponding positive ions. For example, the chlorides of sodium, potassium and rubidium gave ions the ratio of whose e/m was $1/23 : 1/39 : 1/85$ within two percent. None of the halides of magnesium, calcium, strontium, barium, or zinc gave positive ions. No negative ions were obtained from any of the salts. The sharpness of the peaks indicated that all of the ions fell through the same potential drop and hence it may be concluded that they were formed either at or very close to the filament. Under such conditions the work function of the platinum is high enough to remove the extra electrons from any of the negative ions which might have formed.

JUNE, 1940 JOURNAL OF CHEMICAL PHYSICS VOLUME 8

Entropy of Vaporization and Restricted Molecular Rotation in Liquids

R. S. HALFORD
Department of Chemistry, University of California, Berkeley, California
(Received December 18, 1939)

Deviations among entropies of vaporization to constant vapor volume are attributed to restricted rotation of molecules in the liquid. An arbitrary measure of the amount of restriction is defined and the deviations are shown to exhibit a remarkable regularity when compared on this basis. Deviations due to perturbation of vibrations in the liquid must either parallel those due to restricted rotation or be quite small.

WHEN a liquid is caused to vaporize isothermally against its own vapor pressure the entropy of vaporization is given by the well-known relation $\Delta S = \Delta H/T$. ΔH, the heat absorbed, is a characteristic property of each liquid which has approximately the same value over a wide range of temperature for any given liquid. A characteristic temperature can therefore be defined for each liquid such that, at their respective characteristic temperatures, all liquids have the same entropy of vaporization.

Three important attempts have been made to relate the characteristic temperature with other properties of the liquid. The widely used rule of Trouton[1] identifies it with the boiling point of the liquid. The inadequacy of this definition is evidenced by the fact that the corresponding entropies of vaporization show a trend when a wide range of boiling points is considered. A second definition of the characteristic temperature is deduced from the theory of corresponding states. According to this definition, liquids at their characteristic temperatures have the same ratio of vapor volume to liquid volume. A recent discussion, given by Pitzer,[2] makes evident the fact that this rule is not generally obeyed although a few simple substances show a very striking agreement. Large differences in entropy of vaporization are obtained with substances selected at random and Pitzer has discussed the significance of these deviations.

The third definition of a characteristic temperature was proposed by Hildebrand[3] as a

[1] F. Trouton, Phil. Mag. (5) **18**, 54 (1884).

[2] K. S. Pitzer, J. Chem. Phys. **7**, 583 (1939).

[3] J. H. Hildebrand, J. Am. Chem. Soc. **37**, 970 (1915).

modification of Trouton's rule. Liquids are in corresponding states when all are in equilibrium with the same concentration of vapor. This rule meets with considerable success in practical application; there is no trend with temperature and deviations among so-called "normal" liquids are relatively small. Several attempts[4] have been made to furnish the Hildebrand rule with a satisfactory basis in theory. It appears, however, that theoretical considerations always lead to the second definition given above. Excepting the few simple substances which were shown by Pitzer to be in perfect accord with theory, this definition of characteristic temperature cannot compete in practical value with the empirical rule of Hildebrand. A very attractive suggestion concerning the solution of this paradox for the case of complicated polyatomic molecules was made to the author by Professor Pitzer. The theoretical treatments leading to a definition of corresponding states have assumed that the potential energy can be represented as a function of the distance between molecular centers. This assumption will lead rigorously to the definition in terms of equal vapor to liquid volume ratios. However, the most polarizable electrons in the molecules will be the nonbonding valence electrons on outside atoms and the major contribution to the potential energy will come from these. This suggests that the attraction between neighboring molecules may arise largely in the interaction of adjacent outside atoms; in which case, the potential energy should be represented as a function of the distance between these atoms. It can be seen qualitatively that this modification of the theory should lead to something similar to the Hildebrand definition of characteristic temperature. I trust that Professor Pitzer will find the opportunity to elaborate on this suggestion soon. In the meantime it will be tentatively assumed that the comparison of entropies of vaporization at equal vapor volumes is justified.

Recently, Hildebrand[5] has called attention to certain regularities among deviations from his rule and has suggested an interpretation for them. Assuming that the rule would be obeyed for the vaporization of a completely random liquid to a completely random vapor, he points out that any tendency toward order in the liquid (with consequent lower liquid entropy) would increase the entropy of vaporization to a random vapor. Among "normal" liquids the factors tending to produce ordering would be polarity and geometrical shape. Hildebrand showed that the higher entropies of vaporization were observed for those liquids which were most likely to be ordered for just these reasons.

In the subsequent discussion these deviations will be examined from the point of view of hindered rotation of the molecules in the liquid. The suggestion that this phenomenon may be the cause of deviations is not a new one.[2, 4(a, b)] The relation to be demonstrated should be regarded as empirical. The concept of restricted rotation may be synonymous with the ordering proposed by Hildebrand but it is not necessarily so. It is possible to imagine molecules, so packed that dipoles or other identifying axes are oriented at random, but prevented by their shape from executing a complete rotation without interference from their neighbors.

If rotation and vibration, respectively, are not equally excited in liquid and vapor a contribution to the entropy of vaporization can be associated with these degrees of freedom. The contribution from rotational motion can be described qualitatively in terms of a simple model consisting of an assemblage of molecules occupying a certain volume which is subdivided into cubical compartments. The molecules are distributed with one in each compartment and the center of gravity of each molecule is fixed to coincide with the center of its compartment. Initially it will be supposed that the molecules are rotating freely with a Maxwellian distribution of rotational energy in the assemblage. Each compartment is thus large enough to permit a molecule to sweep out a complete rotation within it. Under such conditions the rotational factor for the assembly is the same as that for a gas. Now, if this system is slowly compressed so that the volumes of all compartments are diminished similarly, there will be no change in the rotational factor until a certain critical

[4] (a) R. F. Newton and H. Eyring, Trans. Faraday Soc. **33**, 73, 80 (1936); (b) O. K. Rice, J. Chem. Phys. **5**, 353 (1937); (c) H. Eyring and J. Hirschfelder, J. Phys. Chem. **41**, 249 (1937); (d) J. E. Lennard-Jones, Proc. Roy. Soc. London, **A165**, 1 (1938).

[5] J. H. Hildebrand, J. Chem. Phys. **7**, 233 (1939).

volume is reached. At this point the side of each cubical compartment will be twice the length of the longest rotating arm of the molecule. Any further compression will result in interference among the rotators and a loss of rotational entropy. Torsional oscillation about the diagonals of the cube will persist in diminishing degree over a range of volume and a continuous loss of rotational entropy will accompany the compression. This phenomenon has been discussed quantitatively by Pitzer.[6] The model used here is of course only qualitative and highly simplified but it furnishes a basis for the comparison of actual liquids.

One method of comparison would be to compare the entropy of vaporization with the volume of a liquid at various temperatures, always correcting to the same vapor volume. However, the amount of expansion occurring over the range of temperature where the vapor remains dilute would correspond to only a small portion of the process discussed in connection with the model. The region of concentrated vapor introduces vapor imperfections as an undesirable complication.

On the other hand, if the notion of hindered rotation is to be applied quite generally the phenomenon should occur in very much the same way for all liquids, allowing for individual differences. An estimate of the importance of these differences can be taken from the work of Pitzer who showed that over a wide range of moments of inertia the entropy loss due to a given amount of restriction of rotation is about the same. The individual differences are comparable in magnitude to the errors in the best available entropy values for the liquids in which we are interested. Thus we may expect that in corresponding states of restriction, in the sense of the model, the various liquids will have lost, to a good approximation, the same amount of rotational entropy. If then, the various liquids are found to cover a wide range of restriction under the conditions that their entropies of vaporization have been determined it will be possible to carry out a comparison on the basis of the model.

In order to do so it is necessary to be able to define suitable corresponding states of restriction

[6] K. S. Pitzer, J. Chem. Phys. 5, 469 (1937).

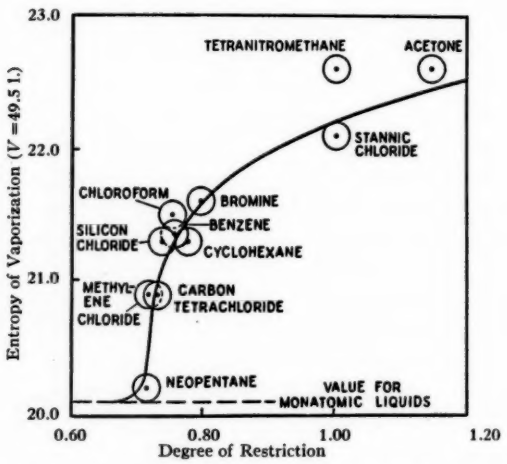

FIG. 1. Hg, Xe and Zn have been used to fix the entropy of vaporization for a monatomic liquid.

for various liquids. In terms of the model these states refer to the volume required by a molecule in order that it may sweep out a complete rotation. It is difficult to define this volume exactly. For a rigid molecule, the distance from the center of gravity to the center of the extreme atom along the longest rotating arm can be given quite accurately. In many cases, accurate electron diffraction data are available; otherwise, distances can be estimated satisfactorily from covalent radii. However, the additional extension of the extreme atom away from the center of gravity is not so simply determined. It should be greater than the covalent radius and possibly somewhat less than the ionic radius for the same atom as a singly charged negative ion. Estimates of such distances are available but they are not sufficiently accurate for the purpose at hand.

In view of this difficulty, corresponding states of restriction will be arbitrarily defined in terms of a volume calculated by assuming that the extension of the extreme atom away from the center of gravity is equal to its covalent radius. The length, so defined, in turn defines a sphere corresponding to complete rotation of this length about the center of gravity. The molal volume calculated for cubic closest packing of these spheres will be called the molal volume of the free covalent rotator. The ratio of the calculated molal volume of the free covalent rotator to the actual molal volume measures the degree of restriction of the liquid. Liquids having the same

degree of restriction are said to be in corresponding states of rotational freedom.

The entropy of vaporization to a vapor volume of 49.5 l. has been plotted against the degree of restriction for a number of liquids in Fig. 1. The close grouping of the points about a single simple curve seems highly significant. The deviations from the curve as drawn are less than might be expected from the errors in the values of the entropies, making no allowance for the individual differences due to different moments of inertia. The horizontal line at a value of 20.1 E.U. is the average for several monatomic substances which agree among themselves within 0.2 E.U. The fact that this entropy value is achieved at a degree of restriction of 0.7 rather than unity is due merely to the arbitrary definition chosen for the length of the rotating arm. In calculating these lengths all data have been taken from Pauling, *The Nature of the Chemical Bond*.[7] When in a terminal position methyl and methylene groups have been assigned an extension of 1.37A, equal to the covalent radius of *C* plus the covalent diameter of *H*. The entropy values were taken from the vapor pressure curves generously provided by Professor Hildebrand and used by him in the preparation of his paper.[5] The entropy values given by the author differ slightly from those given by Professor Hildebrand and the differences, about ± 0.1 E.U. represent the limit of accuracy in reading the plots. The circles enclosing the points in Fig. 1 correspond to this uncertainty in the entropies and to an uncertainty of about 0.01A in the length of the rotating arm. The actual experimental uncertainties may be several times larger in both quantities. These figures are cited to call attention to the truly striking consistency of the points in Fig. 1.

A few remarks may now be made concerning the curve which has been drawn to fit the points. Pitzer's calculations[6] lead to a curve of this shape when the entropy lowering due to restricted rotation is plotted against the value of the restricting potential. Since the relation between the restricting potential and the degree of restriction, as defined here, is unknown, a quantitative application of Pitzer's theory cannot be undertaken. However, it is to be expected that the two quantities would be related in a rather simple way and as a result the shape of the lines in the two types of plot should have some resemblance. While these remarks can hardly be taken as evidence for the interpretation given in the previous discussion they nevertheless add to its plausibility.

A description of the effect of the vibrational factor is not so readily given. One observes however that for the substances included in the figure it must either closely parallel the rotational effect or be very small.

It is interesting to note that the several polar substances included in the plot appear to be displaced upward to a small extent. This may be indicative of the contribution of polarity to the restriction of rotation but the accuracy of the data hardly warrants such a conclusion.

[7] Cornell University Press, Ithaca, New York.

Absolute Reaction Rates and the Photovoltaic Effect*

EDWARD ADLER
Department of Chemistry, Columbia University, New York, New York
(Received April 2, 1940)

IN several recent papers[1,2] the theory of absolute reaction rates has been applied to the study of electrode processes. By an extension to the photovoltaic effect, the experimental dependence of the photo e.m.f. upon the intensity of illumination can be deduced. In a later paper we shall discuss some of the factors complicating the photovoltaic effect, such as "dark" or thermal e.m.f. and variation of resistance with light. We are concerned here only with the primary photo e.m.f., and shall consider only the case in which the photo e.m.f. is positive. (The illuminated electrode becomes increasingly positive.)

Following the treatment in,[1] the current from the electrode for the process $A \rightarrow A^+ + e$ is

$$I_t' = \epsilon k_1 [A] e^{-\epsilon(V_C - V_B)/kT}, \tag{1}$$

where $[A]$ is the activity of atoms A in the surface of the electrode or adsorbed on it, ϵ is the charge of the ion, V_B is the electrical potential of the electrode (or in the adsorbed atomic layer), V_C the potential at the "saddle point," and

$$k_1 = \frac{kT}{h} e^{-\Delta F_1^*/kT}.$$

Similarly, for the discharge of ions in the process $A^+ + e \rightarrow A$, the current due to thermal transfer is

$$I_t'' = \epsilon k_2 [A^+]_{ads} e^{-\epsilon(V_C - V_F)/kT}, \tag{2}$$

where $[A^+]_{ads}$ is the activity of ions A^+ in the adsorbed ionic layer, and V_F is the potential in the adsorbed ionic layer.

In addition, if the electrode is illuminated by radiation of the proper frequency, electrons may be transferred from the electrode to the ionic layer across the potential hill, resulting in the same process, namely, $A^+ + e \rightarrow A$. If J is the intensity of illumination, then the rate of the photo-discharge is $k_3 J$ and $I_p'' = \epsilon k_3 J$.

The total current, accordingly, is

$$I = \epsilon k_1 e^{-\epsilon(V_C - V_B)/kT} [A] - \epsilon k_2 e^{-\epsilon(V_C - V_F)/kT} [A^+]_{ads} - \epsilon k_3 J. \tag{3}$$

At equilibrium, $I = I_D$ the diffusion current, where

$$I_D = \frac{\epsilon D}{l} \{[A^+]_{ads} - [A^+]\}. \tag{4}$$

Setting these two equal, and solving for $[A^+]_{ads}$

$$[A^+]_{ads} = \frac{k_1 e^{-\epsilon(V_C - V_B)/kT} [A] - k_3 J + (D/l)[A^+]}{k_2 e^{-\epsilon(V_C - V_F)/kT} + (D/l)}$$

and substituting in (4)

$$I = \frac{\epsilon D}{l} \left\{ \frac{k_1 [A] e^{-\epsilon(V_C - V_B)/kT} - k_3 J - k_2 [A^+] e^{-\epsilon(V_C - V_F)/kT}}{k_2 e^{-\epsilon(V_C - V_F)/kT} + (D/l)} \right\}. \tag{5}$$

Now, if we assume that $V_B = V$, the potential of the electrode, that $V_F = 0$ and let $V_C = \alpha V$, and note further that at equilibrium,

$$V = V_e, \quad I = 0, \quad [A] = [A^+],$$

then,

$$k_3 J = [A] e^{-\epsilon \alpha V_e/kT} \{k_1 e^{\epsilon V_e/kT} - k_2\}.$$

* Publication assisted by the Ernest Kempton Fund for Physical Research of Columbia University.
[1] Kimball, J. Chem. Phys. **8**, 199 (1940).
[2] Eyring, Glasstone and Laidler, J. Chem. Phys. **7**, 1053 (1939).

Now when $J=0$,

$$\frac{k_1}{k_2}=e^{-\epsilon V_0/kT} \quad (V_0 \text{ is "dark" e.m.f.})$$

and

$$k_3 J=k_2[A]e^{-\epsilon\alpha V_e/kT}\{e^{\epsilon(V_e-V_0)/kT}-1\}. \tag{6}$$

This equation may be simplified in two limiting cases.

Case 1.—Where the active electrode consists of an oxide, sulfide, or halide of copper or silver, selenium, etc., then (V_e-V_0) is of the order of one-tenth of a volt even at moderate light intensities. In this case, at room temperatures $e^{\epsilon(V_e-V_0)/kT}\gg 1$

and

$$k_3 J=k_2[A]e^{\epsilon(V_e-\alpha V_e-V_0)/kT}$$

or, taking logarithms and combining the constant terms, at constant T

$$V_e=C+B\ln J.$$

This is in agreement with the experimental dependence of V_e upon $\ln J$ for active electrodes at moderate illumination intensities.

Case 2.—At very low intensities, or for pure metal electrodes, giving potential differences of the order of microvolts or millivolts,

$$\frac{\epsilon(V_e-V_0)}{kT}\ll 1; \quad \frac{\epsilon\alpha(V_e-V_0)}{kT}\ll 1$$

and

$$k_3 J=k_2[A]e^{-\epsilon\alpha(V_e-V_0)/kT}e^{-\epsilon\alpha V_0/kT}\frac{\epsilon(V_e-V_0)}{kT}$$

$$=k_2[A]e^{-\epsilon\alpha V_0/kT}\frac{\epsilon(V_e-V_0)}{kT}\left\{1-\frac{\epsilon\alpha(V_e-V_0)}{kT}\right\}$$

and, combining constant terms,

$$V_e=C'+B'J.$$

Again, this is in agreement with the experimental linear dependence of V_e upon J at small values of (V_e-V_0), i.e., for very small light intensities or for slight photo-activity.

Thanks are due Professor G. E. Kimball for a very helpful discussion.

LETTERS TO THE EDITOR

This section will accept reports of new work, provided these are terse and contain few figures, and especially few halftone cuts. The Editorial Board will not hold itself responsible for opinions expressed by the correspondents. Contributions to this section should not exceed 600 words in length and must reach the office of the Managing Editor not later than the 15th of the month preceding that of the issue in which the letter is to appear. No proof will be sent to the authors. The usual publication charge ($3.00 per page) will not be made and no reprints will be furnished free.

Lengths and Strengths of Atomic Bonds

It has been claimed that it is possible to construct a table of bond energies applicable to wide classes of molecules, which gives agreement withone one or two kcal./mole with the heats of combustion.[1] Unfortunately "resonating" molecules are found to require special treatment and they are assigned supplementary energies, arbitrarily chosen so that agreement with heats of combustion is obtained. This scheme is essentially concerned with relating molecular structures, as determined by x-ray and electron diffraction studies and spectroscopic observations, to heats of combustion. Consequently, to the individual atoms single-bond, double-bond and triple bond radii are given, which are so chosen as to give, when added together, the best fit with the interatomic distances found in the restricted class of molecules of nonresonating types for which such measurements are available.

The accumulating data seem now to call for a revision of this scheme. The assumption that a C−O bond or a C=O bond e.g. have invariably the same energy and the same length, even if it were permissible as a first assumption, can no longer be justified. The C−O bond in trimethyl carbinol apparently is a number of kcal./mole stronger than in dimethyl ether or methyl alcohol.[2] And the C=O bond is apparently shorter in formaldehyde,[3] acetaldehyde,[4] and glyoxal,[5] than in diketopiperazine.[6] There are similar difficulties with the other bonds. Even within the class of saturated hydrocarbons, there is some evidence that the C−C and C−H bonds vary in strength.[7] That the C−C and C−N bonds vary in length, even in cases in which none of the usual types of resonance is applicable, is shown by the cases of diketopiperazine[6] and glycine.[8] On the whole, the data indicate that we have to anticipate gradations in bond energies and gradations in bond lengths associated with one and the same bond.

It is therefore suggested that the essential objective is to construct strength/length curves for each pair of atoms, alike and different, based upon the single assumption that there is a 1–1 relation between the strengths and the lengths of each such bond. In a more general scheme of this

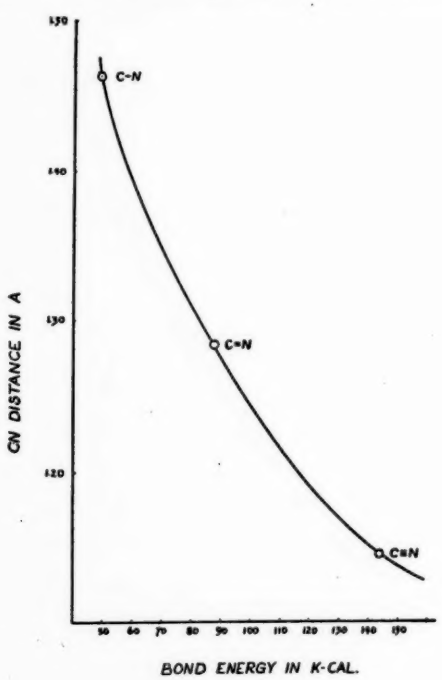

FIG. 1.

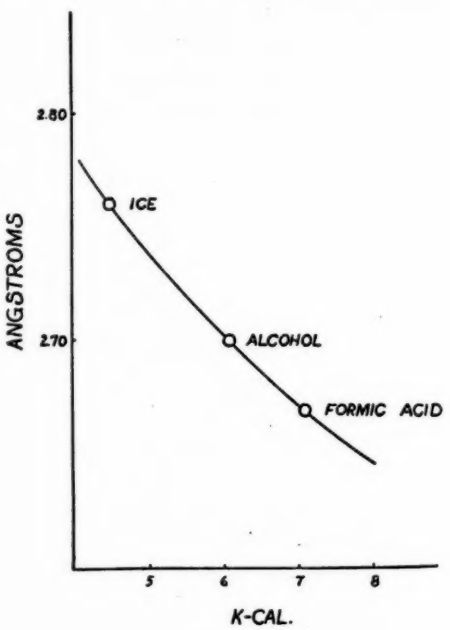

FIG. 2.

kind the difficulties mentioned above disappear. Further, we have an approach to the problem which is at once more direct and more comprehensive in that, regarding a molecule, in the first instance, as a set of atoms at definite distances apart, we view these definite lengths as connoting definite energies and by summing these energies obtain a heat of formation directly related to the structure, without any discussion as to the nature of the bonds. It is more comprehensive since, in such a scheme, benzene and other "resonating" molecules find a place, no arbitrarily chosen resonance energies having to be added so as to tally with the heats of combustion.

As an illustration, Fig. 1 shows a tentative carbon-nitrogen bond curve, based upon the bond energies and atomic radii assumed by Pauling.[1] A curve of this type for the C−C bond has already been attempted.[9] The idea of strength/length bond curves may also be applied to atoms bonded by hydrogen, and Fig. 2 shows a tentative OH···O curve based upon the lengths and strengths given for these bonds in ice, alcohol and formic acid.[1]

Full details of the work, which includes C−N, C−C, C−O and other strength-length curves, based upon a new analysis of the data, will be published shortly.

DOROTHY WRINCH
DAVID HARKER

Department of Chemistry,
The Johns Hopkins University,
Baltimore, Maryland,
May 8, 1940.

[1] Pauling, *The Nature of the Chemical Bond* (1939).
[2] Pauling, J. Am. Chem. Soc. **54**, 3570 (1932).
[3] Stevenson, LaValle and Schomaker, J. Am. Chem. Soc. **61**, 2508 (1939).
[4] Stevenson, Burnham and Schomaker, J. Am. Chem. Soc. **61**, 2922 (1939).
[5] LaValle and Schomaker, J. Am. Chem. Soc. **61**, 3520 (1939).
[6] Corey, J. Am. Chem. Soc. **60**, 1598 (1938).
[7] Fajans, Ber. **53**, 643 (1920); **55**, 2826 (1922); Rossini, J. Research Nat. Bur. Stand. **13**, 21 (1934); Rossini, J. Chem. Phys. **3**, 438 (1935).
[8] Albrecht and Corey, J. Am. Chem. Soc. **61**, 1087 (1939).
[9] Fox and Martin, J. Chem. Soc. 2106 (1938); 884 (1939).

The Dissociation of Iodine

G. M. Murphy[1] calculated the general equation for $\Delta F^0/T$ for the reaction $I_{2(g)}=2I_{(g)}$ and compared the results with the experimental results of Starck and Bodenstein,[2] De Vries and Rodebush[3] and part of those by Braune and Ramstetter.[4] For $I_{(g)}$

$$-\frac{F^0-E_0^0}{T}=\frac{3}{2}R\ln M+\frac{5}{2}R\ln T+R\ln Q-7.267. \quad (1)$$

Or using $M=126.932$, $R=1.9869$ cal. mole^{-1} deg.$^{-1}$, and $Q=4$ this reduces to

$$-\frac{F^0-E_0^0}{T}=11.4375\log T+9.9231_8. \quad (2)$$

By use of the calculated values at five temperatures, Murphy represented this function in the empirical form

$$-\frac{F^0-E_0^0}{T}=\frac{a}{T}+b\log T+cT+dT^2+i \quad (3)$$

with $a=-28.052$, $b=11.1292$, $c=1.907\times10^{-4}$, $d=-4.09\times10^{-8}$, $i=10.7277$, whereas by the theoretical equation, $a=0$, $c=0$, and $d=0$. The values tabulated in Table II of his paper are too high by 0.001, 0.002, 0.001, 0.001, and 0.0 cal. mole^{-1} deg.$^{-1}$, and this is typical of the relation of

TABLE I.

Investigators	No. pos. Δ (log K)	Σ pos. Δ	No. neg. Δ (log K)	Σ neg. Δ	Mean dev.	Mean net dev.
	(*a*) *From Eq. (3) and* $\Delta E_0^0=35{,}795$ *cal.*					
B & R	9	0.489	11	1.071	0.078	−0.029
DeV & R	3	.399	3	0.084	.071	+ .043
S & B	4	.221	1	.048	.054	+ .035
DeV & R / S & B	7	.560	4	.132	.063	+ .039
B & R / DeV & R / S & B	16	1.048	15	1.203	.073	− .005
	(*b*) *From Eq. (2) and* $\Delta E_0^0=35{,}395$ *cal.*					
B & R	1	0.134	19	2.295	0.1215	−0.108
DeV & R	1	.143	5	0.420	.094	− .066
S & B	1	.012	4	.065	.015	− .011
DeV & R / S & B	2	.155	9	.485	.058	− .030
B & R / DeV & R / S & B	3	.289	28	2.491	.099	− .080

Eq. (3) to Eq. (2) at intermediate points. Of course, the solution of the five simultaneous equations, if carried out exactly with the correct values of $-(F^0-E_0^0)/T$, would lead to the constants of Eq. (2). That is, values of a, c, and d would result, which are of such small magnitudes, that when multiplied by the $1/T$, T, and T^2 terms, the contributions to $-(F^0-E_0^0)/T$ are negligible, and they are properly set equal to zero.

Since one of the purposes of the paper was the comparison of the experimental equilibrium constants with those determined from the spectroscopic data, a more fundamental objection may be made to the use of ΔE_0^0 ($=35{,}795\pm100$ cal.) derived from the experimental data. The spectroscopic value by Brown,[5] $D=1.535\pm0.001$ ev. or $\Delta E_0^0=35{,}395\pm23$ cal. appears to be a satisfactory determination. The consistency of the experimental results decreases in the order (1) Starck and Bodenstein (S & B), (2) De Vries and Rodebush (De V & R), (3) Braune and Ramstetter (B & R). Table I shows that the deviations of the experimental values of log K by Starck and Bodenstein from log K derived from Eq. (2) and $\Delta E_0^0=35{,}395$ cal. are less than a third of the corresponding deviations from log K derived from Eq. (3) and $\Delta E_0^0=35{,}795$ cal. The deviations of the results of the first two groups of investigators from the data of purely spectroscopic origin are also less than those from the hybrid equation involving $\Delta E_0^0=35{,}795$ cal.

HUGH M. SPENCER

Cobb Chemical Laboratory,
University of Virginia,
Charlottesville, Virginia,
May 4, 1940.

[1] G. M. Murphy, J. Chem. Phys. **4**, 344 (1936).
[2] G. Starck and M. Bodenstein, Zeits. f. Elektrochemie **16**, 961 (1910); **22**, 327 (1916).
[3] T. De Vries and W. H. Rodebush, J. Am. Chem. Soc. **49**, 656 (1927).
[4] H. Braune and H. Ramstetter, Zeits. f. physik. Chemie **102**, 480 (1922).
[5] W. G. Brown, Phys. Rev. **38**, 709 (1931).

Transition in Nickel Nitrate Hexammoniate

The low temperature crystal structure of nickel nitrate hexammoniate has been investigated by Yü,[1] who found evidences of very high thermal agitation of the nitrate groups in the crystal. We have measured the heat capacity curve for this substance from 54°K to 300°K, using a modified Nernst vacuum calorimeter. The data, shown in Fig. 1, indicate the existence of two regions of high energy absorption, one a typical lambda-type transition extending from 173°K to 247°K, with a maximum value at 243°K, and the other a region of anomalous energy absorption below 85°K.

The lambda transition can be supercooled to liquid-air temperatures and held there indefinitely without transforming; the rate of transformation becomes appreciable only upon warming to about 200°K. Cooling-curve measurements indicate a hysteresis effect of several degrees. In one cooling experiment, the minimum cooling rate occurred at 239°K.

The height of the lambda-peak at 243°K is not determinable; our highest C_p measurement in this region was 1270 calories/mole/degree, certainly a lower limit. The total heat absorption in excess of that represented by the "normal" heat capacity curve was obtained by "heat of transition" measurements extending from 227–247°K, thus including the area which could not be integrated graphically. The excess heat effect (above the "normal" curve from 173–247°K) is 1818 calories/mole. The corresponding entropy is 7.65±0.5 E.U.

This high entropy of transition seems to invalidate any explanation involving rotation of only the nitrate groups in the crystal lattice. The assumption that both the ammonia and nitrate groups are executing rotational oscillations gives fair agreement with the experimental entropy, and with the value of C_p just above the transition. This assumption is in accordance with the theory of Frenkel,[2] and that of Kirkwood,[3] which assume that the active groups are librating both below and above the transition, and that the transition is simply a process of disorientation, or the disordering of these librations with respect to the crystal axes. A more precise check of the assumption could probably be made from an investigation of C_v values in the transition region.[4] If the ammonia groups are librating, as proposed, the prsence of nitrate or similar groups would seem to be required, since cooling-curve measurements on nickel chloride hexammoniate[5] show no indication of a transition. We are investigating ammonium chlorostannate and other substances of similar crystal structure to the nickel hexammoniates, in order to establish more definitely the conditions for this phenomenon.

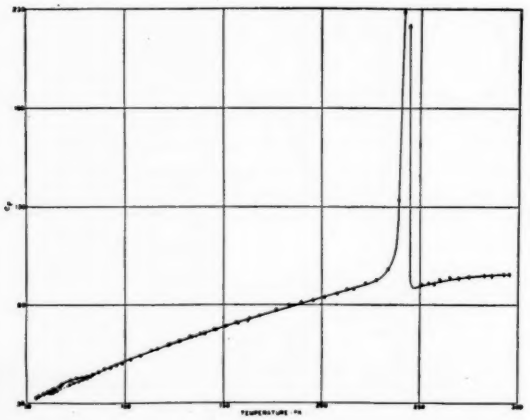

FIG. 1. Heat capacity in calories per degree per mole of nickel nitrate hexammoniate.

The region of anomalous energy absorption below 85°K is of much smaller magnitude, the C_p values being about five percent high. The dotted line in Fig. 1 shows the results of measurements made on a sample which had been partially supercooled through the 243° transition. The presence of the form stable above 243° almost completely eliminates the high energy absorption below 85°. Measurements at temperatures considerably below 54°K will be necessary for a full description of the phenomenon.

A detailed report of the work will be published later. This investigation has been supported by a grant from the University of Missouri Research Council.

EARL A. LONG
FRED C. TOETTCHER*

Department of Chemistry,
University of Missouri,
Columbia, Missouri,
May 3, 1940.

[1] S. H. Yü, Nature **141**, 158 (1938).
[2] J. Frenkel, Acta Physicochemica **3**, 23 (1935).
[3] J. G. Kirkwood, J. Chem. Phys. **8**, 205 (1940).
[4] Cf. A. W. Lawson, Jr., Phys. Rev. **57**, 417 (1940).
[5] Beevers and Jensen, Trans. Faraday Soc. **34**, 1478 (1938).
* Gregory Fellow, 1939–40.

The Mercury Photosensitized Hydrogenation of Ethylene, Propylene, and *n*-Butylene

A convenient method of preparing a free aliphatic radical is by the addition of a hydrogen atom to the corresponding olefine; if the hydrogen atoms are produced by mercury photosensitization their concentration will be low compared with the radical concentration, and subsequent reactions of the radicals with each other may be studied. Thus Taylor and Jungers[1] reported that butane was the predominant product from the mercury photosensitized hydrogenation of ethylene.

In an apparatus similar to that of Taylor and Jungers we have compared the reactions of ethyl, propyl, and butyl radicals formed in a similar fashion. In each case olefine at about forty millimeters pressure, mixed with a sixfold excess of hydrogen, was illuminated at room temperature in the presence of mercury vapor with 2536.7A radiation. The analytical method employed was a suitable adaptation

TABLE I.

Olefine used	Percentage of Olefine to Saturated Products						
	CH_4	C_2H_6	C_3H_8	C_4H_{10}	C_5H_{12}	C_6H_{14}	C_8H_{18}
C_2H_4	2	14	—	84	—	—	—
C_3H_6	2	1	26	5	2	64	—
C_4H_8	3	1	1	29	—	—	66

of that previously described.[2] The results are given in Table I as the means of two concordant experiments with each olefine. In some of the experiments a trap cooled to −78° was used to decrease if possible the amount of lower hydrocarbon products formed, by preventing more extensive secondary reactions of higher hydrocarbons with hydrogen atoms.

There is a significantly greater formation of propane and butane from propylene and butylene than of ethane from ethylene. A possible explanation may be that addition of a hydrogen atom to propylene and *n*-butylene may form the isopropyl and isobutyl radicals as well as the normal radicals. Our earlier work with mercury diethyl indicates that the disproportionation reaction $2C_nH_{2n+1}=C_nH_{2n+2}+C_nH_{2n}$ is not important with the normal radicals, C_2H_5. The reaction may become of greater importance when iso-radicals are involved. It is of interest in this connection to compare the observation of Norrish[3] that considerable amounts of propane and propylene are formed from the photolysis of di-isopropyl ketone, while neither of these products is obtained from di-*n*-propyl ketone.

WALTER J. MOORE, JR.
HUGH S. TAYLOR

Frick Chemical Laboratory,
Princeton University,
Princeton, New Jersey,
May 10, 1940.

[1] H. S. Taylor and J. C. Jungers, J. Chem. Phys. **6**, 325 (1938).
[2] W. J. Moore, Jr., and H. S. Taylor, J. Chem. Phys. **8**, 396 (1940).
[3] R. G. W. Norrish, quoted in Pearson and Glazebrook, J. Chem. Soc. 1777 (1936).

The Thermodynamic Properties of the PN Molecule*

In 1938 Moureu and Wetroff[1] showed that equimolecular quantities of phosphorus and nitrogen, when heated together, form a compound $(PN)_x$. In a more recent paper Moureu and his co-workers[2] show the existence of an equilibrium between $(PN)_x$ and PN, and also one between PN and P_2+N_2. In view of their results, we thought that it might be of interest to calculate from spectroscopic data the thermodynamic properties of a perfect gas composed of PN molecules, and the equilibrium constant for the gaseous reaction

$$P_2+N_2=2PN. \quad (1)$$

By combining the values for the equilibrium constant of reaction (1) with the values of the equilibrium constant for the reaction

$$P_4=2P_2 \quad (2)$$

given by Dushman,[3] the equilibrium constant for

$$P_4+2N_2=4PN \quad (3)$$

can be calculated.

The results of these calculations are listed in Tables I and II.

In the calculation of the thermodynamic functions, the total partition function Q is given by

$$Q=Q_{\text{trans}}\cdot Q_{\text{internal}}\cdot Q_{\text{correction}}.$$

Q_{trans} has been calculated by the usual method assuming a perfect gas. Q_{internal} assumes an harmonic oscillator and a rigid rotator. From the value of $Q_{\text{correction}}$ due to anharmonicity in the oscillation and to the lack of rigidity in the rotation given by Mayer and Mayer,[4] we have calculated the following formulae for the corrections in the thermodynamic functions. The symbols used are defined in reference (4).

$$F_{\text{correction}}=-\frac{RT}{u}\left[8\gamma+\frac{\delta u}{e^u-1}+\frac{2xu^2}{(e^u-1)^2}\right],$$

$$S_{\text{correction}}=R\left[\frac{16\gamma}{u}+\frac{\delta}{e^u-1}+\frac{\delta ue^u}{(e^u-1)^2}+\frac{4xu^2e^u}{(e^u-1)^3}\right],$$

$$H_{\text{correction}}=RT\left[\frac{8\gamma}{u}+\frac{u(\delta e^u-2x)}{(e^u-1)^2}+\frac{4xu^2e^u}{(e^u-1)^3}\right],$$

$$C_{\text{correction}}=R\left[\frac{16\gamma}{u}-\frac{u^2\delta e^u}{(e^u-1)^2}+\frac{2u^2e^u(\delta e^u-4x-2ux)}{(e^u-1)^3}+\frac{12xu^3e^{2u}}{(e^u-1)^4}\right].$$

The molecular constants which we have used were taken from the literature.[5] From the given values of the heats of dissociation, ΔE_0 for reaction (1) is calculated to be −0.2 electron volt.

According to the work of Moureu and his co-workers,[2] PN at 800°C is almost completely dissociated into P_2 and N_2. The difference between this work and the values we have obtained may be attributed to the fact that the E_0 for PN has been determined by an extrapolation method,[5c] and is probably an upper limit. A change in E_0 for PN of only a few tenths of an electron volt would have the effect of lowering the calculated value of K_p.

KENNETH J. MCCALLUM
EDGAR LEIFER**

Havemeyer Laboratories,
Columbia University,
New York, New York,
May 13, 1940.

TABLE I. *The thermodynamic functions of the* PN *molecule. (One mole of the perfect gas at one atmosphere.)*

TEMP. °K	$-(F-F_0)$ CAL.	$(H-H_0)$ CAL.	S CAL./DEGREE	C_p CAL./DEGREE
100.0	3588.0	694.6	42.824	6.9544
298.1	12959.8	2079.1	50.448	7.0973
500.0	23553.6	3565.1	54.235	7.6474
750.0	37538.7	5546.6	57.450	8.1759
1000.0	52209.0	7633.8	59.842	8.4774

TABLE II. *The equilibrium constant for* $P_2+N_2=2PN$.

TEMP. °C	$K_{pe}+\Delta E_0/RT$	$e^{-\Delta E_0/RT}$	K_p
800	6.09	7.87	47.9
900	5.94	6.58	39.1
1000	5.82	5.68	33.1

* Publication assisted by the Ernest Kempton Adams Fund for Physical Research of Columbia University.

[1] Henri Moureu and George Wetroff, Comptes rendus **207**, 915 (1938).

[2] Henri Moureu, Boris Rosen and George Wetroff, Comptes rendus **209**, 207 (1939).

[3] S. Dushman, J. Am. Chem. Soc. **43**, 397 (1921).

[4] Joseph E. Mayer and Maria Goeppert-Mayer, *Statistical Mechanics* (John Wiley and Sons, 1940).

[5] (a) N_2—G. Büttenbender and G. Herzberg, Ann. d. Physik **21**, 577 (1935). (b) P_2—M. F. Ashley, Phys. Rev. **44**, 919 (1933). (c) PN—J. Curry, L. Herzberg and G. Herzberg, Zeits. f. Physik **86**, 348 (1933).

** Fellow of Charles A. Coffin Foundation, 1939–40.

The Entropy of Dimethyl Sulfide from Low Temperature Calorimetric Measurements. Restricted Rotation of the Methyl Groups

In order to arrive at a satisfactory theory for the potential restricting the rotation of methyl groups in many molecules, it is desirable to determine how the magnitude of the barrier depends on the kind of atom to which the methyl groups are bonded. Recently we have obtained an estimate of the barriers in dimethyl sulfide by comparing the entropy obtained from calorimetric measurements extending to low temperatures with that computed from molecular data.

The heat capacities of dimethyl sulfide in the temperature range 13.4 to 291°K, heat of fusion, and heat of vaporization at 291°K were accurately determined in an adiabatic calorimeter equipped with a calibrated platinum resistance thermometer. In addition, precise measurements of the vapor pressure were made from 250 to 293°K. The size of the sample in the calorimeter was 1.4432 moles, with an estimated impurity of 0.007 mole percent. Complete details will be published later.

In Table I are given the entropy changes calculated from our calorimetric data. The final temperature and pressure are those for the directly measured heat of vaporization, 6696 cal./mole, which may be compared with 6690 cal./mole calculated from the Clapeyron relation, assuming that the gas follows the Berthelot equation of state, with critical temperature 503°K and critical pressure 54.6 atmos.[1] This same assumption was made in the correction for gas imperfection.

The calculation of the entropy from molecular data is summarized in Table II. The translational entropy comes from the familiar Sackur-Tetrode equation. The following frequencies and multiplicities,[2] as well as the usual approximation of harmonic oscillation, were used to obtain the vibrational entropy: 284, 695, 742, 1030 (2), 1262 (2), 1323 (2), 1445 (4), and 2900 (6) cm^{-1}. The calculation of the rotational entropy was made by means of the formulas of Crawford,[3] in the derivation of which it is assumed that the potential energy of each methyl group has the form

TABLE I. *Molal entropy of dimethyl sulfide from calorimetric data.*

0–15°K, Debye extrapolation, $h\nu/k=110.4$	0.369
15–174.855°K, graphical	21.156
Fusion, 1908.4/174.855	10.914
174.855–291.06°K, graphical	13.821
Vaporization, 6696/291.06	23.006
Entropy of actual gas, 291.06°K, 365.5 mm	69.27 ±0.1
Correction for gas imperfection	0.08
Entropy of ideal gas, 291.06°K, 365.5 mm	69.35 cal./deg. mole

TABLE II. *Molal entropy of gaseous dimethyl sulfide from molecular data at 291.06°K and 365.5 mm.*

S_{trans}	39.63
S_{vib} (Harmonic)	2.31
S_{rot} ($V=2015$ cal./mole)	27.41
Total entropy ($V=2015$)	69.35 cal./deg. mole
($V=1800$)	69.60
($V=0$)	71.03
($V=\infty$)	64.08

$(V/2)(1-\cos 3\alpha)$, where α is the angular displacement of the methyl group from its equilibrium position. The bond angles and interatomic distances taken were $<C-S-C=102°$, C–S=1.82A,[4] C–H=1.09A, and tetrahedral angles for the methyl groups. These values lead to principal moments of inertia of 45.49, 116.1, and 151.0×10^{-40} g cm^2 and to a moment of inertia 5.303×10^{-40} and reduced moment of inertia 4.818×10^{-40} for each methyl group. Since the ratio of these last two is nearly unity, use of Pitzer's tables[5] does not cause great error at the temperature of interest. Thus the entropy for $V=2015$ cal./mole calculated with the aid of Pitzer's tables is 69.28 cal./deg. mole rather than 69.35 cal./deg. mole by the more accurate method of Crawford.

It is seen that if the values assumed for the structural parameters and for the vibrational frequencies are sufficiently accurate, a potential barrier of about 2000 cal./mole for each methyl group is required for dimethyl sulfide. The fact that the barriers in ethane[6] and in the methyl amines[7] are of about this same magnitude, while that in dimethyl acetylene[8] is negligible, suggests that the restriction is mainly due to the proximity of the methyl groups rather than to the kind of atom to which the methyl groups are attached.

We wish to express our thanks to Professor Alexander Goetz for supplying us with liquid hydrogen.

DARRELL W. OSBORNE*
RUSSELL N. DOESCHER
DON M. YOST

Gates Chemical Laboratory,
California Institute of Technology,
Pasadena, California,
May 11, 1940.

[1] A. Berthoud and R. Brum, J. Chim. Phys. **21**, 143–160 (1924).
[2] R. Fonteyne, J. Chem. Phys. **8**, 60 (1940).
[3] B. L. Crawford, Jr., J. Chem. Phys. **8**, 273 (1940).
[4] L. O. Brockway and H. O. Jenkins, J. Am. Chem. Soc. **58**, 2036 (1936).
[5] K. S. Pitzer, J. Chem. Phys. **5**, 469 (1937).
[6] J. D. Kemp and K. S. Pitzer, J. Am. Chem. Soc. **59**, 276 (1937).
[7] J. G. Aston, C. W. Siller and G. H. Messerly, J. Am. Chem. Soc. **59**, 1743 (1937); J. G. Aston, M. L. Eidinoff and W. S. Forster, J. Am. Chem. Soc. **61**, 1539 (1939).
[8] B. L. Crawford, Jr., and W. W. Rice, J. Chem. Phys. **7**, 437 (1939); D. W. Osborne, C. S. Garner and D. M. Yost, J. Chem. Phys. **8**, 131 (1940).

* A. A. Noyes Fellow in Chemistry.